



University of Kentucky Gill Heart & Vascular Institute

Cardiovascular Research Day

September 10, 2021 - Bill Gatton Student Center

ABSTRACT BOOK

TABLE OF CONTENTS

SCHEDULE	2
POSTER PITCH PARTICIPANTS.....	11
POSTER PARTICIPANTS.....	12
ABSTRACTS.....	13
SURVEY & 2022	101

SCHEDULE

Friday, September 10, 2021

FLRC Day 2

University of Kentucky

Cardiovascular Research Day

Bill Gatton Student Center

Grand Ballrooms



University of Kentucky Gill Heart & Vascular Institute

**Cardiovascular
Research Day**

September 10, 2021 - Bill Gatton Student Center

 8:00 to 9:00 - Busses Depart Outside Marriott Lobby to Gatton Student Center

 8:15 - Continental Breakfast

Session I | Worsham Theater

9:00 - Alan Daugherty, PhD, DSc | Director, Saha Cardiovascular Research Center

Opening Comments

9:05 - Trainee Presentations

Sathya Velmurugan, PhD | Despa Lab – University of Kentucky

Inhibition of Na⁺-glucose cotransporter 1 reduces arrhythmogenesis in diabetic rats

Conner Earl | Goergen Lab – Purdue University

Strain Estimates of Murine Myocardial Infarction Size from Four-Dimensional High-Frequency Ultrasound

9:35 - Distinguished Alumni Speaker

Steven Steinhubl, MD | Scripps Research Translational Institute

Healthcare Transformation and the Need for More Unreasonable Clinician-Researchers

10:05 - 90 Second Poster Pitch

Yonathan Aberra | University of Virginia

Hammodah Alfar | University of Kentucky

Naofumi Amioka | University of Kentucky

Tyler Benson, PhD | University of Cincinnati

Kathryn Gunn, PhD | The University of North Carolina at Chapel Hill


Sohei Ito, MD, PhD | University Kentucky

Sarah Kosta, PhD | University of Kentucky

Jennifer Torres Yee, MD, MSc | University of Kentucky

Lauren Weaver | University of Kentucky

Yingdong Zhu | Northeast Ohio Medical University

 10:15 – Break

Poster Session A | Grand Ballrooms

10:30- Poster Session A

Odd numbered posters presented and judged

Friday, September 10, 2021

FLRC Day 2

Continued



University of Kentucky Gill Heart & Vascular Institute

**Cardiovascular
Research Day**

September 10, 2021 - Bill Gatton Student Center



Session II | Worsham Theater

11:45 - Gill Heart and Vascular Institute Outstanding Contributions to Cardiovascular Research Award

Elizabeth McNally, MD, PhD
Director, Center for Genetic Medicine
Northwestern University Feinberg School of Medicine
The Genetic Landscape of Heart Failure



Lunch Session | Grand Ballrooms

12:30- Buffet Lunch

1:00 - Professional Development Lecture

Amy Herman
Author of “Visual Intelligence”
2016 New York Times Bestseller
Seeing What Matters



2:00 – Break

Session III | Worsham Theater

2:15 - Trainee Presentations

Alexis Smith | Whiteheart Lab – University of Kentucky

α-Synuclein: a VAMP Chaperone in the Platelet Release Reaction

Rupinder Kaur | Graf Lab – University of Kentucky

Trans-intestinal cholesterol excretion is dependent on the luminal cholesterol content

2:45 - 90 Second Poster Pitches

Fathima Nafrisha Cassim Bawa | Kent State University

Hui Chen, MD | University of Kentucky

Brandee Goo, MS | Augusta University

Velmurugan Gopal Viswanathan | University of Kentucky

Shayan Mohammadmoradi, MS | University of Kentucky

Kelsey Pinckard | Ohio State University

Caris Wadding Lee, BS | The University of Cincinnati



3:00 – Break

Friday, September 10, 2021

FLRC Day 2

Continued



University of Kentucky Gill Heart & Vascular Institute

**Cardiovascular
Research Day**

September 10, 2021 - Bill Gatton Student Center

Poster Session B | Grand Ballrooms

3:15 - Poster Session B

Even numbered posters presented and judged



Session IV | Worsham Theater

4:30 - Gill Heart and Vascular Institute Early Career Award

Katherine Gallagher, MD

John R. Pfeifer Professor of Surgery

Associate Professor of Surgery, Section of Vascular Surgery

Associate Professor of Microbiology and Immunology

University of Michigan

Epigenetics in Vascular Disease



Evening Session | Grand Ballrooms

5:15 - Networking Session

6:00 - Dinner & Awards Presentations



6:45 to 7:45 - Busses Depart Gatton Student Center to Marriott City Center

SPONSORS

A special thank you to the sponsors of the
2021 University of Kentucky Cardiovascular Research Day



**GILL FOUNDATION
OF TEXAS**



**THE SAHA FUND FOR
CARDIOVASCULAR
RESEARCH & EDUCATION**

**THE ESTATE & FAMILY OF
MRS. HAGER KOOSTRA**

**MR. & MRS.
BOB ALLEN**

 **CARDIOVASCULAR
RESEARCH PRIORITY AREA**

 **Saha Cardiovascular
Research Center**

 **Saha Aortic Center**

 **HealthCare®
GILL HEART & VASCULAR
INSTITUTE**

INVITED SPEAKERS

GILL HEART AND VASCULAR INSTITUTE OUTSTANDING CONTRIBUTIONS TO CARDIOVASCULAR RESEARCH AWARD



ELIZABETH MCNALLY, MD, PHD
NORTHWESTERN UNIVERSITY

Elizabeth McNally MD Ph is a physician and scientist who directs the Center for Genetic Medicine at Northwestern University's Feinberg School of Medicine. As the Elizabeth J. Ward Professor of Genetic Medicine, Dr. McNally is a cardiologist with expertise in cardiovascular genetics. As a clinician, she developed one of the first Cardiovascular Genetics clinics in the nation, integrating genetic testing into cardiovascular care for patients and families. Dr. McNally's research focuses on understanding genetic mechanisms underlying heritable cardiac disorders. By developing a deeper understanding as to how these genetic mutations exert their effects, she is using these genetic signals to drive the development of new therapies. She has published nearly 300 papers and book chapters. Dr. McNally has a special interest in neuromuscular genetic diseases like muscular dystrophy since often these disorders have accompanying cardiovascular complications. Her translational accomplishments have been recognized through an award from the Burroughs Wellcome Foundation and as a recipient a Distinguished Clinical Scientist Award from the Doris Duke Charitable Foundation. She serves on the Board of Directors for the Muscular Dystrophy Association and is the current Chair for the Council on Basic Cardiovascular Sciences of the American Heart Association. She is a past president of American Society for Clinical Investigation and currently President of the Association of American Physicians. She was elected to the American Academy of Arts and Sciences.

INVITED SPEAKERS

GILL HEART AND VASCULAR INSTITUTE EARLY CAREER AWARD



KATHERINE A. GALLAGHER, MD
UNIVERSITY OF MICHIGAN

Dr. Katherine Gallagher is Professor of Surgery, Professor of Microbiology and Immunology, and the John R. Pfeifer Collegiate Professor of Surgery. Dr. Gallagher graduated with highest honors from the University of Maryland with a B.S. in Physiology and Neurobiology in 1998. During this time, she was a Howard Hughes Fellow at the NIH studying embryonic hair cell regeneration. She graduated with honors (cum laude) from the University of Maryland School of

Medicine in 2002. She did her General Surgery Residency at the University of Maryland from 2002-2009. Concurrently, she pursued Vascular Biology Post-Doctoral T32 Fellowship at the University of Pennsylvania. Dr. Gallagher completed her Vascular Surgery Fellowship at Weill Cornell Medical Center/Columbia University Medical Center in 2011.

Since joining the faculty at the University of Michigan, Dr. Gallagher's research has focused on vascular inflammation and the intercept between epigenetics and peripheral macrophage phenotypes in wound repair and vascular disease. Dr. Gallagher is an NIH-funded researcher with additional funding from the Doris Duke Charitable Foundation, Wylie Scholars, AHA and the ACS. She is a standing member on the BTSS NIH-study section and is a founding member of the NIH-NIDDK Wound Consortium. She has received numerous honors and awards which include the American Heart Association's ATVB Young Investigator of the Year (2019), member of the American Society of Clinical Investigation (ASCI), American Surgical Association, Distinguished Fellow of the Society of Vascular Surgery, and is a Taubman Scholar. She is most excited about training the next generation of surgeon-scientists, with numerous general/vascular surgery residents who have all achieved NIH (F32/T32) and society funding (ACS, AAS/SUS, VESS, SVS).

INVITED SPEAKERS

PROFESSIONAL DEVELOPMENT PRESENTATION



AMY HERMAN

AUTHOR OF “VISUAL INTELLIGENCE”
2016 NEW YORK TIMES BESTSELLER

Amy E. Herman is the founder and president of The Art of Perception, Inc., a New York-based organization that conducts professional development courses to leaders around the world including at the FBI, CIA, Scotland Yard, and the Peace Corps. Herman was also the Director of Educational Development at Thirteen/WNET, the educational public television station serving New York and New Jersey, and the Head of Education at The Frick Collection for over ten years, where she oversaw all of the Collection's educational collaborations and community initiatives.

An art historian and attorney, Herman holds a BA in International Affairs from Lafayette College, a JD from the National Law Center at George Washington University, and an MA in Art History from Hunter College. She is a member of the New Jersey and Pennsylvania Bar Associations. Herman channeled her dual degrees in art and law to create the successful Art of Perception program, and now trains thousands of professionals from Secret Service agents to church fundraisers. Herman is a world-renowned speaker who frequently presents at national and international conventions. She has been featured on the CBS Evening News, the BBC, and in countless print publications including The New York Times, The Wall Street Journal, The London Times, New York Daily News, Smithsonian Magazine, and The Philadelphia Inquirer.

INVITED SPEAKERS

DISTINGUISHED ALUMNI PRESENTATION



STEVEN R. STEINHUBL, MD

SCRIPPS RESEARCH TRANSLATIONAL INSTITUTE

Dr. Steinhubl is a career-long clinician-scientist and the founding Director of Digital Medicine at Scripps Research's Translational Institute. He recently began splitting his time between Scripps and physIQ where he is their Chief Medical Officer. He remains clinically active as a Cardiologist in the Alaska Native Tribal Health Consortium. He received his undergraduate training in chemical engineering at Purdue University, medical degree at St. Louis University and cardiology training at the Cleveland Clinic.

His research has focused on the implementation of clinical programs built specifically around the novel capabilities of digital technologies, especially those made possible through combining novel sensor technologies and AI-based insights to provide personalized, real-time analyses able to detect individual changes in health.

Steve has been the Principal Investigator of dozens of nationwide and global clinical trials and has published ~300 peer-reviewed articles and was the founding Editor-in-Chief of Nature Partner Journal - Digital Medicine. He is also the default breakfast cook at his wife's B&B, Susitna Place, in Anchorage Alaska.

SELECTED ABSTRACTS

Congratulations to the abstracts selected to present at the
University of Kentucky Cardiovascular Research Day

CONNER C. EARL

GOERGEN LAB – PURDUE UNIVERSITY

RUPINDER KAUR

GRAF LAB – UNIVERSITY OF KENTUCKY

ALEXIS SMITH

WHITEHEART LAB – UNIVERSITY OF KENTUCKY

SATHYA VELMURUGAN, PHD

DESPA LAB – UNIVERSITY OF KENTUCKY

POSTER PITCH PARTICIPANTS

YONATHAN ABERRA

UNIVERSITY OF VIRGINIA

HAMMODAH ALFAR

UNIVERSITY OF KENTUCKY

NAOFUMI AMIOKA

UNIVERSITY OF KENTUCKY

TYLER BENSON, PH.D

UNIVERSITY OF CINCINNATI

FATHIMA NAFRISHA CASSIM BAWA

KENT STATE UNIVERSITY

HUI CHEN, MD

UNIVERSITY OF KENTUCKY

BRANDEE GOO, MS

AUGUSTA UNIVERSITY

VELMURUGAN GOPAL VISWANATHAN

UNIVERSITY OF KENTUCKY

KATHRYN GUNN, PHD

THE UNIVERSITY OF NORTH CAROLINA AT
CHAPEL HILL

SOHEI ITO, MD, PHD

UNIVERSITY OF KENTUCKY

SARAH KOSTA, PHD

UNIVERSITY OF KENTUCKY

SHAYAN MOHAMMADMORADI, MS

UNIVERSITY OF KENTUCKY

KELSEY PINCKARD

OHIO STATE UNIVERSITY

JENNIFER TORRES YEE, MD, MSC

UNIVERSITY OF KENTUCKY

CARIS WADDING LEE, B.S

THE UNIVERSITY OF CINCINNATI

LAUREN WEAVER

UNIVERSITY OF KENTUCKY

YINGDONG ZHU

NORTHEAST OHIO MEDICAL UNIVERSITY

POSTER PARTICIPANTS

Yonathan Aberra	35/44	Sidney Johnson	74
Clementine Adeyemi	50	Smita Joshi	60
David Alexander	81	Rupinder Kaur	21
Hammodah Alfar	55	Sarah Kosta	69
Ryan Allen	31	Xian Li	64
Yasir Al-Siraj	66	Ching Ling (Jenny) Liang	22
Naofumi Amioka	47	Andrew Lutkewitte	11
Liya Anto	51	Joshua Lykins	78
Gertrude Arthur	77	Benton Maglinger	57
Keiichi Asano	26	William Massey	37
Jacob Barber	38	Nicholas McVay	63
Shimpi Bedi	41	Maura Mobilia	10
Tyler Benson	45	Shayan Mohammadmoradi	14
Lei Cai	18	Xufang Mu	73
Fathima Nafrisha Cassim Bawa	20	Kellea Nichols	52
Mark Castleberry	23	Makoto Ono	82
Aaron Chacon	61	Danny Orabi	81
Harry Chanzu	62	Lucas Osborn	33
Hui Chen	2	Kelsey Pinckard	48
Taylor Coughlin	46	Brittany Poole	43
Wen Dai	28	Audrey Poupeau	70
Frank Davis	8	Kanakanagavalli Shravani Prakhya ...	65
Jacob DeMott	68	Jordan Reed	27
Renee Donahue	72	Ezekiel Rozmus	56
Conner Earl	9	Hisashi Sawada	79
Daniel Ferguson	42	Luke Schepers	29
Salma Fleifil	39	Martha Sim	80
Brandee Goo	12	Angelica Solomon	40
Velmurugan Gopal Viswanathan ...	58	Scott Street	30
Kailash Gulshan	25	Jennifer Torres Yee	75
Kathryn Gunn	13	Himi Tripathi	5
Taesik Gwag	36	Andrea Trumbauer	1
Dan Hao	71	Sathya Velmurugan	59
Rachel Hart	32	Caris Wadding Lee	4
Robert Helsley	34	Lauren Weaver	19
Madison Hickey	67	Anna Wheless	6
Jordan Howard	53	Kori Williams	16
Brad Hubbard	54	Lin Zhu	49
Sohei Ito	15	Yingdong Zhu	17
Aida Javidan	3		
Uriel Jean-Baptiste	24		

1

Andrea Trumbuer¹ • Victoria Noffsinger¹ • Ailing Ji, PhD¹ • Frederic de Beer, MD² • Adam Dugan³ • Adam Mullick, PhD⁴ • Nancy R Webb, PhD⁵ • Preetha Shridas, PhD³ • Lisa R Tannock, MD³

Saha Cardiovascular Research Center, University of Kentucky¹

Internal Medicine/Saha Cardiovascular Research Center, University of Kentucky²

Biostatistics, University of Kentucky³

Ionis Pharmaceuticals⁴

Pharmacology and Nutritional Sciences/Saha Cardiovascular Research Center, University of Kentucky⁵

Suppression of Serum Amyloid A (SAA) Limits Progression of Obesity-Associated Abdominal Aortic Aneurysms

Staff

Obesity increases the risk for abdominal aortic aneurysms (AAA) in humans, and enhances angiotensin II (AngII)-induced AAA formation in C57BL/6 mice. Obesity is also associated with increases in serum amyloid A (SAA). We previously reported that deficiency of SAA significantly reduces AngII-induced inflammation and AAA in apoE-deficient mice. In this study we investigated whether SAA plays a role in progression of an established AAA in obese C57BL/6 mice.

Approach and results: Male C57BL/6 mice were fed a high fat diet (60% kcal as fat) throughout the study. After 4 months of diet the mice were infused with angiotensin II (AngII) at 1000ng/kg/min until the end of the study. Ultrasound (US) was performed in all mice before and after 28 days of AngII infusion, and mice that had at least a 25% increase in the luminal diameter of the abdominal aorta were stratified by luminal diameter into 3 groups. Group 1 was killed to establish baseline AAA. Groups 2 and 3 continued to receive AngII for a further 8 weeks along with an antisense oligonucleotide (ASO) that suppresses all 3 acute phase SAA isoforms (SAA-ASO), or a control ASO (5 mg/kg/wk). US was repeated at study end to assess AAA progression. Plasma SAA at the end of the experiment was 89.2±83.2 mg/L in the control ASO group, and 18.6±0.7 mg/L in the SAA-ASO group (mean±SD, p=0.008). There was no impact of SAA suppression on body weight, body fat, or blood pressure. After the first 4 weeks of AngII infusion, the average luminal diameter in all mice was 1.81±0.40 mm (mean±SD). Mice that received the control ASO had continued aortic dilation (average luminal aortic diameter 2.06±0.42 mm), whereas the mice that received the SAA-ASO had significant reduction in progression of aortic dilation (average luminal diameter 1.64±0.43 mm, p=0.0015 for interaction between time and group).

Conclusions: We demonstrate for the first time that suppression of SAA protects obese C57BL/6 mice from progression of AngII-induced AAA. Suppression of SAA may be a therapeutic approach to limit AAA progression.

Hui Chen, MD, Masayoshi Kukida, MD ¹ • Dien Ye, MS ¹ • Deborah A. Howatt ¹ • Jessica J. Moorleghen, ² • Hisashi Sawada, MD ¹ • Alan Daugherty, MD, PhD ¹ • Hong S. Lu, MD, PhD ¹
 Saha Cardiovascular Research Center University of Kentucky ¹

Deficiency of Angiotensin-converting Enzyme in Renal Proximal Convoluted Tubules Does Not Attenuate Atherosclerosis in Mice

Postdoc

Objective:

Angiotensin-converting enzyme (ACE) is the enzyme to generate Angiotensin II (AngII), an important contributor to atherosclerosis. ACE is present in all 3 segments (S1, S2, and S3) of proximal tubular cells (PTCs), and AngII concentrations are higher in kidney than in plasma. The purpose of this study was to determine whether ACE in PTCs contributes to atherosclerosis in mice.

Approach and Results:

Female ACE floxed mice and male Ndr1-Cre ERT2 +/- transgenic mice were bred to generate ACE f/f x Ndr1-Cre ERT2 -/- (PTC-ACE +/+) and ACE f/f x Ndr1-Cre ERT2 +/- (PTC-ACE -/-) littermates. Male PTC-ACE +/+ (n=7) and PTC-ACE -/- (n=10) littermates in an LDL receptor -/- background were used for atherosclerosis study. After Cre genotyping using tail DNA, mice (both Cre ERT2 -/- and Cre ERT2 +/-) were injected with 150 mg/kg/day of tamoxifen for 5 consecutive days at the age of 4-6 weeks. Two weeks after the last injection of tamoxifen, mice were fed a Western diet (Envigo, Diet #TD.88137) for 12 weeks to induce hypercholesterolemia. Blood pressure was measured using a tail-cuff system. No difference of blood pressure was detected between the two genotypes (PTC-ACE +/+ vs. PTC-ACE -/-: 126 ± 4 vs. 125 ± 3 mmHg; $P = 0.763$). All study mice were hypercholesterolemic, but plasma cholesterol concentrations were not different between the two genotypes (PTC-ACE +/+ vs. PTC-ACE -/-: 1376 ± 119 vs. 1543 ± 93 mg/dl; $P = 0.28$). PTC-specific deletion of ACE was confirmed after termination using immunostaining of ACE. In mice with Ndr1-Cre ERT2 transgene, immunostaining of ACE in kidney section showed an absence of ACE in S1 and S2 of PTCs, but ACE protein in S3 remained. Deletion of ACE in S1 and S2 of PTCs did not change hypercholesterolemia-induced atherosclerosis in the ascending and aortic arch regions (PTC-ACE +/+ vs. PTC-ACE -/-: $9.6 \pm 0.9\%$ vs. $7.0 \pm 1.9\%$; $P = 0.13$ by Mann-Whitney Rank Sum Test), as measured using an *en face* method.

Conclusion:

ACE deficiency in S1 and S2 of renal proximal tubular cells had no effect on atherosclerosis in hypercholesterolemic mice. Since ACE is more abundant in S3 than in S1 and S2 of PTCs, it would be important to determine the role of ACE in the S3 segment.

Aida Javidan, MS¹ • Weihua Jiang, MS² • Lihua Yang² • Venkateswaran Subramanian, PhD³

Pharmacology and Nutritional Sciences University of Kentucky¹ • Saha Cardiovascular Research Center University of Kentucky² • Physiology University of Kentucky³

Celastrol Supplementation Profoundly Activates Aortic MMP-9 and Abolishes Sexual Dimorphism of Abdominal Aortic Aneurysm in Mice.

Graduate Student

Background and Objective: Abdominal Aortic Aneurysms (AAAs) are permanent dilations of the abdominal aorta with greater than 80% mortality after rupture. AAA prevalence is 4–5 times greater in males than females. AAA formation involves a complex process of destruction of aortic media through degradation of extracellular matrix proteins, elastin and collagen. Angiotensin II (AngII) infusion model of AAA in mice recapitulates major features of human AAA mainly male gender specificity. Celastrol, a pentacyclic triterpene from the root extracts of Thunder God Vine (*Tripterygium wilfordii*), strongly suppressed AngII-induced cardiovascular complications in mice. The purpose of this study is to test the effect of Celastrol supplementation on AngII-induced AAAs in mice.

Methods and Results: Male and female LDL receptor -/- mice (8 weeks old; n= 12 per group) were fed a fat-enriched diet (21% wt/wt fat; 0.15% wt/wt cholesterol) supplemented with or without Celastrol (10mg/kg/day) for 5 weeks. After 1 week of diet feeding, mice were infused with AngII (500 or 1000 ng/kg/min) for 28 days by osmotic minipumps. Dietary supplementation of celastrol significantly promoted AngII-induced abdominal aortic luminal dilation (Con = 1.25 ± 0.05 versus Celas = 1.55 ± 0.09 mm, $P < 0.05$) and external aortic width (Con = 1.01 ± 0.09 versus Celas = 1.62 ± 0.14 mm, $P < 0.05$) in male mice as measured by ultra-sonography and ex vivo measurement, with 90% incidence (10/11) compared to 36% (4/11) in control group. Interestingly, celastrol supplementation to AAA female mice, resulted in a significant increase in AngII-induced aortic luminal dilation (Con = 1.17 ± 0.30 versus Celas = 1.57 ± 0.21 mm, $P < 0.001$) and AAA formation (Con = 0.94 ± 0.03 versus Celas = 1.36 ± 0.25 mm, $P < 0.05$) mice with 80% incidence (12/15) compared to 6% (1/15) in control group. Celastrol supplementation dramatically increased AngII-induced aortic leukocyte accumulation, MMP-9 activity and medial elastin degradation in both male and female mice compared to saline and AngII controls.

Conclusion: These findings demonstrate that celastrol supplementation to LDLr -/- mice ablates sexual dimorphism and promotes AngII-induced AAA formation, which is associated with increased leukocytic infiltration and MMP-9 activation.

Caris Wadding Lee¹ • Shannon Jones² • Kelsey Conrad, PhD¹ • Sarah Anthony, MS¹ • Mete Civelek, PhD³ • Michael Tranter, PhD¹ • A. Phillip Owens III, PhD¹
 Internal Medicine University of Cincinnati¹ • Pathology University of Cincinnati² • Biomedical Engineering University of Virginia³

Protease activated receptor 2 is a critical mediator of the vascular smooth muscle cell synthetic state

Graduate Student

Introduction: The vascular smooth muscle cell (VSMC) is a biologically flexible cell that can differentiate based on various injury states. In atherosclerosis, it is estimated that 50-70% of the macrophages present in plaques may be of VSMC origin. In a potential contribution to this phenotype, protease activated receptor 2 has been associated with VSMC proliferation, migration, and an increased overall synthetic phenotype. The objective of this study is to determine the role of PAR2 in VSMC dedifferentiation in atherosclerosis.

Methods and Results: Our previous studies have demonstrated *Ldlr*^{-/-}/*Par2*^{-/-} were protected from both early (12 weeks) and late-stage (24 weeks) atherosclerosis in the aortic sinus and the en face aorta when compared to littermate *Ldlr*^{-/-}/*Par2*^{+/+} controls. These results also demonstrated this effect was non-hematopoietic, with VSMCs as a potential target. To determine the mechanism of PAR2 in VSMC plasticity, *Par2*^{+/+} and *Par2*^{-/-} VSMCs were treated with cholesterol-methyl- β -cyclodextrin for 72 hours or placebo (water). After cholesterol treatment, *Par2*^{+/+} VSMCs showed a downregulation of VSMCs markers (alpha-actin and myosin heavy chain 11) and upregulation of macrophage markers (CD68 and Mac-2) whereas *Par2*^{-/-} remained unaffected. *Par2*^{-/-} VSMCs also displayed less phagocytic activity with latex beads when compared to *Par2*^{+/+} VSMCs. Krüppel-like factor 4 (KLF4) is a critical mediator of the VSMC synthetic phenotype in vivo. To determine whether PAR2 had any interaction with KLF4, we examined the hybrid mouse diversity panel conducted on ~100 strains of mice with induced atherosclerosis. Interestingly, PAR2 was found to be significantly correlated with KLF4 (top 50 gene; $r = 0.419447$; $p = 2.77 \times 10^{-17}$). This was further confirmed in *Par2*^{-/-} VSMCs, where basal KLF4 mRNA expression was significantly lower versus *Par2*^{+/+} VSMCs. Recent data also connects the RNA binding protein human antigen R (HuR) to PAR2 mRNA stability and VSMC proliferation. As such, we confirm role of HuR in PAR2 stability with the use of actinomycin D. Importantly, 72-hour cholesterol-loaded *Par2*^{-/-} VSMCs demonstrated decreased HuR shuttling to the cytoplasm versus *Par2*^{+/+} VSMCs, demonstrating a role of HuR in the PAR2-induced VSMC synthetic phenotype.

Conclusions: These results suggest that VSMC PAR2 activation mediates the modulation of VSMCs via as yet unspecified interactions with KLF4 and HuR. Future studies will continue to study PAR2 in VSMC plasticity and clonal expansion both in vitro and in vivo.

Himi Tripathi, PhD ¹ • Kazuhiro Shindo, MD, PhD ¹ • Renee Donahue, MS ² • Erhe Gao, MD ³ • Andrew J. Morris, PhD ⁴ • Susan S. Smyth, MD, PhD ⁴ • Ahmed Abdel-Latif, MD, PhD ⁴

Saha Cardiovascular Research Centre University of Kentucky ¹ • Saha Cardiovascular Research Centre University of Kentucky ² • The Center for Translational Medicine, Lewis Katz School of Medicine Temple University, Philadelphia, PA, USA ³ • Gill Heart Institute and Division of Cardiovascular Medicine University of Kentucky ⁴

Myeloid-specific Deletion in Lipid Phosphate Phosphatase3 (plpp3) Increases Cardiac Inflammation

Staff

Introduction and Hypothesis: Acute myocardial infarction (AMI) which commonly leads to heart failure (HF), is among the leading causes of morbidity and mortality worldwide. While the innate immune response after AMI is essential for clearing necrotic cells and initiating myocardial repair, uninhibited inflammatory response is often complicated by adverse ventricular remodeling and HF. Lysophosphatidic acid (LPA), produced by autotaxin (ATX), regulates monocytes and promotes inflammation. Signaling of lipid substrate including LPA is dephosphorylated and terminated by Lipid phosphate phosphatase 3 (LPP3). However, the role of ATX/LPA signaling nexus in cardiac inflammation is poorly investigated.

Hypothesis: We investigated the possible role of Leukocyte-specific Plpp3 KO mice in cardiac and systemic inflammation and resulting adverse cardiac remodeling post-MI.

Methods and Results: To generate mice with leukocyte-specific Plpp3 deletion, female Plpp3^{fl/fl} mice were crossed to male Plpp3 mice expressing Cre recombinase under the control of the LysM promoter to generate lysm-plpp3 mice. These mice and their littermate control underwent MI or sham surgery. Inflammatory cell content was assessed using flow cytometry and immunohistochemistry. Cardiac function and scar size were assessed by echocardiography and Mason Trichrome staining, respectively.

Increased number of Ly6C^{hi} monocytes (CD45⁺/Ly6C/G^{hi}/CD115^{hi}) and pro-inflammatory macrophages (CD45⁺/F4-80⁺/CD11b⁺) (CD45⁺/F4-80⁺/CD86⁺), in cardiac tissue of Cre+LysM mice was observed compared to Cre-fl/fl littermate controls during peak post-MI inflammation, as assessed by flow cytometry. This increase in inflammatory cells and inflammation may be the consequence of the significant increase in bone marrow and/or spleen progenitor cell count and proliferation. Moreover, Cre+LysM mice cardiac functional recovery was also reduced significantly as assessed by echocardiography.

Conclusion: Leukocyte-specific Plpp3 deletion increases the deleterious effects of inflammation on the ischemic myocardium and ATX/LPA signaling could represent a novel therapeutic target for future clinical studies of coronary heart diseases.

Anna Wheless¹ • Saskia Neher, PhD¹

Biochemistry and Biophysics University of North Carolina - Chapel Hill¹

Resolving the Interaction of LPL and ANGPTL4

Graduate Student

Lipoprotein lipase (LPL) is a pillar of the fatty acid allocation system that provides cells with energetic and biosynthetic precursors. Responsive and tissue-specific regulation determines which tissues receive the fatty acids LPL cleaves from the triglycerides found in cores of circulating lipoproteins. Additionally, LPL activity levels govern the concentration of circulating triglycerides, which is linked to cardiovascular health. As a potent physiological inhibitor of LPL, ANGPTL4 is an important player in LPL regulation. A certain mutation in ANGPTL4 is even associated with beneficial lipid profiles in human populations due to a loss of its LPL inhibitory function. Thus, the interaction between ANGPTL4 and LPL is sufficient to modulate global lipid levels, and is consequential for human health. Others have also recognized this and have developed monoclonal antibody therapeutics to bind ANGPTL4 and block its inhibition of LPL, thereby enhancing LPL activity and lowering lipid levels. However, these treatments have historically resulted in lethal side effects in animals. Because the physical properties of these two proteins (particularly ANGPTL4) have made structural studies challenging, there is no structural data for the complex that forms when ANGPTL4 is inhibiting LPL. However, in recent years, the field of cryogenic electron microscopy (cryoEM) has developed rapidly. We are using single-particle cryoEM to obtain high-resolution structural data that will illuminate the ANGPTL4 mechanism of inhibition. Having this structure gives the field a better chance of designing a therapeutic that blocks ANGPTL4 inhibition of LPL without affecting the other known functions of ANGPTL4, and will also contribute to the studies of the other related LPL inhibitors ANGPTL3 and ANGPTL8.

Hemendra Vekaria , PhD ¹ • Danielle Coenen, PhD ² • Patrick Sullivan , PhD ¹ • Sidney Whiteheart, PhD ³

Department of Neuroscience University of Kentucky ¹ • Department of Cellular and Molecular Biochemistry University of Kentucky ² • Department of Cellular and Molecular Biology University of Kentucky ³

Understanding the role of mitochondria in platelet function

Post doc

To mediate hemostasis, platelets use energy-dependent processes (e.g., activation, aggregation, granule secretion, clot formation, and contraction), yet it is unclear what metabolic fuels and energy-producing pathways are required for which platelet function. Platelets have metabolic flexibility, using several fuels (glucose, glycogen, etc.) and switching between glycolysis and oxidative phosphorylation (OxPhos); however, the relative roles of these ATP-generating processes are unclear. We are developing tools and models to study platelet bioenergetics and mitochondrial function in hemostasis.

To study platelet bioenergetics, we developed a continuous tracking clot contraction assay that yields multiple kinetic parameters: lag time, rate, extent, and the area under the curve (AUC). Metabolic inhibitors and a platelet-specific TFAM (Transcription Factor A Mitochondrial) deletion were used to probe the importance of platelet bioenergetics and mitochondrial function. TFAM is a transcription factor that is important for mitochondrial genome compaction (like histones). It is not only essential for maintaining the integrity of the mitochondrial genome but also for transcription of mitochondrial genes which encode for subunits of Electron Transport Chain complexes. To study platelet mitochondrial function, we created a platelet-specific KO of TFAM.

Clot contraction of TFAM^{-/-} platelets (TFAM^{flox/flox}::PF4^{Cre+}) showed defective rate, extent, and AUC at low thrombin concentration (5 mU/mL), but were normal at higher (20 mU/mL). When clot contraction was measured in the presence of a glycolysis inhibitor (2-Deoxyglucose or a glycogen phosphorylase inhibitor (CP 316819), platelets from TFAM mice showed decreased rate and extent of clot contraction. Other low energy-dependent processes such as secretion and aggregation were not affected. Using Bioflux, a microfluidic flow channel system, we have observed that TFAM^{-/-} platelets had an impaired and unstable thrombus formation showing that the formation of thrombi and its stability is energy-dependent and platelet mitochondrial bioenergetics is important for thrombus formation underflow. These experiments are supported by a preliminary *in vivo* Ferric Chloride injury model where we noted an increase in occlusion time but there was no significant change in the tail-bleeding assay.

In conclusion, we have developed a continuous tracking clot retraction assay to study platelet bioenergetics and developed a new mouse model with dysfunctional mitochondrial bioenergetics. We have seen that low energy-demanding processes like secretion and aggregation were not affected in TFAM KOs but clot contraction at low thrombin and thrombus formation under shear was impaired. We also observed no hemostatic effects but impaired thrombosis with our Kos. This model can be an important model to better understand how platelet mitochondrial bioenergetics plays a role in metabolic disorders like diabetes and aging.

Frank M. Davis, M.D.^{1,2}; Lam C. Tsoi, Ph.D.^{3,4,5}; William J Melvin, M.D.¹; Aaron denDekker, Ph.D.¹; Rachael Wasikowski, MS³; Amrita D. Joshi, Ph.D.¹; Sonya Wolf, Ph.D.¹; Andrea T. Obi, M.D.¹; Allison C. Billi, M.D. Ph.D.³, Xianying Xing M.D.³, Christopher Audu, M.D., Ph.D.¹; Bethany B. Moore, Ph.D.^{2,6}; Steven L. Kunkel, Ph.D.⁷; Alan Daugherty, Ph.D.⁸; Hong S. Lu, M.D., Ph.D.⁸; Johann E. Gudjonsson, M.D., Ph.D.³; Katherine A. Gallagher, M.D.^{1,2}

¹Section of Vascular Surgery, Department of Surgery, University of Michigan, Ann Arbor, MI

²Department Microbiology and Immunology, University of Michigan, Ann Arbor, MI

³Department of Dermatology, University of Michigan, Ann Arbor, MI

⁴Department of Computation Medicine and Bioinformatics, University of Michigan, Ann Arbor, MI

⁵Department of Biostatistics, University of Michigan, Ann Arbor, MI

⁶Department of Internal Medicine, University of Michigan, Ann Arbor, MI

⁷Department of Pathology, University of Michigan, Ann Arbor, MI

⁸Department of Physiology, Saha Cardiovascular Research Center, University of Kentucky

Inhibition of Macrophage Histone Demethylase JMJD3 Protects Against Abdominal Aortic Aneurysms

Postdoc

Background: Abdominal aortic aneurysms (AAA) are a life-threatening cardiovascular disease characterized by an inflammatory macrophage phenotype that contributes to pathological vascular remodeling and predisposes patients to the potentially fatal consequence of aortic rupture. Identifying the mechanisms regulating macrophage-mediated inflammation during AAA development are of critical importance to developing novel pharmacological therapies to prevent AAA progression. Recent evidence indicates that that epigenetic enzymes, specifically the histone demethylase JMJD3, play a critical role in establishing tissue macrophage phenotype and inflammation. Here we examined the role of JMJD3 in the development of AAAs and establish JMJD3 as a novel target in the treatment AAA disease.

Methods: The role of JMJD3 in AAA formation was examined in human aortic tissue samples by single cell RNA sequencing and in a myeloid-specific JMJD deficient murine model induced by challenging mice with a combination of a high-fat diet and angiotensin II. We also examined the direct effect of pharmacological inhibition of JMJD3 on macrophage function and AAA expansion.

Results: In human AAA tissue we observed a significant upregulation of *JMJD3* and inflammatory cytokines in aortic macrophages. Mechanistically, we found that interferon (IFN) β regulates *Jmjd3* expression via JAK/STAT1 and JMJD3 induces NF κ B-mediated inflammatory gene transcription in infiltrating aortic macrophages. Single cell transcriptome analysis of human AAA tissues revealed that JMJD3 was increased in myeloid subsets resulting in upregulation of cellular activation and an inflammatory immune response. In the murine model, myeloid-specific JMJD3 depletion (*JMJD3^{f/f}/Lyz2^{Cre+}*) showed significant reduction in angiotensin II-induced AAA formation and inflammation. We also found that pharmacological inhibition of JMJD3 preserved the repressive H3K27me3 on inflammatory gene promoters, reduced inflammatory macrophage phenotype, and prevented pathological aortic remodeling.

Conclusions: These findings identify JMJD3 as a critical regulator macrophage-mediated inflammation in AAAs and identify a mechanistic target for the management of AAA development.

Conner C. Earl^{1,2}, Karthik Annamalai¹, Sydney Q. Clark^{1,2}, Luke E. Schepers¹, Arvin H. Soepriatna^{1,3}, Craig J. Goergen^{1,2}

¹Weldon School of Biomedical Engineering, Purdue University West Lafayette, IN

²Indiana University School of Medicine, Indianapolis, IN

³Center for Biomedical Engineering, Brown University, Providence, RI

Strain Estimates of Murine Myocardial Infarction Size from Four-Dimensional High-Frequency Ultrasound

Graduate Student

Introduction: Coronary heart disease is the number one cause of mortality worldwide, contributing to nearly 15% of all deaths [1]. While two-dimensional ultrasound is often used to evaluate left ventricular function and monitor disease progression, it is insufficient to completely characterize the complex myocardial biomechanics involved in pathologic remodeling leading to heart failure, a common sequela of coronary ischemic injury. Here we present a method for quantifying myocardial mechanics using four-dimensional (4D or 3D plus time) ultrasound imaging in a mouse model of myocardial infarction. The objective of this study is to correlate 3D regional strain metrics derived from 4D ultrasound with left ventricular function in order to estimate infarct size and better characterize post-infarction heart remodeling.

Materials and Methods: We performed left coronary artery ligation surgeries on 5 male, wild-type, C57BL/6J mice (age 14±1 weeks; weight= 27±3 g). We acquired sequential high-frequency 4D ultrasound image data (Vevo2100, FUJIFILM VisualSonics Inc.) prior to surgery and at days 1, 3, 7, 14, 21, and 28 post-ligation, after which, each animal was euthanized and the infarct size was determined via histology [2]. 4D ultrasound images were analyzed using a custom-built graphical user interface in MATLAB (MathWorks, Natick, MA) to identify regions of surface area strain from the 3D segmentation of endocardium below 20%. The estimated size of the infarcted regions from areas of low strain was then correlated with infarct size obtained from histological analysis.

Results and Discussion: Left ventricular ejection fraction (LVEF) dropped from 74.3± 3.7% (mean±SD) at baseline to 42.9±9.6% at day 7 and 36.3±8.8% at day 28 post-infarction. We found that regions with surface area strain value greater than -20% correlated well with infarct size as measured by histology ($R^2=0.92$, $p<0.01$, Figure 1).

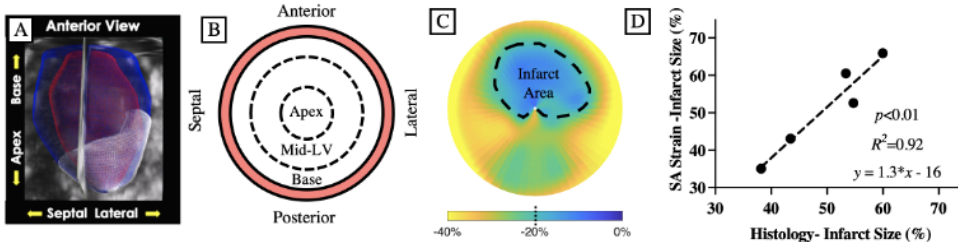


Figure 1: A) Representative 4D ultrasound heart segmentation with epicardial (blue), endocardial (red), and infarct (white) outlined. B) Polar heart map schematic C) Surface area strain plot with estimated infarct area as strain below 20% (dotted line). D) Surface area strain infarct size correlation with histology,

Conclusions: 4D ultrasound allows for robust analysis of murine left ventricular function and may provide a rapid and accurate method to assess the size of myocardial infarction.

***** Selected Abstracts Presentations*****

Maura Mobilia¹ • Callie Whitus¹ • Alexander Karakashian¹ • Hong Lu, MD, PhD² • Alan Daugherty, PhD, D.Sc² • Scott Gordon, PhD²

Saha Cardiovascular Research Center University of Kentucky¹ • Saha Cardiovascular Research Center, Physiology University of Kentucky²

Dennd5b knockout mice are resistant to hepatic steatosis and PCSK9-induced hypercholesterolemia

Staff

Background: Dietary lipid absorption by enterocytes and hepatic lipid metabolism are critical for maintenance of systemic lipid homeostasis. Regulation of lipid processing in both organs can influence plasma lipids and cardiometabolic disease (e.g. obesity and atherosclerosis). We previously demonstrated that the gene *Dennd5b* plays a key role in intestinal lipid absorption. *Dennd5b*^{-/-} mice have impaired lipid absorption and are resistant to diet-induced hypercholesterolemia, atherosclerosis, and obesity. Furthermore, we found that a common human *DENND5B* gene variant is associated with BMI. **Approach:** The goal of the current study was to examine the effect of *Dennd5b* on atherosclerosis in the context of hypercholesterolemia. Because *Dennd5b*^{-/-} mice are resistant to diet-induced hypercholesterolemia, we used adeno-associated viral (AAV) transfection to induce overexpression of the PCSK9 gain-of-function mutation (PCSK9D377Y) in wildtype and knockout mice then kept the mice on western diet for 3 months. During the study, body weight, and plasma lipids were monitored. After 3 months, aortic atherosclerosis and hepatic lipid content were evaluated. **Results:** Wildtype mice experienced significant PCSK9-induced weight gain and increases in plasma cholesterol and triglyceride, however, *Dennd5b*^{-/-} mice are resistant to PCSK9-induced weight gain and hyperlipidemia. Atherosclerosis development, evaluated by *en face* and aortic root sections, was significantly lower in *Dennd5b*^{-/-} compared to wildtype mice. We found that *Dennd5b*^{-/-} mice were also resistant to hepatic lipid accumulation with significantly lower triglyceride levels, but similar total cholesterol content compared to wildtype. To gain insight into the basis for reduced hepatic triglycerides, we performed quantitative PCR to measure expression of genes involved in hepatic lipid metabolism. Key genes involved in hepatic lipid metabolism and lipid storage were differentially expressed in *Dennd5b*^{-/-} including the lipid regulating nuclear receptor *Pparg* and the lipid droplet associated protein *Pnpla3*. Furthermore, hepatic VLDL secretion was increased in *Dennd5b*^{-/-} mice.

Conclusions: These findings suggest a role for *Dennd5b* in regulation of plasma and hepatic lipid levels. Loss of *Dennd5b* appears to be protective against atherosclerosis and fatty liver by altered hepatic lipid metabolism and increased export of hepatic lipids by VLDL secretion. Because *Dennd5b* is highly expressed in intestine and liver, it is unclear if these observations are due to intestinal or hepatic *Dennd5b* activity, or both. We are currently generating tissue-specific knockout mice to examine the function of this protein in these two organs.

Andrew Lutkewitte¹, Brian Finck¹

Washington University in St. Louis

Loss of Lipin 1 in Adipocytes Leads to Hepatic Steatosis, Signatures of Liver Injury, And Insulin Resistance in Mice.

Postdoc

The proper function of adipocytes is vital for preserving systemic metabolic health and excess, insufficient, or dysfunctional adipose tissue drives the development of a number of metabolic diseases including non-alcoholic fatty liver disease, insulin resistance, and type 2 diabetes. There are two major functions of adipose tissue that impact systemic metabolism. The first is to store and, when needed, appropriately release fatty acids. The second is to secrete peptide mediators called adipokines. When these functions are dysregulated, systemic metabolic disease can develop. Adipose tissue stores fatty acids primarily as triglycerides that are generated by the sequential acylation of glycerol-3-phosphate. The penultimate step in this pathway is the dephosphorylation of phosphatidic acid into diacylglycerol by the phosphohydrolase activity of lipin 1, which is encoded by the LPIN1 gene. Importantly, we found that LPIN1 expression is decreased in abdominal fat of patients with obesity and metabolic abnormalities compared to obese metabolically-normal patients and LPIN1 positively correlates to insulin sensitivity in these patients. To further evaluate the role of adipocyte lipin 1 in regulating systemic insulin sensitivity and metabolism, we developed adipocyte-specific lipin 1 knockout (Adn-lipin 1-KO) mice and characterized their phenotype using gold standard measures of insulin sensitivity and a multiomic approach. Loss of adipocyte lipin 1 led to reduced adipose tissue mass across all depots in mice fed a high-fat diet. Lipidomic analyses revealed accumulation of diacylglycerol and triglyceride in both liver and muscle of Adn-lipin 1-KO mice compared to control mice. Increased hepatic lipid accumulation was associated with severe hepatic, skeletal muscle, and adipose tissue insulin resistance compared to littermate controls as determined by hyperinsulinemic-euglycemic clamps. RNA sequencing of liver RNA demonstrated that several genes/gene networks related to insulin resistance and the transition from simple steatosis to nonalcoholic steatohepatitis, including fibrogenic and inflammatory markers, were activated in the knockout mice compared to WT littermates. Lastly, we combined lipidomic and metabolic data with differential expression data from hepatic RNA sequencing using weighted gene co-expression analysis, which revealed that hepatic insulin resistance and steatosis in were strongly linked with signatures of altered lipid synthesis and reduced adiponectin signaling. Indeed, plasma adiponectin concentrations were markedly lower in Adn-lipin 1-KO mice. Finally, transplantation of a small amount of subcutaneous fat from WT donor mice corrected the insulin resistant and fatty liver phenotypes of Adn-lipin 1-KO mice. Together, these data suggest that loss of adipocyte lipin 1 leads to a lean phenotype that is marked by insulin resistance and steatosis potentially driven by reductions in insulin sensitizing adipokines, such as adiponectin.

****Selected Abstracts Presentation****

Brandee Goo, MS¹ • Samah Ahmadih, MD¹ • Abdalrahman Zarzour, MD¹ • Jacob Greenway¹ • David Kim¹ • Mourad Oghi¹ • Yun Lei, PhD² • Xin-Yun Lu, PhD² • Ha Won Kim, PhD¹ • Neal Weintraub, MD¹
Vascular Biology Center Augusta University¹ • Neuroscience and Regenerative Medicine Augusta University²

Role of Histone Deacetylase 9 in the Development of Adipose Tissue Senescence and Mitochondrial Dysfunction

Graduate Student

Background: Senescence is a state in which cells stop replicating that occurs in adipose tissue in the context of aging and obesity. It has recently been shown that elimination of senescent cells can extend health and lifespan in mice. Our previous studies showed that global histone deacetylase 9 (HDAC9) gene deletion protected mice against obesity-associated metabolic disorder. Here, we hypothesized that HDAC9 expression during aging plays an important role in the development of adipose tissue senescence.

Methods and Results: Visceral adipose tissue from 20-month-old wild type (WT) mice showed increased expression of HDAC9 (2 fold) and senescence markers, p16 (5 fold) and p21 (2 fold) compared to 3-month-old mice, as examined by qRT-PCR. Furthermore, HDAC9 expression in human subcutaneous adipose tissue positively correlated with age ($r^2=0.088$, $p=0.034$). Therefore, to determine if HDAC9 knockout (KO) would protect mice against adipose tissue aging, we aged WT and KO mice to 1-year-old. KO mice were protected against the development of age-associated weight gain. Furthermore, body composition analysis attributed the difference in body mass to adiposity, as KO mice had reduced fat mass percentage compared to WT mice (12% vs 20%, $p=0.048$) and no difference in lean mass percentage. Intriguingly, adipose tissues from KO mice exhibited reduced levels of senescence-associated beta-galactosidase (SABG) staining and lower expression of p16 and p21 (0.7 fold and 0.5 fold, respectively). Preadipocytes reside in adipose tissue and replenish aged or dying adipocytes, thus they play an important role in regulating adipose tissue health and senescence. Interestingly, reduced SABG staining was also observed in early passage primary preadipocyte culture derived from HDAC9 KO adipose tissue as compared to WT (17% vs 30% SABG+). Next, we measured adipose tissue mitochondrial function which is mechanistically linked to cellular senescence. Interestingly, HDAC9 gene deletion significantly increased adipose tissue mitochondrial oxygen consumption rate (e.g. increased basal respiration, proton leak and ATP production), as measured by the Seahorse Analyzer. Mitochondria are dynamically regulated by fusion and fission. Following C6 ceramide stress, fission marker DRP1 expression was increased in WT but not KO adipocytes *in vitro*, suggesting a role of HDAC9 in adipocyte response to ceramide.

Conclusion: HDAC9 plays a crucial role in the development of adipose tissue senescence, possibly through regulating mitochondrial function and dynamics. Thus, HDAC9 may be a promising target to combat the development of a senescent phenotype and to maintain healthy adipose tissue.

Support or Funding Information: This work was supported by grants HL124097, HL126949, HL134354, AR070029 and AG064895 (N.L.W) from the National Institutes of Health.

Kathryn Gunn, PhD¹ • Aspen Gutzsell, PhD¹ • Yongmei Xu, PhD² • Jian Liu, PhD² • Saskia Neher, PhD¹

Biochemistry and Biophysics University of North Carolina, Chapel Hill¹ • Chemical Biology and Medicinal Chemistry, Eshelman School of Pharmacy University of North Carolina, Chapel Hill²

Angiotensin-Like Proteins 3 And 4 Both Form Homotrimers That Non-Competitively Inhibit Lipoprotein Lipase

Postdoc

Elevated plasma triglycerides are a risk factor for coronary artery disease (CAD). Lipoprotein lipase (LPL) reduces triglycerides by hydrolyzing them from triglyceride-rich lipoproteins (TRLs) to release free-fatty acids, which is essential for maintaining healthy plasma triglyceride levels in the blood. LPL activity is regulated in a nutritionally responsive manner by macromolecular inhibitors including angiotensin-like proteins 3 and 4 (ANGPTL3 and ANGPTL4). However, the mechanisms by which ANGPTL3 and ANGPTL4 inhibit LPL have been unclear, in part due to challenges in obtaining pure ANGPTL3 for study and conflicting evidence for the ANGPTL4 inhibition mechanism. We found that ANGPTL3 forms elongated, flexible trimers and hexamers when produced in *E. coli*, whereas ANGPTL4 formed only elongated flexible trimers. To clarify the physiologically relevant oligomer of ANGPTL3, we expressed ANGPTL3 in HEK293 cells and found it only formed trimers. We compared the inhibition of ANGPTL3 and ANGPTL4 homotrimers using human very-low-density lipoproteins (VLDL) as a substrate and found both were non-competitive inhibitors with only 2-fold difference in inhibition constant. Heparin has previously been reported to interfere with ANGPTL3 binding to LPL and we found that ANGPTL3 inhibition is abolished by binding to low molecular weight heparin, whereas ANGPTL4 inhibition is not. This effect is caused by heparin binding to ANGPTL3, rather than binding to LPL as had been previously hypothesized. Our data show new similarities and differences in how ANGPTL3 and ANGPTL4 regulate LPL and opens new avenues of investigating the effect of heparin on LPL inhibition by ANGPTL3.

Shayan Mohammadmoradi^{1,2}, Hisashi Sawada^{1,3}, Sohei Ito¹, Dien Ye¹, Adam E. Mullick⁴, Deborah A. Howatt¹, Michael K. Franklin¹, Hong S. Lu^{1,2,3}, Alan Daugherty^{1,2,3}

¹Saha Cardiovascular Research Center, University of Kentucky

²Department of Pharmacology and Nutritional Sciences, University of Kentucky

³Department of Physiology, University of Kentucky

⁴Ionis Pharmaceuticals, Inc

Sustained Inhibition of High Mobility Group Box 1 mRNA by Antisense Oligonucleotides Demonstrated a Protracted Half-life of the Protein

Graduate Student

Background and Objectives: High-mobility group box 1 (HMGB1) is a highly conserved nonhistone DNA-binding nuclear protein that is present in almost all eukaryotic cells. HMGB1 is proposed to exert effects on several forms of vascular disease including atherosclerosis, pulmonary hypertension, and abdominal aortic aneurysm. However, the lack of a viable whole-body genetic deletion has increased interest in pharmacological approaches to sufficiently inhibit HMGB1 to investigate its role in pathological conditions. In the current study, we assessed the efficacy of a novel antisense oligonucleotides (ASOs) approach to deplete HMGB1 in mice.

Methods and Results:

Either ASOs (25 mg/kg/day) or phosphate-buffered saline (PBS) were injected intraperitoneally into male C57BL/6J mice (8-10-week-old). ASOs were injected at day 0 and day 3 in the initial week and once a week for the duration of the study. Mice were terminated at either 2, 4, or 12 weeks after the initial injection of ASOs (N = 5/group). Since HMGB1 is highly abundant in the kidney and liver, mRNA and protein abundance of HMGB1 were examined subsequently in these organs by qPCR and Western blot analyses.

ASO administration resulted in a 90% decrease of *Hmgb1* mRNA abundance in the kidney and liver by 2 weeks of ASO injection. The decreased *Hmgb1* mRNA abundance was observed consistently at both week 4 and 12. Surprisingly, ASOs failed to deplete HMGB1 protein abundance in the kidney and liver at 2- and 4-week time intervals. However, HMGB1 protein abundance was markedly reduced to less than 20% in kidney and liver tissues at week 12, indicating an extended protein half-life.

Conclusion: These findings reveal the protracted interval need to deplete HMGB1 protein depletion after mRNA inhibition.

Sohei Ito, Satoko Ohno-Urabe, Michael K. Franklin, Jessica J Moorleghen, Deborah A. Howatt, Hisashi Sawada, Hong S. Lu, Alan Daugherty

Saha Cardiovascular Research Center University of Kentucky ¹ • Department of Physiology University of Kentucky ²

Inducible Deletion of Fibrillin-1 in Smooth Muscle Cells Has Modest Effects on Thoracic Aortic Dilatation in Adult Mice

Postdoc

Introduction:

Fibrillin-1 (*Fbn1*) mutations are associated with thoracic aortic aneurysms (TAAs) in patients with Marfan syndrome. Constitutive deletion of *Fbn1* leads to neonatal death due to aortic rupture in mice. However, the role of *Fbn1* in maintaining aortic integrity during the adult phase remains unclear. Since smooth muscle cell (SMC) is a major constituent of the aortic media, this study examined whether deletion of *Fbn1* in SMCs of adult mice leads to compromise of aortic integrity.

Methods and Results:

Fbn1 floxed mice were generated that included insertion of tdTomato as a reporter for gene deletion. Female *Fbn1* floxed mice were bred with male *Fbn1* floxed mice expressing CreER^{T2} driven by an *Acta2* promoter. Tamoxifen (75 mg/kg/day) was injected intraperitoneally for 5 days into male *Fbn1* floxed littermate mice that were either Cre negative or positive (n=6-8/genotype, 5-week-old) to create sm*Fbn1*^{+/+} and ^{-/-} mice, respectively. Gene recombination was confirmed by the presence of tdTomato in sm*Fbn1*^{-/-} mice using PCR and confocal microscopy. To investigate the impact of SMC-specific *Fbn1* deletion, male sm*Fbn1*^{+/+} and ^{-/-} littermates terminated at two intervals, 5 and 36 weeks after completion of tamoxifen injections. In situ aortic images were captured, and aortic diameters were subsequently measured at three regions, ascending, arch, and descending thoracic aortas. Five weeks after tamoxifen injection, aortic diameters of sm*Fbn1*^{+/+} and ^{-/-} mice were not different. Despite the long-term deletion of *Fbn1* in SMCs, aortic dilatation was not observed in any regions of aortas in sm*Fbn1*^{-/-} mice compared to wild type littermates 36 weeks after tamoxifen injection. Next, we investigated whether *Fbn1* deletion in SMCs augmented angiotensin II (AngII)-induced thoracic aortic dilatation. AngII was infused subcutaneously into male sm*Fbn1*^{+/+} and ^{-/-} littermates for 12 weeks (n=11-12/genotype), started 2 weeks after completion of tamoxifen injections. AngII-induced aortic dilatations were augmented modestly by SMC-specific *Fbn1* deletion (^{+/+} 1.7±0.0, ^{-/-} 1.9±0.1 mm, P=0.047).

Conclusion:

Deletion of *Fbn1* in SMCs did not cause spontaneous TAA formation and had modest effects on AngII-induced TAAs in adult mice. *Fbn1* in SMCs does not exert a critical role in mice after the aortic structure has formed.

Kori Williams,¹ • Isha Chauhan² • Gregory Graf, PhD¹

Pharmaceutical Sciences University of Kentucky College of Pharmacy¹ • College of Arts and Sciences University of Kentucky²

Characterization of Sitosterolemia-Associated ABCG8 Mutants

Graduate Student

Sitosterolemia is a rare, autosomal recessive form of familial hypercholesterolemia (FH) caused by mutations in either ABCG5 or ABCG8 that is distinguished from other forms of FH by the accumulation of phytosterols in plasma. ABCG5 and ABCG8 form a heterodimer that is located at the apical surface of hepatocytes and enterocytes and promotes the secretion of cholesterol and phytosterols. Over 20 missense mutations in ABCG8 have been identified in patients with clinically confirmed Sitosterolemia. We established a classification system for mutants of ABCG8 based on the underlying molecular mechanism for ABCG5 ABCG8 dysfunction (maturation, trafficking, activity, etc.) Small molecule modulators of ABC transporters known as “correctors” and “potentiators” can rescue mutants of ABCB4 (PFIC3) and ABCC7 (CF) with impaired folding, stability, or activity. We have generated the missense mutants of ABCG8 within the cytosolic domain that are associated with Sitosterolemia and determined their impact on ABCG5 ABCG8 maturation and stability in cultured cells. The effects of potentiators, correctors, and regulators of proteostasis on the rescue ABCG8 mutants in vitro and in vivo are ongoing.

Yingdong Zhu
Northeast Ohio Medical University

Hepatic Mir-34a Regulates the Development of Non-Alcoholic Fatty Liver Disease

Graduate Student

Hepatic miR-34a expression is elevated in diet-induced or genetically obese mice and patients with non-alcoholic steatohepatitis (NASH), yet hepatocyte miR-34a's role in the progression of non-alcoholic fatty liver disease (NAFLD) from non-alcoholic fatty liver (NAFL) to NASH remains to be elucidated. Mice overexpressing or deficient in hepatocyte miR-34a and control mice were fed a diet enriched in fats, cholesterol, and fructose (HFCF) to induce NASH. C57BL/6 mice with NASH were treated with an miR-34a inhibitor or a scramble control oligo. The effect of miR-34a on the development, progression, and reversal of NAFLD was determined. The hepatocyte-specific expression of miR-34a aggravated HFCF diet-induced NAFLD. In contrast, germline or adult-onset deletion of hepatocyte miR-34a attenuated the development and progression of NAFLD. In addition, pharmacological inhibition of miR-34a reversed HFCF diet-induced steatohepatitis. Mechanistically, hepatocyte miR-34a regulated the development and progression of NAFLD by inducing lipid absorption, lipogenesis, inflammation, and apoptosis but inhibiting fatty acid oxidation. Hepatocyte miR-34a is an important regulator in the development and progression of NAFLD. MiR-34a may be a useful target for treating NAFLD.

Lei Cai, Peter I. Hecker, Tong Li, Joseph D. Layne, Zhen Wang, Sierra M. Paxton, Courtney R. Burkett, Margery A. Connelly[@], Ryan E. Temel

Nurtion and Pharmacology University of Kentucky ¹ • Physiology University of Kentucky ² • Physiology University of Kentucky ³ • Research and Development Labcorp (Liposcience) ⁴

Microrna-33a/B Antagonism Does Not Impact Atherosclerosis Regression And Stabilization In A Nonhuman Primate Model

Staff

The two members of the microRNA-33 (miR-33) family miR-33a and miR-33b coordinately regulate lipid metabolism. Antagonism of miR-33 in mice reduced atherosclerosis by stimulating reverse cholesterol transport and dampening plaque inflammation. However, these studies were of limited translational value since mice express only miR-33a. We and others published that miR-33 antagonism in nonhuman primates (NHPs), which like humans express both miR-33a and miR-33b, resulted in a favorable plasma lipid profile including increased HDL cholesterol (HDL). Based upon these results, we hypothesized that antagonizing miR-33a/b would regress or stabilize atherosclerotic lesions in NHPs. Male cynomolgus monkeys were fed an atherogenic diet and after 20 months a subset (progression; n=12) was euthanized to characterize atherosclerosis development. The remaining animals were switched to a standard NHP "chow" diet and treated for 6 months with saline (vehicle; n=12) or the miR-33a/b antagonist RG428651 (anti-miR-33; n=12). Due to chow being a hypocholesterolemic diet, both the vehicle and anti-miR-33 groups displayed rapid, sustained, and similar decreases in cholesterol and particle concentrations of VLDL and LDL. Treatment with anti-miR-33a/b significantly increased HDL and large HDL particle (HDL_L) concentrations and decreased medium HDL_L concentration. The alteration of HDL levels was accompanied by a significant elevation in the hepatic protein level of ABCA1, an essential factor in nascent HDL production and a miR-33 target. Cholesterol efflux from J774 macrophages was significantly greater with serum HDL from NHPs treated with anti-miR-33 compared to vehicle. However, coronary arteries from animals treated with anti-miR-33 or vehicle had atherosclerotic lesions with similar size and composition (CD68+ macrophage foam cells, α -actin+ smooth muscle cells or collagen). The two regression groups also had similar levels of cholesteryl ester, a marker of foam cell content, in the thoracic and abdominal aorta and carotid and iliac arteries. The iliac arteries from NHPs treated with anti-miR-33 or vehicle showed similar expression of genes associated with inflammation, lipid metabolism, cell death and proliferation. In conclusion, our results indicate that in spite of seemingly beneficial changes in circulating HDL levels and HDL efflux capacity, miR-33a/b antagonism for 6 months did not stimulate plaque regression or stabilization. This work was supported by NIH grants R01 HL111932 and P20 GM103527.

Lauren M Weaver ¹ • Madeline J Stewart ¹ • Shuo Zhou, PhD ¹ • Charles D Loftin, PhD ¹ • Fang Zheng, PhD ¹ • Chang-Guo Zhan, PhD ¹

Pharmaceutical Sciences University of Kentucky College of Pharmacy

An mPGES-1 Inhibitor Alters the Growth of Abdominal Aortic Aneurysms in Mice

Graduate Student

Abdominal aortic aneurysm (AAA) is a deadly, permanent balloon of the aortic artery. Surgery is the only option available to patients, but it is risky. In addition, there are currently no FDA-approved pharmacological treatments for AAA available. Notably, microsomal prostaglandin E2 synthase-1 (mPGES-1) is recognized as a promising target for development of a next generation of anti-inflammatory drugs. Through computational modeling and *in vitro* experiments, we have recently discovered a novel type of mPGES-1 inhibitors as possible anti-inflammatory drug candidates. The purpose of this study was to assess the capability of an mPGES-1 inhibitor to alter the growth of AAA in the angiotensin (Ang)-II induced mouse model.

For 28 days, male *ApoE*^{-/-} were infused with Ang-II (1,000 ng/kg/min) plus either drug (500 mg/ml) starting day 0 (pretreatment group, *N* = 5), drug (500 mg/ml) starting day 5 (intervention group, *N* = 5) or no drug (control group, *N* = 5). On day 5, ten mice were divided into the intervention and control groups, with equal aortic diameters. Maximal aortic diameter was measured by ultrasound on day 0 (baseline), 2, 5, 7, 12, 16, 21, and by *ex vivo* on 28. Blood PGE₂ concentrations were determined on day 0 and day 28.

On day 28, there was no difference between the maximal aortic diameters of the pretreatment and intervention groups (1.1±0.00 mm, 1.0±0.00 mm) and a significant difference between both groups and the control group (2.09±0.58 mm). The maximal aortic diameter of the pretreatment group was not different between day 0 and day 28 (0.99±0.05 mm, 1.10±0.00 mm). PGE₂ levels decreased in the pretreatment and intervention groups from day 0 to day 28 (4.5 to 2.9 ng/ml and 9.5 to 6.0 ng/ml, respectively) and increased in the control group (5.3 to 12.1 ng/ml).

In summary, this mPGES-1 inhibitor was able to both prevent the formation and reverse the progression of AAA in these mice. This change in maximal aortic diameter was significantly correlated with the change in the PGE₂ levels. These preliminary results show promise for the use of an mPGES-1 inhibitor in the treatment of AAA.

Fathima Nafrisha Cassim Bawa (1), Yanyong Xu (2), Raja Gopaju (2), Yingdong Zhu (1), Shaoru Chen (2), Kavitha Jadhav (1), Yanqiao Zhang (2)

(1) School of Biomedical Sciences, Kent State University, Kent, Ohio

(2) Department of Integrative Medical Sciences, College of Medicine, Northeast Ohio Medical University, Rootstown, Ohio

Retinoic Acid Receptor Alpha Protects Against Diet Induced Hepatic Steatosis Via Retinoid Signaling

Graduate Student

Nonalcoholic Fatty Liver Disease (NAFLD) is often characterized by accumulation of lipid in the liver. It presents a pathological spectrum of changes from simple steatosis to liver fibrosis. Since liver is the main organ involved in retinoid signaling, the impairment of this pathway is known to be associated with the progression of NAFLD. Many studies have shown that retinoic acid treatment can ameliorate insulin resistance and obesity. We hypothesize that Retinoic acid receptor Alpha (Rar α) in hepatocytes play a significant role in mediating retinoid signaling to protect against NAFLD and obesity. To further investigate the role of hepatic Rar α , we conducted in vivo studies using liver specific Rar α knockout mice. Rar α floxed mice were injected with AAV8-TBG-Cre or AAV8-TBG-Null to generate liver-specific Rar α knockout mice (L-Rar $\alpha^{-/-}$) and the control mice (Rar $\alpha^{fl/fl}$). These mice were gavaged with either vehicle or all-trans retinoic acid (AtRA; 15mg/kg/day) along with high fat/high cholesterol/high fructose (HFCF) diet for 16 weeks. The data showed that AtRA treatment can reduce body fat content and increase energy expenditure in the control mice but not in L-Rar $\alpha^{-/-}$. Hepatic lipid analysis has shown that AtRA can reduce hepatic triglyceride levels in control mice in greater extent compared to L-Rar $\alpha^{-/-}$. Furthermore, hematoxylin and eosin (H and E) and Oil Red O staining of liver sections from L-Rar $\alpha^{-/-}$ mice displayed higher lipid droplet deposition compared to the control mice even with AtRA treatment. The RNA Seq analysis showed upregulation of genes related to lipid accumulation. The qPCR analysis confirmed the significant increase in lipid uptake gene Cd36, triglyceride synthesis genes like Vlcad and Mcad and lipid droplet forming genes like Cidea and Cldec in L-Rar $\alpha^{-/-}$ compared to the control in AtRA treated groups. Similar observations were collected in a different study where control mice and L-Rar $\alpha^{-/-}$ mice were fed an HFCF diet for 20 weeks, followed by 10 weeks of treatment with either vehicle or AtRA. Both our prevention and intervention study has shown that knocking down Rar α in hepatocytes can increase steatosis and obesity. Our data demonstrate that the retinoid signaling protects against the development of hepatosteatosis and obesity in a Rar α -dependent manner.

Rupinder Kaur¹, Auriona Hodges¹, Garrett Anspach¹, Gregory Graf¹.

¹Department of Pharmaceutical Sciences, College of Pharmacy

Alterations in lipoprotein profile do not alter routes of cholesterol elimination

Graduate Student

Reverse cholesterol transport (RCT) is the active process of mobilizing peripheral cholesterol for excretion through the hepatobiliary (transhepatic cholesterol elimination, THCE) or intestinal (transintestinal cholesterol elimination, TICE) pathways. TICE relies on the plasma compartment for delivery of cholesterol, presumably through lipoprotein carriers. However, the exact source of this cholesterol is controversial. We previously showed that expression of Cholesterol Ester Transferase Protein (CETP) in mice results in increased Low-Density Lipoprotein (LDL) levels and promotes cholesterol elimination through THCE and away from TICE. Furthermore, the ApoB100 transgenic mouse displays reduced cholesterol clearance compared with ApoB48, and when crossed with a CETP transgenic, exhibits a humanized lipoprotein profile on Western Diet. Using a previously published surgical procedure to measure simultaneous biliary and intestinal cholesterol secretion, we investigate how changes in the lipoprotein profile affect routes of cholesterol elimination. C57BL/6 mice expressing *ApoB100*, *CETP*, or both transgenes were maintained on Standard Rodent Chow and placed on Western Diet at 8 weeks of age for 4 weeks. Pre/post-diet MRI, plasma, and 72-hour fecal collection were obtained. After 4 weeks, mice underwent a 30 min bile collection and dissection - consisting of liver, 5 segments of the intestine, and euthanasia via cardiac puncture - or simultaneous TICE and THCE surgery. In both females and males, CETP/ApoB100 and ApoB100 transgenic mice showed a robust increase in the LDL fraction and increased concentration of total plasma cholesterol. This alteration did not lead to any significant differences in body weight, adiposity, total fecal cholesterol secretion, or total biliary cholesterol secretion and composition. Gender differences were observed when examining routes of cholesterol elimination, yet significant differences across the four genotypes were not detected. Based on the present data, we conclude that alterations in lipoprotein profile do not alter routes of cholesterol elimination. Remarkably, differences in hepatic cholesterol accumulation were observed, with ApoB100 and CETP/ApoB100 mice displaying the highest prevalence and severity of hepatic steatosis. Ongoing studies investigate the CETP/ApoB100 transgenic mouse as a viable model for Non-Alcoholic Fatty Liver Disease.

Ching L. Liang, Masayoshi Kukida¹ • Dien Ye¹ • Deborah Howatt¹ • Yuriko Katsumata² • Hisashi Sawada³ • Jessica Moorleggen¹ • Alan Daugherty³ • Hong Lu³

Saha Cardiovascular Research Center University of Kentucky¹ • Department of Biostatistics; Sanders-Brown Center on Aging University of Kentucky² • Saha Cardiovascular Research Center; Saha Aortic Center; Department of Physiology University of Kentucky³

Angiotensin II Type 1a Receptor Deletion in Renal Proximal Tubular Cells Does Not Attenuate Atherosclerosis in Hypercholesterolemic Mice

Staff

Objective: AngII (Angiotensin II) acts through AT1aR (AngII type 1a receptor) to promote atherosclerosis. Despite the consistency that genetic deletion of AT1aR markedly attenuates atherosclerosis, it remains undefined in which cell types that AT1aR contributes to atherosclerosis formation. Since renal AngII is associated with increased atherosclerosis in hypercholesterolemic mice, and AT1aR is abundant on PTCs (proximal tubular cells), the present study investigated the effects of AT1aR deletion in PTCs on atherosclerosis in hypercholesterolemic mice. **Approach and Results:** First, both male and female LDL receptor $-/-$ mice were fed a Western diet and infused with either vehicle or losartan for 12 weeks. Losartan led to more profound increases of plasma renin concentrations and greater reduction of systolic blood pressure in female than in male mice, whereas atherosclerosis was attenuated by losartan equivalently in both sexes. Secondary, we determined whether the effects of losartan were attributed to inhibition of AT1aR on PTCs. To generate PTC-specific AT1aR $-/-$ mice, AT1aR floxed mice were bred with mice expressing Cre under the control of the N-myc downstream regulated gene 1. These mice were injected with 150 mg/kg/day of tamoxifen for 5 days to activate Cre at the age of 4 - 6 weeks. RNAscope detected AT1aR mRNA in both PTCs and glomeruli; mRNA of AT1aR was absent in PTCs, but not glomeruli, of PTC-specific AT1aR $-/-$ mice. Two weeks after completion of tamoxifen injection, these mice in LDL receptor $-/-$ background were fed Western diet for 12 weeks. Deletion of AT1aR in PTCs did not affect plasma renin concentrations, blood pressure and atherosclerosis in either sex. Finally, to investigate the impacts of PCT-specific AT1aR deletion under the conditions with enhanced AngII stimulation, AngII was infused subcutaneously for 12 weeks. There were no differences in both blood pressure and atherosclerosis between genotypes. **Conclusion:** Although pharmacological inhibition of AT1aR reduced atherosclerosis profoundly in both sexes, PTC-specific AT1aR deletion did not affect atherosclerosis in hypercholesterolemic mice. Our future study will determine whether the presence of AT1aR in both PTCs and glomeruli are needed to promote atherosclerosis.

Mark Castleberry, PhD¹ • Chase Raby, MS¹ • Ryan Allen, PhD¹ • MacRae Linton, MD¹ • Kasey Vickers, PhD¹
Medicine Vanderbilt University Medical Center¹

Macrophages Store LDL-Delivered Microbial Small RNAs in Lipid Droplets.

Postdoc

Low-density lipoproteins (LDL) are causal factors in atherosclerosis. Inflammation is a driving force for both atherogenesis and advanced lesion progression. LDL stimulates inflammation in the lesion; however, the mechanism by which LDL activates macrophages and promotes atherosclerosis inflammation remains to be fully defined. Recently, we reported that LDL is enriched with microbial small RNAs (msRNA) derived from bacteria in the microbiome and environment. Most importantly, we showed that LDL-delivered msRNA activated toll-like receptor 8 (TLR8) in recipient macrophages and inhibition of this pathway reduced atherosclerosis. Nevertheless, the processes by which macrophages store and catabolize exogenous LDL-delivered msRNA are unknown. We ***hypothesize that LDL-delivered msRNA is stored in lipid droplets of macrophages***. LDL was found to transport approximately 37µg of total RNA per mg of protein, and macrophages were found to take up LDL-msRNAs through an LDL receptor-independent process (pinocytosis). Confocal microscopy and RNA quantification of purified organelles indicate that macrophage lipid droplets (LD) contain RNA and that LDL treatment increases LD-associated RNA. Macrophages transfected with msRNA fluorescence-labeled (msRNA-Cy5) contain signal in both the organic and aqueous phases after Bligh-Dyer lipid extraction, indicating a potential acyl esterification of the msRNA. To evaluate LDL-msRNA delivery to macrophages *in vitro*, cells were treated with reconstituted LDL (rLDL) loaded with msRNA-Cy5. Utilizing confocal microscopy, rLDL was found to deliver msRNA-Cy5 to macrophages. Ongoing research aims to determine the subcellular processing of LDL-delivered msRNA in macrophages; however, results from microscopy studies support that the endo-lysosome and LD compartments are involved. Moreover, rLDL provides a powerful tool for the study of LDL-msRNA delivery to macrophages by reducing the heterogeneity of lipid cargo that may confound analyses, while enabling the enrichment of specified RNA cargo for cellular delivery. These results support that i) LDL can transfer pro-inflammatory msRNA to macrophages, ii) LDL treatment increases LD-associated RNA, and iii) RNA can be isolated by organic lipid extraction.

Uriel L. Jean-Baptiste (1)(2), Ming Jing Wu(1), Saskia B. Neher (1)

(1)Department of Biochemistry and Biophysics, University of North Carolina at Chapel Hill

(2)UNC McAllister Heart Institute Integrative Vascular Biology (IVB) Trainee

Unravelling the mysteries of Endothelial Lipase (EL) and it's inhibition by ANGPTL3

Graduate Student

Heart disease encompasses several conditions that, collectively, are the cause of 1 out of 4 deaths in America each year, according to the CDC. These conditions are complex diseases that require the collaborative energy of scientists from multiple fields to be effectively understood and remedied. Through our work with lipoprotein lipase (LPL), the Neher lab has actively contributed to the ongoing effort to understand and combat these conditions. Of the commonly known lipases, LPL is the most famous member of the family. Its inhibition by the Angiopoietin-like family of proteins (ANGPTLs) has been well characterized by our lab.[1] [2] Furthermore, a beautiful cryo-EM reconstruction of a helical LPL oligomer has also been solved by our lab at 3.8-Å resolution.[3] It is fair to say that we are highly adept at working with lipases and their interacting partners. Using our previous work with LPL as a foundation, I will venture into the lesser-known endothelial lipase (EL) that is also important for heart disease. EL is an HDL-specific lipase that is implicated to reduce levels of plasma triglycerides (TGs), LDL-C, and HDL-C. This is important for familial hypercholesterolemia patients (FH) who experience excessively high levels of plasma LDL-C levels, however, EL has proven to be an enigmatic protein. For example, EL acts on HDL, the “good cholesterol”, and Loss of EL results in increased HDL, but population studies do not show a clear cardioprotective phenotype. Also, loss of ANGPTL3, an EL inhibitor, reduces HDL, yet that is shown to be cardioprotective. Using several biophysical techniques, such as cryo-EM and mass photometry, and an established kinetic assay in our lab that directly measures free fatty acids, we will unravel the inner-workings of EL and its interaction with ANGPTL3. Overall, the success of this work can vastly expand our knowledge of EL and its inhibition by ANGPTL3 and can greatly contribute to our effort to combat heart disease.

Alicia Traugher^{1,2}, Mariam Khan^{1,2}, and Kailash Gulshan^{*1,2}

¹Center for Gene Regulation in Health and Disease, College of Science and Health Professions, Cleveland State University, Cleveland, OH 44115, USA. ²Department of Biological, Geological and Environmental Sciences, Cleveland State University, Cleveland OH 44115, USA.

ROLE OF PIP2 and GASDERMIN D MEDIATED IL-1B RELEASE IN INFLAMMATION AND ATHEROSCLEROSIS.

Faculty

Introduction: The CANTOS trial showed that anti-IL-1 β therapy met the primary trial endpoint, *a reduction in a composite of heart attack, stroke, and cardiovascular death*. The N-terminal fragment of Gasdermin D (GsdmD) binds phosphatidylinositol 4, 5-bisphosphate (PIP2), resulting in pore formation on the cell membrane and release of mature IL-1 β . PIP2 also plays a role in GsdmD independent release of IL-1 β and in the generation of nascent HDL by ABCA1-apoA1 pathway.

Objectives: To determine the effect of PIP2 levels and localization in macrophages on ABCA1 mediated cholesterol efflux and GsdmD mediated IL-1 β release.

Methods and results: We investigated the correlation between cellular levels of PIP2 and ABCA1 expression/function. PIP2 levels were markedly higher in foam cells vs. control macrophages (~ 22 % increase, N=3, *P=0.05). Expression of TMEM55b, a PIP2 phosphatase, in BHK cells resulted in ~ 70 % decrease in ABCA1 mediated cholesterol efflux to apoA1 (N=4, P<0.0001) and greatly reduced levels of ABCA1. Chemical inhibition of PI5PK2 α , a PIP2 biosynthetic enzyme, in THP-1 cells showed a dose-dependent decrease in ABCA1 levels and cholesterol efflux to apoA1. The GsdmD^{-/-} mice were less prone to Nlrp3 inflammasome mediated defect in RCT. Using LDLr ASO-induced hyperlipidemia in mice, we found that GsdmD^{-/-} KO mice exhibit ~42% decreased atherosclerotic lesion area in females and ~33% decreased lesion area in males vs. WT mice. We tested the effect of Miltefosine, an FDA-approved drug that disrupts PIP2 plasma membrane localization and IL-1b release, on atherosclerosis in hyperlipidemic mice. The apoE^{-/-} KO mice fed with Miltefosine gained significantly less weight vs. control mice fed with WTD, and showed significantly decreased atherosclerotic lesions (\geq 50% smaller vs. controls; mean \pm SD, p<0.001 in females with N=10, and p<0.04 in males with N=12).

Conclusion: Cellular PIP2 levels and localization regulate RCT and inflammation by regulating ABCA1, GsdmD, and IL-1 β pathways.

Keiichi Asano¹, Anna Cantalupo¹, Jens Hansen,¹ Bart Spronck², Jay D. Humphrey², Ravi Iyengar¹ and Francesco Ramirez¹

¹Department of Pharmacological Sciences, Icahn School of Medicine at Mount Sinai, New York, NY; ²Department of Biomedical Engineering, Yale University, New Haven, CT

AT1R blockade together with AT2R stimulation prevents aortic aneurysm in mice with progressively severe Marfan syndrome

Faculty

Angiotensin II receptor signaling regulate vascular tone by stimulating either vasoconstriction (AT1R) or vasodilation (AT2R). AT1R antagonism (via losartan) has been shown to mitigate thoracic aortic aneurysm (TAA) progression in mouse models of Marfan syndrome (MFS). Here we monitored multiple pathological readouts of TAA in MFS mice chronically treated for 90 days with either losartan, the AT2R agonist C21, or both. While C21 had no apparent effects on arterial disease by itself, it significantly enhanced losartan's efficacy by preventing death of MFS mice from ruptured TAA during the treatment period. Specifically, the combination therapy normalized the diameters of the aortic root and ascending aorta, the architecture of the vessel wall, endothelial-dependent relaxation, and circumferential wall strength (a strong biomechanical indicator of aneurysmal vulnerability). Computational analyses of bulk RNASeq data predicted that the combination therapy largely decreased expression of abnormally upregulated genes, principally those associated with inflammatory pathways. By contrast, these *in silico* analyses predicted no modifications of signaling pathways associated with dysregulated mitochondrial energy metabolism. Ongoing investigations are using single cell RNASeq to identify the different cell types targeted by the two drugs used in combination therapy, as well as potential cell-cell interactions that underlie the efficacy of the combination therapy.

Jordan Reed ¹ **Johan Bjorkegren**²• **Mete Civelek, PhD** ³

Biomedical Engineering University of Virginia ¹ •Department of Genetics and Genomic Sciences, Icahn School of Medicine at Mount Sinai, Biomedical Engineering, Center for Public Health Genomics University of Virginia ³

Novel genetic regulators of body fat distribution in humans, ABI3BP, RBL2, CBX3, and ATP13A1, uncovered using network modeling approaches

Graduate Student

Body fat distribution (BFD) is a complex trait that describes the non-uniform storage of fat in various adipose tissue depots. Excess storage in the abdominal region is a well-established risk factor for Type II Diabetes (T2D). This trait is sexually dimorphic; males tend to store more fat in abdominal depots. The comparative storage between abdominal and lower body depots is approximated in large studies by the waist-to-hip ratio adjusted for body mass index (WHRadjBMI). While genome-wide association studies (GWAS) have uncovered novel loci and genes associated with WHRadjBMI, a majority of these genes are understudied. The link between gene expression and differential fat storage remains largely unknown. Monogenic forms of lipodystrophy can cause altered fat distribution. Many genes that are associated with BFD are expressed in adipose tissue and effect adipocyte differentiation, proliferation and storage. Genes that are differentially regulated or expressed between fat depots may lead to preferential fat storage in one depot that alters WHRadjBMI. We aimed to identify novel genetic regulation of genes associated with WHRadjBMI in both sexes and fat depots using systems biology approaches.

We modeled sex- and depot-specific adipose tissue gene-gene interactions on a large scale by creating directed networks from a curated geneset of ~8,000 putative BFD-related genes. Included in this set were ~ 450 genes associated with WHRadjBMI in GWAS using both colocalization and nearest-gene methods. We used 2 independent cohorts of adipose tissue gene expression data to create 8 sex- and depot-specific independent networks. Because of the unique structure of these models, we could predict genes whose expression regulates the expression of many others in the network using a Bayesian Network approach. We then chose genes that regulated the expression of many WHRadjBMI GWAS genes in the network. We found that ABI3BP is an important regulator in female lower body (subcutaneous) fat networks, while RBL2 is an important regulator of male abdominal fat networks. Both genes have been shown to drive adipocyte differentiation. We also found that CBX3 and ATP13A1 are important regulators in male networks of both fat depots. CBX3 is located near a WHRadjBMI GWAS locus and may play a role in lipolysis. Atp13a1 affects body fat percentage and lean mass when knocked out in mice. Single-cell data shows that these genes are highly expressed in adipocytes and pre-adipocytes.

Genes ABI3BP, RBL2, CBX3, and ATP13A1 and others may play an important role in the differential fat storage in adipose tissue that contributes to overall BFD. In future studies, we will manipulate the expression of these genes in adipocytes of both sexes and depots to assess their role in adipocyte function and fat storage.

****Selected Abstracts Presentation****

Wen Dai, MD¹, Hayley Lund, BS² • George Kuriakose, MS³ • Ira Tabas, MD, PhD³ • Ze Zheng, MD, PhD^{1,2}

Blood Research Institute, Versiti Blood Center of Wisconsin¹ • Medicine Medical College of Wisconsin² • Medicine Columbia University Irving Medical Center³

Silencing Hepatocyte Tissue Plasminogen Activator Increases Plasma Apob Lipoprotein-Cholesterol By Promoting MTP-Mediated VLDL Lipidation

Postdoc

Tissue plasminogen activator (tPA) is a key protein that promotes blood clot lysis, a fibrinolysis process. Lower tPA activity was associated with higher atherogenic cholesterol levels in humans, but the mechanism remains unknown. Our group recently reported that hepatocytes, which assemble and secrete apoB lipoproteins, are a source of plasma tPA. We now show a novel role of hepatocyte tPA in determining blood apoB lipoprotein-cholesterol levels via limiting microsomal triglyceride transfer protein (MTP)-mediated VLDL lipidation.

To elucidate the role of hepatocyte-derived tPA in lipid metabolism, we silenced hepatocyte-tPA in mice via AAV8-H1-sh-tPA. We found that hepatocyte-tPA silencing increased plasma cholesterol, triglyceride, and apoB in fat-fed wild-type (WT) and *Ldlr*^{-/-} mice. Fractionation of plasma lipoproteins by fast protein liquid chromatography or ultracentrifugation showed increased cholesterol and apoB in VLDL and LDL fractions. Silencing tPA in Western diet-fed *Ldlr*^{-/-} mice exacerbated atherosclerosis compared with mice treated with AAV8-H1-scrambled-RNA. Using poloxamer P407 to inhibit VLDL hydrolysis, we found that hepatocyte-tPA-silenced WT mice showed an increased rate of increase of plasma triglycerides, suggesting enhanced hepatic VLDL production. In both WT and *Ldlr*^{-/-} mice, silencing hepatocyte-tPA led to higher triglyceride-to-apoB ratios in plasma VLDL, suggesting enhanced intrahepatic VLDL lipidation. We replicated our findings in cultured human primary hepatocytes by showing that silencing tPA increased secretion of lipid-rich apoB into the medium. Using microsomes isolated from control and tPA-silenced hepatocytes, we tested microsomal lysates in a donor vesicle @ LDL neutral lipid transfer assay ± MTP-inhibitor. The microsomes from the tPA-silenced vs. control hepatocytes showed increased MTP-dependent lipid transfer activity despite similar MTP protein in both groups of microsomes. These data reveal a new role of tPA in limiting hepatocyte lipoprotein secretion and protecting against atherosclerosis and suggest a mechanism for the association of lower tPA with higher plasma cholesterol in humans.

****Larry Rudel Award Lecture****

Luke Schepers, Hannah Cebull 1 • Alycia Berman, PhD 1 • Evan Phillips, PhD 2 • Joseph Gruber 3 • McKenna Hillsdon-Smith 3 • Claudia Albrecht 3 • Craig Goergen, PhD 3

Weldon School of Biomedical Engineering Purdue University 1 • Department of Pharmaceutical Sciences University of Illinois at Chicago 2 • Weldon School of Biomedical Engineering Purdue University 3

Murine Aortic Dissection Timing Correlates with Animal Age

Graduate Student

Introduction: Acute aortic dissections are a serious vascular disease characterized by a tear in the intimal layer of the aorta, and separation of the intima and media layers to create a false lumen. While incidence of aortic dissections is low (~6/100,000 people), it is associated with high mortality rates ranging from 13-49% depending on type and severity [1]. Here, we investigate hemodynamic and morphological changes that occur within the murine aorta of both young and old mice shortly after a dissection has developed using *in vivo* ultrasound and *ex vivo* scanning electron microscopy (SEM). Here we examined the hypothesis that mouse age affects development of aortic dissections due to systemic infusion of angiotensin II.

Materials and Methods: Male, Apolipoprotein E-deficient, C57Bl/6J mice (n=63) were anesthetized using 2-3% isoflurane, and we surgically implanted mini osmotic pumps (Alzet, DURECT Corp, Cupertino, CA). Pumps were loaded with angiotensin II according to body weight and elution rate at a dose of 1000 ng/kg/min. Mice underwent ultrasound imaging (FUJIFILM VisualSonics, Vevo3100) at baseline before pump implant and every 24-36 hours from days 3-14 post-implant to check for dissections of the suprarenal abdominal aorta. One final dissection check was performed at day 28. Mice that developed dissections were euthanized either same day or three days after the dissection was detected. The aorta was extracted, washed in sodium cacodylate buffer, and fixed in glutaraldehyde for SEM and histology.

Results and Discussion: 37/63 mice developed dissections during the 28-day pump implantation. An interesting trend observed during this study is that young mice between 10-20 weeks of age tend to develop dissections earlier after pump implant (6.4±2.5 days) compared to older mice over 40 weeks of age (10.1±1.3 days), suggesting a different response from older mice (p<0.001; Figure 1A). No significant difference in mean or peak velocity was observed between young and old mice at baseline (Figure 1B). However, aortic dissections of differing severities were observed in this study with some developing large, open false lumens, whereas others immediately developed clot structures in the false lumen (Figure 1D). SEM imaging and histology are currently being used to identify and quantify differences in both thrombus formation and wall composition at multiple locations along the vessel in both young and old groups (Figure C&D).

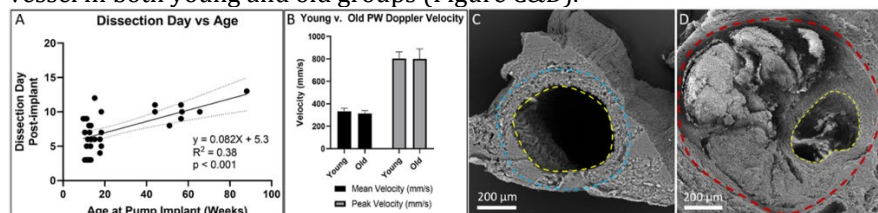


Figure 1: Aortic dissection development and morphology. A. Older mice developed dissections later after pump implant compared to younger mice. B. Mean and peak baseline velocities of both young and old mice, no significant difference observed. C. SEM image of healthy aorta without dissection with intima (yellow) and adventitia (blue) shown. D. SEM image of dissected aorta with true lumen on right (yellow) and partially thrombosed false lumen (red).

Conclusions: Young hyperlipidemic mice tend to develop suprarenal aortic dissections earlier than old mice, despite similarities in baseline hemodynamics. Future work will be needed to correlate differences in wall composition from young and old mice using SEM and histology with dissection timing.

Acknowledgments: Andrew Otte¹, John W. Weisel² and Irina N. Chernysh² for help developing the SEM imaging technique.

Scott E. Street¹, John T. Melchior^{1,7}, Esmond Geh², Amy S. Shah², W. Gray Jerome³, Rachel Hart³, Jay W. Heinecke⁴, Yi He⁴, Tomas Vaisar⁴, Ivan S. Yuhanna⁵, Chieko Mineo⁵, Philip W. Shaul⁵, Michael S. Gardner⁶, Zsuzsanna Kuklenyik⁶ and W. Sean Davidson¹

¹Department of Pathology and Laboratory Medicine, University of Cincinnati, Cincinnati, OH, ²Department of Pediatrics, Division of Endocrinology, Cincinnati Children's Hospital, Cincinnati OH, ³Department of Pathology, Microbiology and Immunology, Vanderbilt University Medical Center, Nashville, TN, ⁴Department of Medicine, University of Washington, Seattle, WA and ⁵Center for Pulmonary and Vascular Biology, Department of Pediatrics, University of Texas Southwestern Medical Center, Dallas, TX, ⁶Clinical Chemistry 2

Distinct Composition and Function of Isolated Human High Density Lipoprotein Subspecies

Staff

High-density lipoproteins (HDL) are heterogeneous in size, composition, and functionality. HDL can host up to 95 different proteins that segregate into distinct subspecies. Unfortunately, the composition/function relationships of these subspecies are poorly understood. The two major apolipoproteins, APOA1 and APOA2, account for 70% and 20% of HDL protein, respectively. We previously used immunoaffinity chromatography to subspeciate HDL by the presence (LpA-I/A-II) or absence (LpA-I) of apoA-II. We observed that APOA2 exhibited a profound impact on the HDL proteome and function and that LpA-I segregated into two remarkably distinct size species (LpA-I_{large} with a diameter of ~11 nm and LpA-I_{small} at ~9 nm by electron microscopy). We hypothesize that compositional/functional properties not only vary between LpA-I and LpA-I/A-II, but also between the different sized LpA-I species. After immunoaffinity separation, LpA-I species were isolated by high-resolution gel filtration chromatography along with size-matched LpA-I/A-II species for direct comparison. In addition to known differences between LpA-I and LpA-I/A-II, we found clear proteomic differences between LpA-I_{large} and LpA-I_{small}, with proteins like apoH, PLTP and fibronectin enriched in the former and complement C1S enriched in the latter. Ion mobility and quantitative mass spectrometry showed that both LpA-I_{large} and LpA-I_{small} contained 3 and ~3.7 molecules of APOA1 per particle. Lipidomics showed LpA-I species contained more surface lipids and decreased neutral core lipids vs. LpA-I/A-II at both sizes. LpA-I_{small} was moderately more effective than LpA-I_{large} in promoting cholesterol efflux, but the presence of apoA-II dramatically enhanced ABCA1 mediated cholesterol efflux for both sizes, despite the fact that these were fully lipidated particles. LpA-I were more effective vs LpA-I/A-II in preventing the binding of LDL to arterial proteoglycans. The ability to stimulate endothelial nitric oxide synthase activity was dependent on particle size, with small particles stimulating greater activity, but independent of apoA-II. Collectively, these results add credence to the growing realization that HDL is composed of distinct compositional entities with unique functionalities.

Ryan Allen ¹ • Danielle Michell ¹ • Ashley Cavnar ¹ • Wanying Zhu ¹ • Neil Makhijani ¹ • Danielle Contreras ¹ • Elizabeth Semler ² • Carlisle DeJulius ³ • Mark Castleberry ¹ • Youmin Zhang ¹ • Marisol Ramirez-Solano ⁴ • Shilin Zhao ⁴ • Craig Duvall ³ • Amanda Doran ¹ • Quanhu Sheng ⁴ • MacRae Linton ¹

Department of Medicine Vanderbilt University ¹ • Department of Molecular Physiology and Biophysics Vanderbilt University ² • Department of Biomedical Engineering Vanderbilt University ³ • Department of Biostatistics Vanderbilt University ⁴

LDL Delivery of Microbial Small RNAs Drives Atherosclerosis through Macrophage TLR8

Faculty

Low-density lipoproteins (LDL) are a causal factor for atherosclerosis, a key pathological process in cardiovascular disease. Within atherosclerotic lesions, macrophages present a spectrum of phenotypes that mediate both disease pathogenesis and resolution. Inflammatory macrophage phenotypes are well-established to be pro-atherogenic, but the natural factors that promote polarization remain incompletely understood. Here, we demonstrate that microbial small RNAs (msRNA) are enriched on LDL and drive pro-inflammatory macrophage polarization and cytokine secretion via activation of toll-like receptor 8 (TLR8). Removal of msRNA cargo during LDL reconstitution yields particles that are taken up by macrophages but fail to stimulate inflammatory activation. Using loss-of-function and gain-of-function studies, we demonstrate that TLR8 is both necessary and sufficient for LDL-induced activation of macrophages. Unexpectedly, we discovered that TLR8 recognition of msRNA could be competitively antagonized by chemically modified oligonucleotides containing locked-nucleic acid bases (nt-LNA). Pre-treatment of macrophages with nt-LNA was found to prevent LDL-induced macrophage polarization *in vitro*, and re-organize lesion macrophage phenotypes *in vivo*, as determined by single-cell RNA sequencing. Critically, we demonstrate that nt-LNA treatment reduced plaque burden in 4-week and 10-week atherosclerosis progression studies in *Apoe*^{-/-} mice fed a western diet, as well as in a short-term *Ldlr*^{-/-} regression model. Furthermore, we have characterized novel genetic models to link naturally increased LDL-msRNA abundance with susceptibility to atherosclerosis, as well as models with reduced LDL-msRNA content that are association with protection against atherosclerosis in the setting of severe hyperlipidemia. These results identify LDL-msRNA as novel stimuli for atherosclerosis-associated inflammation and support alternative functions of LDL beyond cholesterol transport.

Rachel Hart ¹ • Shimpi Bedi, PhD ² • Chongren Tang, PhD ³ • Jay Heinecke, MD ³ • W. Sean Davidson, PhD ² • Jere Segrest, MD, PhD ⁴ • W. Gray Jerome, PhD ¹

Pathology, Microbiology, and Immunology Vanderbilt University Medical Center ¹ • Pathology and Laboratory Medicine University of Cincinnati ² • Department of Medicine University of Washington

- Seattle ³ • Department of Medicine Vanderbilt University Medical Center ⁴

ABCA1 Occurs in Specific Clusters Corresponding to Cytoplasmic Microdomains.

Staff

ABCA1 is a plasma membrane protein that plays a key role in cellular cholesterol homeostasis and possibly in regulation of other cellular processes. Its role as a major transporter of phospholipid and cholesterol to extracellular apolipoproteins such as apolipoprotein A-I (APOA1) is well accepted. Thus, ABCA1 is an important component for removal of excess cholesterol from cells. However, the exact mechanism by which this export occurs has not been established and a number of models have been proposed. ABCA1 has also been shown to be a signaling receptor, transducing extracellular signals to intracellular pathways. Moreover, ABCA1 has been implicated in mobilizing cholesterol from intracellular pools to the plasma membrane for efflux. However, the mechanisms for these have not been fully established. To provide information towards resolving these key questions around ABCA1 structure and function, we characterized the cellular morphology associated with areas of ABCA1 expression on the cell surface by quantitative TEM and SEM imaging. BHK cells expressing mifepristone-inducible human ABCA1 where incubated with 10 µg/ml APOA1 for 3 h, the cells were fixed and immunogold labeled for APOA1 to identify areas of its binding to the cell surface. The immunostaining identified areas of apoA-I binding to ABCA1 as evidenced by a 27X increase in immunolabel in cells overexpressing ABCA1 compared to basal expression levels. The distance of immunogold particles from the cell surface was consistent with the predicted size of the ABCA1 extracellular domain, providing further confidence that the immunolabel indicated areas of ABCA1 surface expression. Scanning electron microscopy indicated that ABCA1 was not uniformly distributed across the surface of the cell. Rather, in both the basal state and after mifepristone treatment, ABCA1 occurred in distinct clusters with large amounts of membrane between the clusters. The number and size of clusters increased significantly with mifepristone treatment. A key feature of the cytoplasm in areas of ABCA1 clusters was a significant increase in image density directly below the plasma membrane compared to areas away from the clusters. This suggests a specific accumulation of proteins in these areas that may be related to ABCA1s signaling and/or cholesterol mobilization properties. Although not yet quantified, there also appeared to be a lack of cytoskeletal elements in areas near the ABCA1 clusters. In summary, our early studies strongly suggest ABCA1 clusters in discrete areas corresponding to areas of local cytoplasm organization and concentration of proteins and where some cytoplasmic elements are excluded.

Lucas J. Osborn^{1,2}, Karlee Schultz^{1,*}, William Massey^{1,2,*}, Beckey DeLucia¹, Ibrahim Choucair¹, Venkateshwari Varaharajan¹, Kevin Fung¹, Anthony J. Horak III¹, Danny Orabi^{1,2,3}, Ina Nemet¹, Laura E. Nagy⁴, Zeneng Wang¹, Daniella Allende⁵, Naseer Sangwan¹, Adeline M. Hajjar¹, Philip P. Ahern^{1,2}, Stanley L. Hazen¹, J. Mark Brown^{1,2,#}, Jan Claesen^{1,2,#}

¹Department of Cardiovascular and Metabolic Sciences and Center for Microbiome and Human Health, Lerner Research Institute of the Cleveland Clinic; Cleveland, OH, USA.

²Department of Molecular Medicine, Cleveland Clinic Lerner College of Medicine of Case Western Reserve University; Cleveland, Ohio, USA.

³Department of General Surgery, Cleveland Clinic; Cleveland, OH, USA.

⁴Department of Inflammation and Immunity, Lerner Research Institute of the Cleveland Clinic; Cleveland, OH, USA.

⁵Robert J. Tomsich Pathology and Laboratory Medicine Institute of the Cleveland Clinic; Cleveland, OH, USA.

A gut microbial metabolite of dietary polyphenols reverses obesity-driven hepatic steatosis

Postdoc

The interaction between gut microbial metabolism and dietary input plays a central role in human health and disease. Consumption of diets rich in colorful fruits and vegetables has been negatively associated with cardiometabolic disease (CMD)-related mortality. Mechanistically, this effect has been attributed to the activity of flavonoids, the most abundant and diverse class of polyphenols in these plant-based diets. Upon reaching the colon, select commensal gut bacteria can catabolize these flavonoid substrates into smaller monophenolic acids. While these monophenolic acids are significantly more bioavailable than the parent flavonoid molecule, their contribution to ameliorating CMD remains poorly understood. Here we show that a single microbe-derived monophenolic acid, 4-hydroxyphenylacetic acid (4-HPAA), is sufficient to reduce the burden of high fat diet (HFD)-induced CMD. We found that supplementing a HFD with flavonoid-rich elderberry extract significantly attenuated HFD-induced obesity and that 4-HPAA was enriched in the portal plasma of these mice. Moreover, continuous subcutaneous delivery of 4-HPAA was sufficient to reverse HFD-induced hepatic steatosis. This anti-steatotic effect is associated with the activation of AMP-activated protein kinase alpha (AMPK α). In a large survey of healthy human gut metagenomes, less than one percent contained all four bacterial genes required to catabolize flavonols into 4-HPAA. Our results demonstrate the gut microbial contribution to the metabolic benefits associated with flavonoid consumption and underscore the rarity of this process in human gut microbial communities. This highlights the importance of factoring in the gut microbiota metabolic capacity in the design of dietary interventions to complement traditional CMD treatment strategies.

****Larry Rudel Award Lecture****

Robert Helsley, PhD¹ • Se-Hyung Park, PhD¹ • Hemendra Vekaria, PhD² • Patrick Sullivan, PhD² • Jesse Meyer, PhD³ • Birgit Schilling, PhD³ • Ronald Kahn, MD⁴ • Samir Softic, MD¹

Pediatrics and Gastroenterology University of Kentucky¹ • Spinal Cord and Brain Injury Research Center University of Kentucky² • Chemistry & Mass Spectrometry Buck Institute for Research on Aging³ • Medicine Joslin Diabetes Center⁴

KHK Promotes Hepatic Lipid Deposition by Repressing CPT1a-Mediated Fatty Acid Oxidation

Postdoc

Background: Increased intake of fructose and high fat diet (HFD) have been linked to the development of obesity and non-alcoholic fatty liver disease (NAFLD). Dietary fructose strongly supports lipogenesis but our lab has reported that fructose also impairs hepatic fatty acid oxidation (FAO). Here we demonstrate that ketohexokinase (KHK), the rate-limiting enzyme of fructolysis, impairs carnitine palmitoyltransferase 1a (CPT1a)-mediated FAO.

Methods: Six-week-old C57BL/6 male mice were fed chow or HFD (60% fat) and supplemented with either tap water or 30% (w/v) fructose or glucose solution in water for two weeks. Livers and serum were harvested for western blot, qPCR, H&E staining, hepatic and serum lipid analysis, mass spectrometry-based lipidomics and acetyl-proteomics. Mouse AML12 hepatocytes were engineered to overexpress (OE) KHK or to knockout (KO) CPT1a using lentivirus or CRISPR/Cas9 nickase, respectively. FAO and glycolytic rates were assessed using Seahorse.

Results: Fructose supplementation on chow and HFD induced hepatic KHK protein ~2-3 fold compared to water control. Mice supplemented with glucose on HFD also had increased KHK due to enhanced endogenous fructose production as evident by increased aldose reductase (~2 fold) and sorbitol dehydrogenase (~3 fold) protein in the liver. All mice with elevated KHK exhibited downstream upregulation of aldolase B and triokinase/FMN cyclase protein levels, as well as decreased CPT1a protein and long chain acylcarnitines in the liver. Interestingly, only mice with increased KHK fed HFD, but not chow, developed severe hepatic steatosis. Cultured KHK OE hepatocytes reduced CPT1a protein by 70% with concomitant decrease in FAO and enhanced triglyceride accumulation when treated with free fatty acids (FFA). CPT1a KO cells resembled KHK OE cells in terms of decreased FAO and FFA enhanced lipid accumulation. Mechanistically, diet-induced upregulation of KHK in mice was associated with increased acetylation of CPT1a at lysine residues 195, 508, and 634, likely contributing to decreased CPT1a protein stability.

Conclusions: Increased hepatic KHK is associated with reduced CPT1a-mediated FAO leading to elevated lipid deposition in the liver when fed a HFD. These data support a mechanism by which sugar and fat synergistically enhance NAFLD development.

Yonathan Tamrat Aberra^{1,2*}, Mete Civelek^{1,2}

¹ Department of Biomedical Engineering, University of Virginia, Charlottesville, VA

² Center for Public Health Genomics, University of Virginia, Charlottesville, VA

Functional Annotation of Genetic Loci Associated with Body Fat Distribution and Type 2 Diabetes

Graduate Student

Metabolic Syndrome (MetSyn) is a cluster of conditions that increases risk of cardiovascular disease, stroke and Type 2 Diabetes (T2D). Body fat distribution (BFD) plays an integral role in MetSyn; excess abdominal body fat accumulation is a stronger risk factor than overall adiposity.¹ BFD is clinically measured by calculating the ratio of waist-to-hip circumference (WHR), and is estimated to have 40-80% heritability, which suggests a strong genetic component.¹ Genetic loci associated with BFD identified in genome-wide association studies (GWAS) are predicted to act through adipose tissues, but the molecular mechanisms regulating the accumulation of adipose tissue in various fat depots are poorly understood.² Colocalization analysis (COLOC) has emerged as a powerful tool to functionally annotate genetic loci. By integrating information from expression quantitative trait locus (eQTL) and GWA studies, COLOC allows for hypothesis prioritization for experimental characterization. Using 3 independent COLOC approaches, we analyzed 605 genetic loci associated with T2D and WHR independent of overall obesity (adjBMI). Our results revealed 74 genetic loci associated with both traits using at least 2 methods. We further performed COLOC with adipose tissue eQTL datasets, and identified the colocalization of 21 adipose tissue eQTLs with both T2DadjBMI and WHRadjBMI loci. The majority of the genetic signals in these 21 loci were co-located with adipose tissue transcriptional regulatory elements, including enhancer-promoter regions and transcription start sites. Of particular note, the locus containing the gene encoding ADAM Metallopeptidase With Thrombospondin Type 1 Motif 9 (*ADAMTS9*) was one where the adipose tissue eQTL, T2DadjBMI GWAS, and WHRadjBMI GWAS signals colocalized. *ADAMTS9* is specifically expressed in visceral adipose tissue³ and is a protease that cleaves the large aggregating proteoglycans. It was also predicted to act through adipose tissue to affect risk of T2D development using the Tissue of ACTION scores for Investigating Complex trait Associations at Loci (TACTICAL).⁴ Although it has previously been shown to play a major role in insulin sensitivity, the exact mechanisms associating the gene with BFD and T2D remain poorly characterized.⁵ Further work will incorporate additional tissue annotation and genomic annotation data to more fully annotate genetic loci associated with T2DadjBMI and WHRadjBMI. We aim to use this annotation to prioritize high-impact genes for experimental characterization and the development of drug targets for Metabolic Syndrome.

References: [1] Pulit SL, et al. *Human Molecular Genetics*, 2019. [2] Rask-Andersen MA., et al. *Nature Communications*, 2019. [3] GTEx Consortium. *Nature Genetics*, 2013. [4] Jason M. Torres, et al., *The American Journal of Human Genetics*, 2020. [5] AS Graae, et al.

Taesik Gwag¹, Eric Ma¹, Changcheng Zhou² and Shuxia Wang¹

¹Department of Pharmacology and Nutritional Sciences, University of Kentucky, Lexington VA Medical Center, Lexington KY 40502. ² Division of Biomedical Sciences, School of Medicine, University of California, Riverside

Anti-CD 47 antibody treatment attenuates liver inflammation and fibrosis in experimental non-alcoholic steatohepatitis models

Staff

Abstract

Background and Aims: With the epidemic burden of obesity and metabolic diseases, nonalcoholic fatty liver disease (NAFLD) including steatohepatitis (NASH) has become the most common chronic liver disease in the western world. NASH may progress to cirrhosis and hepatocellular carcinoma. Currently no treatment is available for NASH. Therefore, finding a therapy for NAFLD/NASH is in urgent need. Previously we have demonstrated that mice lacking CD47 or its ligand thrombospondin1 (TSP1) are protected from obesity-associated NAFLD. This suggests that CD47 blockade might be a novel treatment for obesity-associated metabolic disease. Thus, in this study, the therapeutic potential of a humanized anti-CD47 antibody in NAFLD progression was determined.

Methods: Both diet-induced NASH mouse model and human NASH organoid model were utilized in this study. NASH was induced in mice by feeding with diet enriched with fat, sucrose and cholesterol (AMLN diet) for 20 weeks and then treated with anti-CD47 antibody or control IgG for 4 weeks. Body weight, body composition and liver phenotype were analyzed.

Results: We found that anti-CD47 antibody treatment did not affect mice body weight, fat mass, or liver steatosis. However, liver immune cell infiltration, inflammation and fibrosis were significantly reduced by anti-CD47 antibody treatment. *In vitro* data further showed that CD47 blockade prevented hepatic stellate cell activation and NASH progression in a human NASH organoid model.

Conclusion: Collectively, these data suggest that anti-CD47 antibody might be a new therapeutic option for obesity-associated NASH and liver fibrosis.

William Massey¹ • **Venkateshwari Varadharajan, PhD**¹ • **Rakhee Banerjee, PhD**¹ • **Anthony Horak**¹ • **E. Ricky Chan, PhD**² • **J. Mark Brown, PhD**¹

Cardiovascular and Metabolic Sciences Lerner Research Institute, Cleveland Clinic¹ • Institute for Computational Biology Case Western Reserve University²

Membrane Bound O-Acyltransferase 7 (MBOAT7) Driven Lysophosphatidylinositol (LPI) Acylation in Adipocytes Contribute to Systemic Glucose Homeostasis.

Graduate Student

Non-alcoholic fatty liver disease (NAFLD) is a growing health problem that affects roughly one-third of adults in the United States. Unfortunately, development of therapeutic strategies to arrest the progression of NAFLD to end stage liver disease has been hampered by lack of mechanistic understanding of liver disease progression. An important advance has occurred within the past several years, where several genome-wide association studies (GWAS) have found that a single nucleotide polymorphism (SNP) near the gene encoding membrane-bound *O*-acyltransferase 7 (*MBOAT7*) is associated with liver disease progression. In fact, this common *MBOAT7* variant (rs641738), which reduces *MBOAT7* expression, is associated with increased risk of NAFLD, non-alcoholic steatohepatitis (NASH), alcoholic liver disease (ASH), and liver fibrosis in those chronically infected with viral hepatitis. Although these recent genetic studies clearly implicate *MBOAT7* function in liver disease progression, the mechanism(s) by which *MBOAT7* regulates liver disease are currently unknown. The *MBOAT7* gene encodes an acyltransferase enzyme that specifically esterifies arachidonyl-CoA to lysophosphatidylinositol (LPI) to generate the predominant molecular species of phosphatidylinositol (PI) in cell membranes 38:4 PI. We recently published that *Mboat7* loss of function in mice, using an antisense oligonucleotide (ASO) knockdown approach, is sufficient to promote hepatic steatosis and systemic insulin resistance in the setting of high fat diet. However, ASOs can have off target effects and lack tissue specificity. To further understand the cell autonomous roles of *Mboat7* in HFD-induced metabolic dysfunction, we generated both hepatocyte-specific and adipocyte-specific knockout mice. Interestingly, hepatocyte-specific *Mboat7* deletion promoted hepatic steatosis, whereas adipocyte-specific *Mboat7* deletion promoted systemic glucose intolerance and hyperinsulinemia. Here, we will discuss high fat diet-driven metabolic disease in hepatocyte- and adipocyte-specific *Mboat7* knockout mice. Collectively, these studies show that *MBOAT7* plays cell autonomous roles in lipid and glucose homeostasis, and provide new clues into potential mechanisms by which genetic variation in the human *MBOAT7* locus can impact metabolic disease.

Jacob L. Barber, MS¹ • Brittany Crawford, MS² • Prasun K. Dev, MS¹ • Jeremy M. Robbins, MD³ • Prashant Rao, MD³ • Michael Mi, MD³ • Sujoy Ghosh, PhD⁴ • Clary Clish, PhD⁵ • Daniel H. Katz, MD³ • Robert E. Gerszten, MD³ • Claude Bouchard, PhD⁶ • Mark A. Sarzynski, PhD¹

Exercise Science University of South Carolina¹ • Epidemiology and Biostatistics University of South Carolina² • Division of Cardiovascular Medicine Beth Israel Deaconess Medical Center³ • Centre for Computational Biology Duke- National University of Singapore Medical School⁴ • Metabolomics Platform Broad Institute of Harvard and MIT⁵ • Human Genomics Laboratory Pennington Biomedical Research Center⁶

Circulating Proteomic Signatures Of Plasma Triglycerides And Triglyceride-Rich Lipoproteins

Graduate Student

Background: Elevated triglyceride (TG) levels are associated with increased CVD risk. Plasma TG levels correspond to the sum of the TG content in TG-rich lipoproteins (TRLs) and their remnants. As clinical trials of TG-lowering agents have produced inconsistent results, recent studies, including mendelian randomization and genome wide association studies, have attempted to elucidate the causal role of TG on CVD risk. The associations of TG and TRLs with plasma proteins, critical mediators of biological processes, have not been widely explored and may inform our understanding of TG biology.

Purpose: To identify circulating proteins associated with plasma TG and TRL levels.

Methods: We measured 4,979 circulating proteins using an aptamer-affinity based platform (SomaScan) in 652 black and white adults from the HERITAGE Family Study. Fasting plasma TG levels were measured using enzymatic methods. Seven TRL particle traits (concentration of total, very-large, large, medium, small, and very-small TRL; mean TRL size) were quantified by NMR spectroscopy using LabCorp's LipoProfile-4 algorithm. To construct a proteomic signature of each TG trait, we employed a two-step statistical pipeline. In all statistical modeling, protein and TG variables were natural log transformed. Multivariable linear regression models adjusted for age, sex, race, and BMI were used to examine the association between each TG trait and individual protein, with FDR<0.05 considered statistically significant. Proteins that remained significant after FDR were entered into a LASSO regression model with 10-fold-cross-validation. Proteins retained after LASSO were carried forward to pathway enrichment analysis, conducted using IMPaLA (Integrated Molecular Pathway Level Analysis).

Results: The multivariable linear regression models yielded 1,009 circulating proteins significantly associated with plasma TG and between 25 to 878 proteins with the TRL traits. Following LASSO regression of significant proteins, 136 proteins remained in the model for plasma TG and between 22 to 158 proteins for the seven TRL traits. After LASSO feature reduction, there was little overlap of proteins across the TG and TRL traits. However, the ApoC-III protein appeared in 7 of 8 signatures, WNT5A in 6 of 8, and seven proteins (including ApoJ and PAFAH) in 5 of 8. The complement and coagulation cascade, chylomicron assembly and remodeling, HDL remodeling, and insulin-like growth factor transport and uptake were the top biological mechanisms identified by pathway analysis of the protein signatures across TG and TRL traits.

Conclusions: We observed significant associations between TG-related traits and a large panel of circulating proteins, with the proteomic signatures of these traits seemingly distinct from each other. These results suggest that the circulating proteins associated with TG and TRLs may be involved in important cardiometabolic pathways and provide insights into targets for future research.

Salma Fleifil¹ • Bailey Stone¹ • Lei Cai, PhD² • Ryan E. Temel, PhD² • A. Phillip Owens III, PhD³

Internal Medicine Division of Cardiovascular Health & Disease University of Cincinnati¹ • Pharmacology and Nutritional Sciences University of Kentucky² • Internal Medicine Division of Cardiovascular Health & Disease University of Cincinnati³

MicroRNA-33a/b Inhibition Attenuates Tissue Factor Activity and the Activation of Coagulation in Mice and Nonhuman Primates

Staff

Background: Dyslipidemia in atherosclerotic disease is associated with increased cardiovascular morbidity and mortality. Hypercholesterolemia is linked to a prothrombotic state due to increases in the procoagulant protein tissue factor (TF), which is highly expressed in atherosclerotic plaques. We recently demonstrated that acute hypercholesterolemia can induce the activation of coagulation with time-dependent increases in monocyte TF activity and microvesicle (MV) TF activity in both mice and non-human primates (NHPs).

Objective: Our objective for the current study was to determine the effect of chronic dyslipidemia and subsequent correction of hypercholesterolemia with either standard chow or antagonism of the lipid metabolism regulating microRNA-33 (miR-33) on the activation of coagulation in NHPs.

Methods and Results: Thirty-six male Cynomolgus monkeys (*Macaca fascicularis*) were fed a fat and cholesterol enriched diet (38% fat kcal, 1.0 mg/kcal cholesterol) for a period of 20 months, at which time a subset was euthanized and atherosclerotic development characterized (n = 12). The remaining monkeys were switched to a standard chow diet and treated for 6 months with either saline (n = 12) or the miR-33a/b antagonist RG428651 (anti-miR-33a/b; n = 12). Blood was collected and citrated plasma processed at day 0 (baseline), 8 months, 20 months (peak experimental) as well as 22 and 26 months (intervention). Total plasma cholesterol was significantly elevated (491% increase compared to baseline; P < 0.001) in 20-month NHPs. Circulating MVs, MV TF, monocyte TF activity, thrombin antithrombin (TAT), and D-dimer were significantly augmented at 20 months compared to baseline (P < 0.05). After 6 months of intervention, vehicle and anti-miR-33a/b attenuated plasma cholesterol by 84% and 79% respectively and approached baseline cholesterol measurements (P < 0.001). Importantly, anti-miR-33a/b significantly decreased MV TF and TAT levels compared to the chow intervention (P < 0.05). To determine if miR-33 had acute effects on the activation of coagulation, C57BL/6J mice were pre-treated with anti-miR-33 (n = 10) or placebo (saline, n = 10) for 17 days prior to injection with a lethal dose of LPS (7.5mg/kg). After 5 hours of LPS administration, TAT was significantly attenuated in anti-miR-33 treated mice compared to control littermates (P < 0.05).

Conclusion: Our results demonstrate that chronic hypercholesterolemia augments circulating plasma MVs, plasma MV TF activity, monocyte TF activity, and coagulation variables (TAT and D-dimer) in NHPs. The prothrombotic state induced by hypercholesterolemia was attenuated by chow feeding with additional significant benefit from the miR-33a/b antagonist RG428651. Future studies will examine the mechanistic role of anti-miR-33 in the activation of coagulation via potential alterations in phosphatidylserine, TLR4, or MV formation.

Angelica Solomon, MS, Mohamed Abo-Aly, MD, Elica Shokri, MD, Mohammed Anwer, MD, Samiullah Arshad, MD, Lakshman Chelvarajan, PhD, , Ahmed Abdel-Latif, MD, PhD
University of Kentucky

CD14+ CD16++ Monocytes predict clinical outcomes in patients with ST-Elevation Myocardial Infarction

Medical Student

Introduction: Nonclassical monocytes (CD14+CD16++) play different roles in cardiovascular disease progression. CD14+CD16++ cells can have both proinflammatory functions and atheroprotective properties.

Hypothesis: The predictive value of CD14+CD16++ cells to clinical outcomes in patient with STEMI has not been well studied.

Methods: We recruited 100 patients with STEMI who underwent primary PCI. Blood samples were collected at the time of presentation to the hospital (within 6 hours from onset of symptoms) then at 3, 6, 12 and 24 hours after presentation. Monocytes were defined as CD45+/HLA-DR+ and then subdivided based on the expression of CD14, CD16, CCR2, CD11b and CD42. The primary endpoint was a composite endpoint of all-cause death, hospitalization for heart failure, stent thrombosis, in-stent restenosis, and recurrent myocardial infarction. Univariate and multivariate cox proportional hazards models were performed, including age, sex, body mass index, diabetes mellitus, hypertension, congestive heart failure, and troponin-I.

Results:

The mean age of our cohort was 58.9 years old and 25% of our patients were females. Patients with high level (above the median) of CD14+CD16++ monocytes showed increased risk for the primary endpoint in comparison to patients with low level; adjusted hazard ratio (aHR) for CD14+/ CD16++ cells is 4.3 (95% confidence interval [95%CI] 1.2-14.8, p= 0.02), aHR for CD14+/ CD16++/CCR2+ cells is (95%CI 1.06-13.7, p= 0.04), aHR for CD14+/ CD16++/CD42b+ cells was 3.3 (95%CI 1.07-10.6, p=0.03), aHR for CD14+/ CD16++/CD11b+ is 5.1 (95%CI 1.4-18.0, p=0.009), and aHR for CD14+ HLA-DR+ is 7.5 (95% 2.0 -28.5, p=0.002).

Conclusions:

Our study shows that CD14+ CD16++ Monocytes and their subsets expressing CCR2, CD42 and CD11b could be important predictors of clinical outcomes in patients with STEMI. Further studies with larger sample sizes and different coronary artery disease phenotypes are needed to verify our findings.

Shimpi Bedi¹, Jamie Morris¹, Rachel C. Hart², W. Gray Jerome², W. Sean Davidson¹

¹ Department of Pathology and Laboratory Medicine, University of Cincinnati, Cincinnati OH

² Vanderbilt University School of Medicine, Nashville TN

Characterization of ApoA-I Mediated Activation of Lecithin: Cholesterol Acyltransferase on High Density Lipoproteins

Postdoc

Lecithin:cholesterol acyltransferase (LCAT) is responsible for esterifying the bulk of plasma cholesterol to cholesteryl ester on lipoproteins. Its maximal activity requires its cofactor apolipoprotein A-I (APOA1), typically in high density lipoproteins (HDL). However, the molecular basis of this interaction has not been fully elucidated. Our previous work has implicated a region around helices 4 and 6 that line up on opposite sides of two antiparallel APOA1 molecules on the HDL surface. We performed site-directed mutagenesis within and around these regions and assessed the impact on LCAT activation. Mutations at E111, R153, and V156 strongly inhibited LCAT activation whereas control mutations at E191 had minimal impact. Chemical cross-linking studies identified 10 cross-linked peptides in APOA1 that correspond to the helix 4/6 epitope, but also some more distant sites in helices 7 and 8. Negative stain electron microscopy on APOA1-containing reconstituted HDL particles incubated with LCAT showed that up to two LCAT molecules could bind to each particle. These appeared to interact with the edges of the discoidal particles. To provide landmarks in the images that could help us locate the LCAT binding sites within the APOA1 sequence, we engineered APOA1 mutants that contained multiple copies of helix 5. These particles increased in diameter (10.4 nm, 11 nm, and 12 nm) as the number of helix 5 copies increased from 2 to 4. Furthermore, the presence of helix 5 copies did not adversely affect the LCAT esterification reaction. Ongoing work will determine how the introduction of helix 5 repeats affects the spacing of bound LCAT molecules. Our current working model is that LCAT binds to an intermolecular epitope comprised of helices 4 and 6 of APOA1 to execute cholesterol esterification. LCAT may also bind to proximal sites that are not catalytically active. These studies offer important new insight into the mechanism of cholesterol esterification in the plasma.

Daniel Ferguson, PhD, Nicole K.H. Yiew, PhD¹ • Kyle S. McCommis, PhD¹ • Jerry R. Colca, PhD² • Brian N. Finck, PhD¹
Nutrition Sciences Washington University in St Louis¹ • Cirius Therapeutics Inc.²

Mechanisms of Metabolic Crosstalk between Mitochondrial Pyruvate Carrier Inhibition and Branched Chain Amino Acid Catabolism in Hepatocytes

Postdoc

The mitochondrial pyruvate carrier (MPC) has emerged as a therapeutic target for treating insulin resistance, type 2 diabetes, and nonalcoholic steatohepatitis (NASH). However, the molecular mechanisms by which MPC inhibition leads to metabolic improvements are incompletely understood. We evaluated whether MPC inhibitors might correct abnormalities in branched chain amino acid (BCAA) metabolism, which are predictive of developing diabetes and NASH in people. Circulating BCAA concentrations were assessed in plasma collected in EMINENCE (NCT02784444), a randomized, placebo-controlled trial of the MPC inhibitor MSDC-0602K in people with NASH. MSDC-0602K treatment, which led to marked improvements in insulin sensitivity and other diabetes endpoints, decreased plasma concentrations of BCAAs (leucine, isoleucine, and valine) compared to baseline while placebo had no effect. The rate-limiting enzyme in BCAA catabolism is the mitochondrial branched chain ketoacid dehydrogenase (BCKDH). BCKDH activity is suppressed by phosphorylation mediated by a kinase (BDK) and activated by the BCKDH phosphatase (PPM1K). In Huh7 or HepG2 cells, MPC inhibition with UK-5099, 7ACC2, or MSDC-0602K markedly reduced BCKDH phosphorylation, suggesting an increase in BCKDH activity. Chemical inhibition or siRNA-mediated silencing of BDK had no effect on the suppression of BCKDH phosphorylation by MPC inhibitors. In contrast, PPM1K knockdown completely prevented the effects of MPC inhibition on phospho-BCKDH. Lastly, we quantified BCKDH phosphorylation in liver of wild-type and hepatocyte-specific MPC2 knockout (LS-Mpc2^{-/-}) mice after 20 weeks of high fat diet. LS-Mpc2^{-/-} mice exhibited reduced phosphorylation of BCKDH compared to wild-type mice. Lean LS-Mpc2^{-/-} mice also exhibited reduced plasma BCAA concentrations after an overnight fast. These data demonstrate novel metabolic cross talk between mitochondrial pyruvate and BCAA metabolism and suggest that MPC inhibition leads to lower plasma BCAA concentrations and BCKDH phosphorylation via the phosphatase PPM1K.

Brittney Poole¹ • **Isha Chauhan**² • **Gregory Graf, PhD**³

College of Medicine University of Kentucky¹ • College of Arts and Sciences University of Kentucky² • Pharmaceutical Sciences University of Kentucky College of Pharmacy³

Characterization of Sitosterolemia-Associated ABCG5 Mutations

Graduate Student

Familial Hypercholesterolemia (FH) is defined by elevated plasma LDL cholesterol in excess of 190 mg/dl and is most commonly caused by mutations in the LDL receptor, Apolipoprotein B, or PCSK9 genes. Sitosterolemia is a rare form of FH distinguished from others by accumulation of phytosterols and recessive inheritance. Sitosterolemia is caused by mutations in either *ABCG5* or *ABCG8*, genes encoding two ABC half-transporters forming an obligate heterodimer. This mediates sterol transport into bile and the intestinal lumen. We established a classification system delineating the molecular mechanism for Sitosterolemia-associated missense mutations in *ABCG5* and *ABCG8* including impairments including maturation, activity, stability, and trafficking of the complex. We used site-directed mutagenesis to generate disease-causing mutants that reside within the cytosolic domain of *ABCG5*. Our analysis to date indicates most mutations result in the failure of maturation of the *ABCG5* *ABCG8* complex. Small molecule chaperones (correctors), activity modulators (potentiators), and regulators of proteostasis have been shown to correct specific mutants of ABC transporters associated with Progressive Familial Intrahepatic Cholestasis type-3 (PFIC3) and Cystic Fibrosis (CF). We hypothesize these may be useful in the treatment of Sitosterolemia for specific mutations in *ABCG5*.

Yonathan Tamrat Aberra^{1,2}, Mete Civelek^{1,2}

1 Department of Biomedical Engineering, University of Virginia, Charlottesville, VA

2 Center for Public Health Genomics, University of Virginia, Charlottesville, VA

Functional Annotation of Genetic Loci Associated with Body Fat Distribution and Type 2 Diabetes***Graduate Student***

Metabolic Syndrome (MetSyn) is a cluster of conditions that increases risk of cardiovascular disease, stroke and Type 2 Diabetes (T2D). Body fat distribution (BFD) plays an integral role in MetSyn; excess abdominal body fat accumulation is a stronger risk factor than overall adiposity.¹ BFD is clinically measured by calculating the ratio of waist-to-hip circumference (WHR), and is estimated to have 40-80% heritability, which suggests a strong genetic component.¹ Genetic loci associated with BFD identified in genome-wide association studies (GWAS) are predicted to act through adipose tissues, but the molecular mechanisms regulating the accumulation of adipose tissue in various fat depots are poorly understood.² Colocalization analysis (COLOC) has emerged as a powerful tool to functionally annotate genetic loci. By integrating information from expression quantitative trait locus (eQTL) and GWA studies, COLOC allows for hypothesis prioritization for experimental characterization. Using 3 independent COLOC approaches, we analyzed 605 genetic loci associated with T2D and WHR independent of overall obesity (adjBMI). Our results revealed 74 genetic loci associated with both traits using at least 2 methods. We further performed COLOC with adipose tissue eQTL datasets, and identified the colocalization of 21 adipose tissue eQTLs with both T2DadjBMI and WHRadjBMI loci. The majority of the genetic signals in these 21 loci were co-located with adipose tissue transcriptional regulatory elements, including enhancer-promoter regions and transcription start sites. Of particular note, the locus containing the gene encoding ADAM Metallopeptidase With Thrombospondin Type 1 Motif 9 (*ADAMTS9*) was one where the adipose tissue eQTL, T2DadjBMI GWAS, and WHRadjBMI GWAS signals colocalized. *ADAMTS9* is specifically expressed in visceral adipose tissue³ and is a protease that cleaves the large aggregating proteoglycans. It was also predicted to act through adipose tissue to affect risk of T2D development using the Tissue of ACTION scores for Investigating Complex trait Associations at Loci (TACTICAL).⁴ Although it has previously been shown to play a major role in insulin sensitivity, the exact mechanisms associating the gene with BFD and T2D remain poorly characterized.⁵ Further work will incorporate additional tissue annotation and genomic annotation data to more fully annotate genetic loci associated with T2DadjBMI and WHRadjBMI. We aim to use this annotation to prioritize high-impact genes for experimental characterization and the development of drug targets for Metabolic Syndrome.

References: [1] Pulit SL, et al. *Human Molecular Genetics*, 2019. [2] Rask-Andersen MA., et al. *Nature Communications*, 2019. [3] GTEx Consortium. *Nature Genetics*, 2013. [4] Jason M. Torres, et al., *The American Journal of Human Genetics*, 2020. [5] AS Graae, et al. *Diabetes Metabolism*, 2019.

Tyler W. Benson, PhD¹ • Kelsey Conrad, PhD² • Jacob DeMott, Other¹ • Robert N. Helsley, PhD³ • Rebecca C. Schugar, PhD⁴ • Anders Wanhainen, MD, PhD⁵ • Robert Koeth, MD⁴ • Zeneng Wang, PhD⁴ • J. Mark Brown, PhD⁴ • Stanley L. Hazen, MD, PhD⁴ • A. Phillip Owens III, PhD¹

University of Cincinnati¹ • Denison University² • University of Kentucky³ • Cleveland Clinic⁴ • Uppsala University, Sweden⁵

Meta-organismal derived trimethylamine N-oxide (TMAO) augments abdominal aortic aneurysm (AAA) formation

Postdoc

Introduction: Recent studies identify trimethylamine N-oxide (TMAO) as a gut microbiota-generated proatherogenic and prothrombotic metabolite that contributes to the development and progression of several cardiovascular diseases. However, the association between TMAO and abdominal aortic aneurysm (AAA) has not yet been explored. Our study investigates the role of diet derived TMAO in the setting of AAA.

Methods/Results: Plasma concentrations of TMAO were significantly higher in patients with AAA (n = 237) versus controls (n = 115; P < 0.001). Further, we observed a dose-dependent association between higher TMAO concentrations and fast growing aneurysms (n = 92; vs slow growing n = 145; P < 0.001; adjusted quartile 4 odds ratio 93.7). To investigate the role of TMAO in AAA, male *Ldlr*^{-/-} mice were fed a cholesterol-rich (0.2%) control (0.07% choline) or high choline (1.2% wt/wt) diet with or without broad-spectrum antibiotics for two weeks prior to and throughout angiotensin II (AngII) infusion (1,000 ng/kg/min) for 4 weeks. Choline fed mice had elevated plasma trimethylamine (TMA) and TMAO along with increased AAA incidence and abdominal diameter relative to control fed mice. Antibiotic treatment diminished the effects of the choline diet, however, TMAO supplementation in combination with antibiotics restored the AAA phenotype. Mice treated with FMC, an inhibitor of the CutC/D enzymatic complex, exhibited reduced choline-induced plasma TMA/TMAO and AAA formation with supplemental TMAO reversing these effects. Intervention with FMC in established AAAs reduced aneurysm progression with long term AngII treatment. Dietary addition of the FMO3 inhibitor 3,3'-diindolylmethane (DIM) reduced choline-induced AAA incidence and aneurysm diameter, which was confirmed by significantly lower AAA incidence and rupture-induced death in FMO3 deficient mice. Choline augmented aneurysm formation was confirmed in the topical elastase model of aneurysm, which was subsequently blunted by FMC treatment. RNA seq analysis revealed that the putative receptor for TMAO, protein kinase R (PKR)-like endoplasmic reticulum kinase (*Perk*), increased by 256-fold in aortas from choline-fed mice versus control. Experiments in abdominal aortic vascular smooth muscle cells affirmed TMAO-induced PERK up-regulation.

Conclusions: TMAO positively correlates with aneurysmal growth rate in human AAA patients and appears causal to increased aortic diameter and AAA incidence in mice potentially via a PERK dependent mechanism. Disruption of meta-organismal TMAO production diminishes AAA incidence and growth in two mouse models of AAA, indicating therapeutic potential.

Taylor Coughlin ¹ • Mona Mirheydari, PhD ¹ • Caris Wadding Lee ¹ • Kevin Haworth, PhD ¹ • A Phillip Owens III, PhD ¹
Internal Medicine University of Cincinnati ¹

Transcranial disruption of the blood brain barrier using focused ultrasound insonation of microbubbles

Staff

Background: Alzheimer's disease (AD), which affects 5.7 million Americans, is a progressive and fatal neurodegenerative disorder characterized by irreversible cognitive decline, memory derangement, and changes in behavior. Increasing evidence links AD and cardiovascular disease (CVD) via similar cardiometabolic and lifestyle risk factors occurring late in life (hypercholesterolemia, and chronic inflammation). Moreover, intracranial atherosclerosis, is significantly augmented in AD patients and is a risk factor for advanced AD. We have demonstrated protease-activated receptor 2 (PAR2) is a critical regulator of atherosclerosis. Importantly, PAR2 has widespread effects on the peripheral nervous system, where it plays crucial roles in inflammation, neuronal signaling, pain, and is associated with cerebral ischemia, neurodegeneration, and neuroinflammation. However, a definitive role of PAR2 in AD pathology remains unknown.

Problem: While we have a targeted PAR2 peptidic inhibitor (PZ-235), targeted delivery of therapeutic agents to the brain is difficult due to the presence of the blood-brain barrier. Tight junctions formed by endothelial cells coupled with highly regulated transport systems creates a formidable barrier to the brain parenchyma. Focused ultrasound causing the gentle oscillation of microbubbles has been shown to disrupt the BBB transiently, locally, and noninvasively. The objective of this study was to demonstrate this capability in a manner applicable to future studies to deliver therapeutics for the treatment of AD.

Methods: C57BL/6J mice (n = 8) were anesthetized and stabilized onto a stereotaxic frame. Skull landmarks were established using a grid positioning method targeting the hippocampus and ultrasound coupling gel was applied. A degassed/deionized water bath was coupled to the skull and the ultrasound transducer aligned with the positioning grid. Microbubbles (Optison 5ul/g) co-injected with Evans Blue Dye (1%) via the retro-orbital plexus and focused ultrasound insonation was initiated within 15 seconds post injection. Sonication was performed at 500 kHz using a 10 ms pulse duration at 2 Hz pulse repetition frequency for two minutes. Motor function was observed for 2 hr post-insonation. The mice were then euthanized and perfused. Brains were then sliced and imaged coronally to examine dye intensities between treated and untreated hemispheres.

Results: Microbubble oscillations associated with BBB opening were monitored by the detection of ultraharmonic microbubble ultrasound emissions. The threshold for detecting these emission in vitro was determined to be 0.4 MPa peak negative pressure, consistent with values reported in the literature. In this study 8 mice were exposed to focused ultrasound. Ultraharmonic emissions were observed in two mice. Petechial hemorrhage was not observed in any mice. This study shows that focused ultrasound can be safely applied without damage to the brain tissue.

Naofumi Amioka, Kukida Masayoshi, Dien Ye, Deborah A Howatt, Jessica J. Moorleghen, Alan Daugherty, Hong S Lu

Affiliations:

Saha Cardiovascular Research Center and Department of Physiology, University of Kentucky, Lexington, KY, USA.

Induction of Human Angiotensinogen in Hepatocytes and Human Renin in Renal Proximal Tubule Cells Does Not Accelerate Atherosclerosis In Mice

Postdoc

Objective:

Hepatocyte-produced angiotensinogen (AGT) can be filtered by glomeruli and retained in renal proximal tubules. Renin protein has also been detected in proximal tubules (PTC) of kidney. However, it is unknown whether AGT and renin in proximal tubules contribute to atherosclerosis. This study aimed to determine whether hepatocyte-derived AGT interacts with renin in proximal tubules to promote atherosclerosis.

Approach and Results:

Transgenic mice expressing human renin driven by a kidney androgen-related protein promoter (KAP-hREN) in an LDLR $-/-$ background were administered subcutaneously with testosterone (15 mg/mouse, constant release for 60 days) to activate the human renin transgene in PTCs. To induce synthesis of human AGT in hepatocytes, adeno-associated viral (AAV; 3×10^{10} genomic copies/mouse) vector containing human AGT with a liver-specific promoter was injected intraperitoneally. Three groups of male littermates were administered testosterone: (1) wild type mice administered null AAV (n=11), (2) KAP-hREN transgenic mice administered null AAV (n=7), and (3) KAP-hREN transgenic mice (n=8) administered AAV containing human AGT. Two weeks after administration of testosterone and AAVs (either null or human AGT), all mice were fed a Western diet for 6 weeks. Induction of human renin was confirmed by mRNA abundance of human renin in kidney of KAP-hREN transgenic mice. In mice administered human AGT AAV, presence of human AGT was detected in plasma with a human AGT ELISA kit. Induction of both human AGT in liver and human renin in proximal tubules did not affect plasma cholesterol concentrations or systolic blood pressure. Atherosclerotic lesion sizes, as quantified by percent lesion area using an *en face* method, were not different among the 3 groups (Group 1 vs 2 vs 3: $3.7 \pm 0.4\%$ vs $3.3 \pm 0.9\%$ vs $2.3 \pm 0.3\%$; $P = 0.19$).

Conclusions:

Induction of human AGT in hepatocytes and human renin in proximal tubules does not augment atherosclerosis in hypercholesterolemic mice.

Kelsey M. Pinckard¹, Lisa A. Baer¹, Katherine R. Wright¹, Shanna Hamilton¹, Diego Hernandez-Saavedra¹, Shinsuke Nirengi¹, Jorge Vinales¹, Nickolai P. Seculov¹, Neil Schwieterman¹, Ty Saldana¹, Eaman A. Abay¹, Vikram K. Shettigar¹, Mark T. Ziolo¹, Dmitry Terentyev¹, Loren Wold¹, and Kristin I. Stanford¹

¹ Department of Physiology and Cell Biology, The Ohio State University Wexner Medical Center, Columbus, OH 43210

Maternal Exercise Preserves The Cardiac Health Of Adult Offspring

Graduate Student

Cardiovascular disease is the leading cause of death in the United States, and recent studies have shown that maternal obesity during pregnancy is associated with elevated risk for the development of both cardiovascular and metabolic disease in adult offspring. Regular exercise is an important therapeutic used in patients to prevent the onset of both metabolic and cardiovascular disease. Studies in our lab and others have shown that in a rodent model, maternal exercise improves the metabolic health of adult offspring from chow-fed dams and negates the detrimental effects of maternal high-fat diet (HFD) on offspring metabolic health. However, the effects of maternal exercise on the cardiac health of adult offspring has not been investigated. Here, we investigated the role of maternal exercise on offspring cardiac health. To do this, C57BL/6 female mice were chow-fed and sedentary (CS) or subjected to treadmill exercise (CT, 1 hr/day, 0.8 miles/hr, 5 days/wk) or voluntary wheel exercise (CW) for two weeks prior to mating and throughout gestation. All offspring were sedentary and chow-fed throughout their lifespan. Female offspring from CS dams showed an age-induced decline in ejection fraction (EF; 59.9% at 8wks of age, 48.8% at 52 wks of age); however, EF was preserved in offspring from CT (60.9% at 8wks of age, 55.5% at 52wks of age) and CW (59.5% at 8wks of age, 56.1% at 52wks of age) dams. Additionally, female and male offspring from CW dams had increased LV systolic and diastolic function compared to offspring from sedentary dams at 52 weeks of age. After observing these striking effects, we investigated the effects of maternal exercise in the presence of maternal high-fat diet (HFD). To do this, C57BL/6 female mice were fed a HFD (60% kcal from fat) and divided into sedentary (HS) or wheel-exercised (HW) for two weeks prior to mating and throughout gestation. Starting at 8 weeks of age, female offspring from HS dams had significantly reduced LV EF ($P=0.02$) compared to offspring from CS dams. Importantly, this effect was prevented in offspring from HW dams. To determine if these changes in offspring cardiac function were mediated at the cellular level, cardiomyocytes (CMs) were isolated from offspring at 12 weeks of age and underwent functional testing. CMs from HS offspring had reduced peak shortening, kinetics and calcium flux compared to CMs from CS offspring. The negative effects of a maternal HFD on CM function, however, were not seen in offspring from HW dams. Together, these data indicate that maternal exercise preserves cardiac function in adult offspring and negates the negative effects of a maternal HFD, at least partially through improved CM function. By further elucidating the mechanism behind the beneficial effects of maternal exercise on offspring cardiac function, we could potentially develop a therapeutic method to preserve offspring cardiac health and prevent the detrimental effects of maternal obesity or HFD.

Lin Zhu, MD, PhD ¹ • Julia An, ¹ • Sophia Yu, MD ¹ • Emery Edington, Other ¹ • Bridget Litts, ¹ • John Stafford, MD, PhD ¹
Medicine Vanderbilt Medical Center ¹

Sex Differences in Improvements of CVD Risk Factors by Exercise or Low-fat diet in Mice

Faculty

We hypothesized that a healthy diet and exercise individually improve energy metabolism through different pathways in males and females. Understanding the mechanism for how healthy diet vs. exercise improves metabolic outcomes is important for intervention through lifestyle change to target risk factors for obesity-associated diseases in specific populations. Adult mice were fed a high-fat diet (HFD) for 12 weeks, then divided into 4 groups and followed for 6 weeks: a. HFD; b. HFD + exercise; c. diet was switched to chow; d. diet-switch + exercise. Instead of acute metabolic effects, we investigated the sustained effects of exercise training by examining tissue glucose uptake and glucose and lipid metabolism 48 hours after the last exercise session. Diet-switch and exercise reduced obesity and triglyceride contents in tissues in both sexes. Exercise promoted muscle glucose uptake and reduced liver glucose uptake more significantly in male mice than in female mice. Diet-induced fatty liver was more significantly reduced by diet-switch than exercise training in female mice, while the fatty liver was similarly improved by a healthy diet and exercise training in male mice. Glucose uptake in adipose tissues was higher in females than males. Diet-switch, but not exercise, decreased glucose uptake in brown fat, which effect was greater in females than males. Furthermore, the expression of genes involved in lipid biosynthesis and catabolism in fat tissues was higher in female mice than in male mice. Our results indicate that: 1) adipose tissue nutrient storage is the major energy reservoir that protects against obesity-related metabolic changes in females; 2) with regard to improving metabolic outcomes, diet-switch benefits females more and exercise benefits males more; for both sexes 3) exercise training is more effective in preventing fatty liver than diet-switch, and 4) both diet-switch and exercise promote fat oxidation in muscles.

Clementine Adeyemi¹ • **Jamie Morris**¹ • **Debi Swertfeger, PhD**² • **Brynne Whitacre, MS**¹ • **W. Sean Davidson, PhD**¹
Pathobiology and Molecular Medicine University of Cincinnati¹ • Department of Biomedical Informatics Cincinnati Children's
Hospital Medical Center²

The Role of Apolipoprotein A-II in Triglyceride Metabolism

Graduate Student

Hypertriglyceridemia is a major health issue in the US, leading to acute pancreatitis and potentially cardiovascular disease. In the circulation, triglycerides (TG) are carried on TG-rich lipoproteins (TRL) including very low-density lipoprotein (VLDL) and chylomicrons. TG is hydrolyzed by lipoprotein lipase (LPL) residing on the vascular surface. LPL is regulated by a host of apolipoproteins on TRL, but the interplay of these factors is not fully understood. Based on literature reports that suggest that human apolipoprotein A-II (APOA2) modulate LPL activity, we added APOA2 to human plasma and assessed the impact on exogenous human LPL function. APOA2 dose dependently inhibited LPL hydrolysis of plasma TG, primarily in the VLDL fraction, as assessed by gel filtration chromatography. APOA2 also reduced TG hydrolysis when isolated VLDL was the substrate. APOA2 incubation with plasma increased APOA2 levels in VLDL but did not have major impacts on the apolipoprotein C class of proteins known to regulate LPL. APOA2, however, dose dependently drove apolipoprotein E (APOE) from the VLDL particles as assessed by quantitative mass spectrometry and immunoblotting. Since APOE is a major ligand for TRL remnant uptake in the liver, we assessed the effects of APOA2 incubation on VLDL remnant uptake in cultured hepatocytes. APOA2 addition caused a 47% reduction in lipoprotein binding to hepatocytes. Our current working model states that APOA2 increases plasma TG levels via an inhibitory effect on LPL activity and a reduction in remnant particle uptake in the liver. Current work is examining the molecular mechanism behind both effects. This understanding of factors affecting plasma TG clearance may open new avenues toward therapeutic interventions for hypertriglyceridemia.

Liya Anto, Other ¹ • Courtney L Millar, PhD ² • Mi-Bo Kim, PhD ¹ • Anisha Jain, Other ¹ • Anthony Provas, PhD ³ • Ji-Young Lee, PhD ¹ • Frank C. Nichols, PhD ⁴ • Christopher N. Blesso, PhD ¹

Department of Nutritional Sciences University of Connecticut ¹ • The Marcus Institute for Aging Research Harvard University ² • Center for Environmental Sciences and Engineering University of Connecticut ³ • Department of Periodontology UConn Health, Farmington ⁴

Microbiota-derived serine-glycine lipid 654 is reduced by high fat diet and attenuates hepatic injury, dyslipidemia, and atherosclerosis in LDL-recept

Graduate Student

Oral and gut Bacteroidetes have been shown to produce unique classes of serine-glycine bacterial lipids (BLs) that signal through Toll-like receptor 2 (TLR2). These BLs include lipid 654 (L654), a major serine-glycine lipodipeptide species found in Bacteroidetes. We have found that, compared to chow-fed mice, Bacteroidetes-derived BLs, including L654, are markedly reduced in the feces of high-fat diet (HFD)-fed obese mice, with reductions seen in as little as 2 weeks after HFD feeding. This suggests that HFD-fed, obese mice are exposed to fewer gut Bacteroidetes-derived BLs than chow-fed, lean animals. The role of gut microbiome-derived serine-glycine BLs in the development of chronic disease is currently unclear. Thus, we sought to examine the bioactivity of L654 on atherosclerosis progression and liver injury. We fed *Ldlr*^{-/-} mice a high-fat, added cholesterol diet (n = 15/group) for 14 weeks. In the last 7 weeks of HFD, mice were intraperitoneal (I.P.) injected 3 times per week with either 1 mg of L654, a major bacterial serine dipeptide lipid, or a saline-ethanol vehicle (groups BL and Vehicle, respectively). We found I.P. administration of L654 to HFD-fed *Ldlr*^{-/-} mice could significantly lower cholesterol in both serum (-24%) and liver (-35%) compared to Vehicle. BL-injection also significantly lowered aortic root plaque accumulation (-39%), serum ALT (-43%) as a marker of liver injury, and hepatic inflammation compared to vehicle control-injected mice. Liver transcriptomics analysis via RNA-Seq found 187 differentially expressed genes, of which, 183 of these genes were downregulated by L654. Gene ontology shows the changes were highly enriched in collagen-containing extracellular matrix pathways. There were also changes in phagosome-related pathways and a reduction in IFN γ -responsive MHC-class II gene expression, which is consistent with an effect on liver tolerance. Genes expressed by activated hepatic stellate cells were also reduced with L654. These changes were confirmed with real-time RT-qPCR. Conditions where gut microbiome-derived serine-glycine BLs are lost (e.g., when fed HFD or with obesity) may exacerbate development of atherosclerosis and liver injury, while correction of such BL depletion may attenuate these disorders. To confirm this hypothesis, we injected either 1 μ g of L654 or saline, every 48 hours intraperitoneally in *ApoE*^{-/-} mice (n=15/group) for 7 weeks. The animals were fed on chow throughout the study period to induce atherosclerosis and liver injury without reducing the levels of gut BLs such as L654. There was no significant difference in atherosclerosis progression, liver inflammatory markers, and liver and serum lipids between the two groups. These findings suggest that gut Bacteroidetes-derived BLs are lost with high-fat diet, and chronic exposure to the microbiota-derived serine-glycine lipodipeptide, L654, may prevent atherosclerosis progression and liver injury via hypolipidemic and anti-inflammatory effects.

Kellea Nichols ¹ • Audrey Poupeau, PhD ¹ • Eva Gatineau, PhD ¹ • Gertrude Arthur ¹ • Frederique Yiannikouris, PhD ¹
Nutritional Sciences and Pharmacology University of Kentucky ¹

Adipose-derived human soluble (pro)renin receptor causes resistance to Losartan treatment in high-fat diet male and female mice

Graduate Student

Obesity, affecting more than 37% of the US, contributes to hypertension. Despite the use of one or more anti-hypertensive treatments, 48% of the hypertensive population remains with resistant hypertension, which prompts the development for new therapeutic targets. We demonstrated that obesity increased the expression of prorenin receptor (PRR) in the adipose tissue and elevated plasma soluble PRR (sPRR). In addition, the infusion of mouse sPRR increased blood pressure in male mice fed high fat-diet (HF); indicating that adipose-derived sPRR could increase circulating sPRR and contribute to hypertension. However, there is a critical gap in the functional role of human sPRR in obesity-hypertension. In this study, we aim to define whether adipose-derived human sPRR contributes to obesity-hypertension.

Human sPRR-Myc-tag transgenic mice were bred with mice expressing adiponectin/Cre to selectively express human sPRR in adipocytes (adi-HsPRR). Adi-HsPRR and control littermate (CTL) male and female mice were fed HF-diet for 20 weeks (N=8-15/group). Body weight was assessed weekly and body composition monthly. Blood pressure was measured by telemetry after 15 weeks of diet.

Adipose-derived human sPRR did not significantly elevate body weight or fat mass (Male: CTL. 18.3±1.0g; adi-HsPRR. 17.5±0.8g. Female: CTL. 15.6±1.5g; adi-HsPRR. 11.9±1.3g; p>0.05). Systolic blood pressure (SBP) significantly increased in HF-fed male and female mice however; adipose-derived human sPRR did not further elevate SBP (24h SBP. Male: CTL. 136.0±1.7 mmHg; adi-HsPRR: 133.4±1.5 mmHg; Female: CTL. 131.9±2.8 mmHg; adi-HsPRR: 130.6±3.1 mmHg; p>0.05). Surprisingly, the anti-hypertensive effect of losartan (Los) to lower blood pressure was significantly reduced in adi-HsPRR male and female mice (Male: CTL. ΔSBP: -12.1±1.5 ΔmmHg; adi-HsPRR: -7.8±0.6 ΔmmHg; Female: CTL. ΔSBP: -13.4±1.1 ΔmmHg; adi-HsPRR: -5.7±2.3 ΔmmHg; p<0.05). In 3T3-L1 cells, sPRR significantly increased phosphorylation of ERK1/2, which was not completely blunted by Los indicating that human sPRR could act as a partial agonist of AT1R or activate ERK1/2 independently of AT1R. Our data suggests that adipose-derived sPRR does not stimulate AT1R-mediated contractility, instead impairs Los efficacy.

Jordan Howard ¹ • **Rebecca Phillip, MD** ² • **Thomas Tribble** ³ • **John Gurley, MD** ⁴ • **Sibu Saha, MD** ²

University of Kentucky College of Medicine University of Kentucky ¹ • University of Kentucky Cardiothoracic Surgery University of Kentucky ² • University of Kentucky ECMO University of Kentucky ³ • University of Kentucky Cardiology University of Kentucky ⁴

LAVA-ECMO: A Single Center Experience

Graduate Student

Introduction:

Extracorporeal Membrane Oxygenation (ECMO) is a rescue device commonly used in contemporary medical practice. The University of Kentucky has one of the premier ECMO programs in the country with 120-130 ECMO cases per year. A small number of patients on ECMO develop left ventricle distension. Left Atrial Venoarterial (LAVA) ECMO is one of the methods used to manage this complication. LAVA-ECMO was first performed at the University of Kentucky in February of 2017. The purpose of this study was to review our experience with LAVA-ECMO at UK Healthcare.

Methods:

With IRB approval, we reviewed 33 patient charts who were treated with LAVA-ECMO. We compiled demographic data, clinical diagnoses, mortality, pre-LAVA echocardiogram and lab values, post-LAVA lab values, treatment characteristics, and complications. Of the 33 patients, 7 were female and 26 were male with a median age of 55 years

Conclusion:

There are many methods to manage left ventricle distension in ECMO patients. LAVA-ECMO is an effective means of managing this serious complication.

Brad Hubbard, PhD¹ • Meenakshi Banerjee, PhD² • Shravani Prakhya² • Smita Joshi, PhD² • Hemendra Vekaria, PhD³ • Kathryn Saatman, PhD¹ • Martha Sim² • Jeremy Wood, PhD² • Sidney Whiteheart, PhD² • Patrick Sullivan, PhD⁴

Physiology University of Kentucky¹ • Molecular and Cellular Biochemistry University of Kentucky² • SCoBIRC University of Kentucky³ • Neuroscience University of Kentucky⁴

Mechanisms of thromboinflammation following experimental traumatic brain injury

Faculty

Traumatic brain injury (TBI) results in dynamic secondary and systemic mechanisms that contribute to comorbidities, such as deep vein thrombosis. Indeed, patients with TBI are at higher risk of blood clot formation due to TBI-induced hypercoagulability. Clinically, platelet dysfunction and elevated leukocyte levels have been reported following severe TBI. We seek to understand aspects of systemic pathobiology related to thromboinflammation after TBI. To investigate mechanisms of thromboinflammation, we employed two distinct, well-established models of TBI: the contusion-producing controlled cortical impact (CCI) model and the diffuse closed head injury (CHI) model. Whole blood was collected at 6h and 24h post-injury to examine parameters of hematology and leukocyte-platelet aggregation. Platelets were isolated to examine mitochondrial respiration and glycolytic profiles using Seahorse XFe96 Flux Analyzer. Finally, thrombin generation and microvesicle tissue factor were measured in platelet-poor plasma. CCI resulted in an early drop in blood leukocyte counts, while CHI increased blood leukocyte counts early after injury. Platelet-neutrophil aggregation was decreased acutely after CCI compared to sham. Furthermore, platelet bioenergetic coupling efficiency was transiently reduced at 6h and increased at 24h post-CCI. After CHI, oxidative phosphorylation in intact platelets was reduced at 6h and increased at 24h compared to sham. Finally, thrombin generation, initiated with the addition of phospholipid, was greater in CCI-injured animals compared to sham. This is accompanied by significant increases in microvesicle tissue factor early after CCI. Taken together, these data highlight preclinical recapitulation of critical changes in thromboinflammation after head injury.

Hammodah R. Alfar, MS¹ • Martha M.S. Sim, MD¹ • Melissa Hollifield, MS² • Dominic W. Chung, Other³ • Xiaoyun Fu, Other⁴ • Meenakshi Banerjee, PhD¹ • Xian Li, PhD⁵ • Alice C. Thornton, MD⁶ • James Z. Porterfield, MD, PhD⁷ • Jamie L. Sturgill, PhD⁷ • Gail A. Sievert,⁸ • Marietta Barton-Baxter, Other⁸ • Kenneth S. Campbell, PhD⁸ • Jerold G. Woodward, PhD⁹ • Jose A. Lopez, Other³ • Jeremy P. Wood, PhD¹ • Beth A. Garvy, PhD² • Sidney W. Whiteheart, PhD¹
 Department of Molecular and Cellular Biochemistry University of Kentucky¹ • Department of Microbiology, Immunology and Molecular Genetics University of Kentucky² • Department of Biochemistry University of Washington³ • Bloodworks Northwest Bloodworks Northwest⁴ • Saha Cardiovascular Research Center University of Kentucky⁵ • Division of Infectious Disease University of Kentucky⁶ • Department of Microbiology, Immunology and Molecular Genetics University of Kentucky⁷ • Center for Clinical and Translational Science University of Kentucky⁸ • 2Department of Microbiology, Immunology and Molecular Genetics University of Kentucky⁹

Early vs. Late Coagulopathies: Differences between SARS-CoV-2/COVID-19 and HIV1/AIDS

Graduate Student

Background

Currently, we are living in two pandemics: SARS-CoV-2/COVID-19 and HIV1/AIDS. Both of these viral infections are associated with an increased risk of developing cardiovascular complications (CVC). SARS-CoV-2 infections are associated with coagulopathies especially in elderly patients and patients with other comorbidities at the early stages of the disease. The infection is characterized by elevated D-dimer, prolonged prothrombin time (PT), and mild thrombocytopenia. Early reports suggested that inflammation, platelet activation, or endotheliopathy drives the coagulopathies in these patients. On the contrary to SARS-CoV-2, HIV1 infection by itself increases the risk of developing occlusive CVC twofold, independent of age, lifestyle, and the presence of comorbidities. Therefore, we aim to investigate the similarities and differences between the two viral infections in inducing CVC.

Aims

- To assess the similarities and differences between SARS-CoV-2 and HIV1 infection in inducing CVC
- To follow recovered SARS-CoV-2 infected individuals to assess their susceptibility to long term inflammation and increased risk of developing CVC
- Characterize the inflammatory response in Post-Acute Sequelae of COVID-19 (PASC) patients

Methods

This study was approved by the Institutional Review Board. Citrated plasma was collected from consenting HIV1+ (19 naïve, 11 on antiretroviral therapy, ART) or SARS-CoV-2+ (28 inpatients, 49 outpatients) and healthy controls (31). Our study includes PASC patients (~25%), who are negative for the viral infection but still have symptoms of exhaustion.

Results

In contrast to HIV1, SARS-CoV-2 infection activates and mediates endothelial cell damage, induces the innate immune cells to release pro/anti-inflammatory in the ICU patients as measured by increased levels of vWF, E-Selectin, IL-6, IL-8, IL-10, TNF- α , Myeloperoxidase (MPO), and Monocyte Chemoattractant protein-1 (MCP-1). Interestingly, PASC patients and outpatients did not have an increase in the aforementioned cytokines and their levels did not change over time after recovery. However, neither one of these viral infections was associated with increased levels of platelet activation markers such as PF4, IL-1 β , and sCD40L.

Conclusions

- SARS-CoV-2/COVID-19 and HIV1/AIDS induce different cytokine responses that might be responsible for the endothelial activation observed in SARS-CoV-2/COVID-19 which might precipitate CVC in patients with other comorbidities.
- Recovered SARS-CoV-2/COVID-19 patients did not have elevated levels of inflammatory cytokines or endothelial activation markers
- PASC patients did not have a different pattern of immune response compared to other patients

Ezekiel Rozmus, Don E. Burgess, Allison R. Hall, Jennifer L. Smith, Elizabeth A. Schroder, Brian P. Delisle ¹
Physiology University of Kentucky ¹

Analysis of KCNH2 variants to determine risk of Long-QT Syndrome development

Graduate Student

A major challenge in preventing sudden death associated with inherited arrhythmia syndromes lies in identifying people at risk before they suffer a life-threatening cardiac event. Congenital long QT syndrome (LQTS) delays ventricular repolarization and increases the risk for fatal tachyarrhythmias. Most LQTS cases are directly linked to mutations in genes that encode cardiac ion channels. Genetic screening for mutations associated with LQTS cannot be used as a diagnostic tool, because many rare non-synonymous genetic variants in LQTS-susceptibility genes are thought to be neutral and not cause disease. The purpose of this project was to develop strategies that facilitate the early identification of risk in candidate LQTS-associated mutations from a large biobank.

We identified twelve genetic variants of uncertain significance in the LQTS-associated gene *KCNH2* from a large biobank. We studied the functional properties of the *KCNH2*-encoded Kv11.1 channel protein variants using heterologous expression. Western blot analysis of HEK293 cells expressing the variants was used to estimate their trafficking efficiency, and voltage clamp analysis was used to measure current density and changes in Kv11.1 channel gating. Computational simulations were performed to determine which functional changes predicted a prolongation in the ventricular action potential duration, which can correspond with a prolonged QT interval.

Western blot analysis of cells expressing most of the Kv11.1 channel variants suggested that they trafficked similar to the wild-type (WT) Kv11.1 channels. Two variants, S320L- and G749V-Kv11.1 showed decreased trafficking. Voltage-clamp analysis showed the cells expressing S320L or G749L also had decreased maximal currents. Voltage clamping analysis also demonstrated that currents measured from cells expressing Kv11.1 channel proteins with the S320L variant had slower deactivation kinetics. In contrast cells expressing the Kv11.1 channel L552S and R1033W variants showed an acceleration in the recovery from inactivation. In silico modeling suggests that only the G749L variant produced a functional phenotype that is expected to cause ventricular action potential prolongation similar to other LQTS-associated mutations.

We screened a dozen variants of uncertain significance in the LQTS-associated gene *KCNH2*. The data suggest that combining genetic and functional testing might be able to distinguish candidate LQTS-linked variants. We expect this strategy will serve as a platform for using genetic sequencing and functional screening to aid in the early identification and personalized treatment of people with LQTS. Although several variants demonstrated changes in gating activity, we cannot conclude that all dysfunctional variants contribute to a prolongation of the action potential or associate with LQTS. Therefore, we can conclude that the only a subset of dysfunctional Kv11.1 channel variants are expected to associate with LQTS.

Benton Maglinger, MS¹ • Christopher McLouth, PhD² • Jacqueline Frank, Other³ • Madison Sands, MS³ • Lila Sheikhi, MD³ • Shivani Pahwa, MD⁴ • David Dornbos III, MD⁵ • Chintan Rupareliya, MD³ • Jordan Harp, PhD⁶ • Amanda Trout, PhD³ • Jadwiga Turchan-Cholewo, PhD³ • Ann Stowe, PhD³ • Justin Fraser, MD⁵ • Keith Pennypacker, PhD³
 Neurology University of Kentucky¹ • Behavioral Science University of Kentucky² • Neurology University of Kentucky³ • Radiology University of Kentucky⁴ • Neurosurgery University of Kentucky⁵ • Neuropsychology University of Kentucky⁶

Influence of Body Mass Index on Adenosine Deaminase and Infarct Volume in Mechanical Thrombectomy Subjects

Graduate Student

Background: Emergent Large Vessel Occlusion (ELVO) strokes are devastating ischemic vascular events for which novel biomarkers and therapies are needed. The purpose of this study is to investigate the role of Body Mass Index (BMI) on protein expression and signaling at the time of ELVO intervention. Uncovering relationships between BMI, proteomic expression, and stroke outcome measures will aid in personalizing prognosis and future treatment of ELVO stroke.

Methods: The Blood And Clot Thrombectomy Registry And Collaboration (BACTRAC) is a continually enrolling tissue bank (clinicaltrials.gov NCT03153683) from stroke patients undergoing mechanical thrombectomy (MT). N=61 human carotid plasma samples were analyzed for inflammatory and cardiometabolic protein expression by Olink Proteomics. Statistical analyses used t-tests, linear, logistic, and robust regressions, to assess the relationship between BMI, proteomic expression, and stroke related outcomes.

Results: The 61 subjects studied were broken into three categories: Normal weight (BMI 18.5-24.9) which contained 19 subjects, Overweight (BMI 25-30) which contained 25 subjects, and Obese (BMI ≥ 30) which contained 17 subjects. Normal BMI group was a significantly older population (mean 76 years) when compared to Overweight (mean 66 years) and Obese (mean 61 years) with significance of $p=0.041$ and $p=0.005$, respectively. When compared to Normal weight and Overweight categories, the Obese category had significantly higher levels of adenosine deaminase (ADA) expression ($p=0.01$ and $p=0.039$, respectively). Elevated levels of ADA were found to have a significant positive correlation with both infarct volume and edema volume ($p=0.013$ and $p=0.041$, respectively), and were associated with a more severe stroke (NIHSS on discharge) and greater stroke-related disability (mRS on discharge) with significance of $p=0.053$ and $p=0.032$, respectively). When controlling for age and sex, increased infarct volumes were predicted by higher ADA levels in the Obese population ($p=0.009$), while increased ADA levels were not predictive of increased infarct volumes in the Normal weight category.

Conclusions: When examined according to BMI, subjects undergoing mechanical thrombectomy for ELVO demonstrate significant differences in the expression of certain plasma proteins including ADA. The protein ADA is a deaminating enzyme that degrades adenosine, which has been shown to be neuroprotective in ischemia. Levels of ADA were found to be significantly higher in the Obese population when compared to Normal or Overweight groups. Increased levels of ADA in the Obese group were predictive of increased infarct volumes. Further testing will explore the relationship of BMI and ADA on cognitive function outcomes utilizing MoCA scores at both discharge as well as 90-day follow ups. These data provide novel biomarker candidates as well as treatment targets while increasing the personalization of stroke prognosis and treatment.

Velmurugan Gopal Viswanathan, PhD¹ • Sathya Velmurugan, PhD¹ • Deepak Kotiya, PhD¹ • Sanda Despa, PhD² • Florin Despa, PhD¹

Pharmacology and Nutritional Sciences University of Kentucky¹ • Pharmacology and Nutritional Sciences University of Kentucky²

Diabetic cardiomyopathy is partially reversed by knocking-down human amylin in mice with conditional expression of human amylin in the pancre- β -cells

Postdoc

Rationale: Amylin dyshomeostasis is associated with diabetic cardiomyopathy in humans and in rodents expressing human amylin in the pancreatic β -cells.

Objective: To study whether lowering human amylin in the circulation reverses diabetic cardiomyopathy in mice with pancreatic-specific expression of human amylin.

Methods: Humanized amylin mouse model was generated by targeted replacement of rodent amylin by floxed human amylin gene (HuAmy^{f/f}) and was made conditional with pancreas-specific Cre-ERT² mice. Wild type (WT), amylin knock-out (AKO), HuAmy^{f/f} and Cre-ER-HuAmy^{f/f} mice (n=10/group) were fed with high fat diet (HFD) for 4 mo from 3 mo of age to enhance amylin secretion. Cre-ER-HuAmy^{f/f} mice were treated tamoxifen (or vehicle) to downregulate amylin after 2 mo of HFD. Metabolic and cardiac phenotypes were measured terminally at 4 mo of HFD.

Results: In comparison to WT and AKO mice, HuAmy^{f/f} mice show increased insulin resistance and glucose intolerance, hyperglycemia, enhanced HOMA-IR, insulin resistance, decreased AKT signaling with decreased ejection fraction, decreased fractional shortening, increased left ventricular mass, and increased left ventricular internal diameter. Human amylin knockdown in Cre-ER-HuAmy^{f/f} mice partially reverses metabolic and cardiac phenotype similar to WT and AKO mice.

Conclusions: Reducing amylin dyshomeostasis slows the progression of diabetic cardiomyopathy in mice transgenic for human amylin. Further studies are needed to uncover molecular mechanisms by which anti-amylin therapies improve heart function in the setting of type-2 diabetes.

Sathya Velmurugan, PhD¹ • Hailey Mair¹ • Guo Yin, PhD¹ • Florin Despa, PhD¹ • Sanda Despa, PhD¹
Pharmacology and Nutritional Sciences University of Kentucky¹

Inhibition of Na⁺-glucose cotransporter 1 reduces arrhythmogenesis in diabetic rats

Postdoc

Rationale: Type-2 diabetes (T2D) is associated with a higher risk for arrhythmias, but the underlying mechanisms are incompletely elucidated. The expression and function of the Na⁺-glucose cotransporter 1 (SGLT1) are elevated in T2D hearts, which may result in larger myocyte Na⁺ concentration ([Na⁺]_i) and thus promote the occurrence of pro-arrhythmogenic Ca²⁺ sparks and waves. Moreover, SGLT1 is electrogenic and may depolarize the myocytes at rest.

Objective: To test the effect of SGLT1 inhibition on the electrical signaling in diabetic hearts.

Methods/Results: Rats expressing human amylin in the pancreatic β-cells (*HIP rats*) were used as a model of late-onset T2D and their WT littermates served as controls. [Na⁺]_i (measured with the fluorescent indicator SBFI), Ca²⁺ spark frequency (measured in cells loaded with Fluo-4 using the linescan mode of a confocal microscope) and incidence of ventricular arrhythmias (measured by surface ECG in anesthetized rats) were exacerbated in HIP versus WT rats, while the resting membrane potential (E_m; assessed by patch-clamp) was depolarized. SGLT1 inhibition with phlorizin (250 μM; 2 hours incubation) reduced [Na⁺]_i and Ca²⁺ spark frequency and normalized resting E_m in myocytes from diabetic HIP rat. Moreover, perfusion with phlorizin (50 μM) reduced the duration of arrhythmias induced by a stress test with caffeine and isoproterenol in Langendorff-perfused hearts.

Conclusion: SGLT1 inhibition improves the electrical activity of T2D hearts.

Smita Joshi, PhD¹ • Sidney W. Whiteheart, PhD¹
Molecular and Cellular Biochemistry University of Kentucky¹

Vesicle-Associated Membrane Proteins (VAMPs) regulate platelet cargo distribution

Postdoc

Platelets are crucial to maintaining the vascular microenvironment. Upon vascular injury, they interact with extracellular matrix proteins and release cargo contents from their granules. These cargo are either synthesized by megakaryocytes or platelets (from residual mRNAs) or endocytosed from plasma. *De-novo* synthesized or endocytosed cargo travel through specialized compartments like endosomes or multivesicular bodies and are packaged in granules. Platelets have three types of granules—delta, alpha, and lysosomes. While delta granules contain cargo important for amplifying platelet responses, lysosomal cargo are important for clot remodeling. Alpha granules have the most diverse composition including growth factors, cytokines, chemokines, and angiogenesis regulators, which are important in inflammation, immunity, wound healing, and many other processes.

Platelet granule release is mediated by Soluble N-ethylmaleimide Sensitive Factor Attachment Protein Receptors (SNAREs) and their regulators. To drive secretion, vesicle (v)-SNARE on granules and target (t)-SNARE on the plasma membrane (PM) form a *trans*-bilayer complex that mediates membrane fusion. Apart from granule secretion, the VAMPs also play a role in intracellular trafficking. VAMP-3 mediates endocytosis while VAMP-7 and VAMP-8 are considered endosomal v-SNAREs. Platelets contain Vesicle-Associated Membrane Protein (VAMP)-2, -3, -4, -5, -7, and -8 although, VAMP-4 and -5 are present in trace amounts. To study how VAMPs regulate platelet cargo levels, we generated several VAMP-deficient mouse strains that lack either one VAMP isoform or combinations of VAMPs. The theoretical levels of VAMPs in these platelets vary from 100% to trace amounts based on previous mass-spec and quantitative blotting analysis. Using commercial antibody arrays, we probed for 53 different cargo proteins in VAMP-deficient platelets. Cargo levels were minimally affected (relative to wild-type) in VAMP7^{-/-} platelets and drastically reduced in NBL2^{-/-} platelets. (NBL2 is a sorting protein whose deletion causes Grey Platelet Syndrome). While all strains showed some decreases, VAMP-(2/3)^{Δ/Δ}(7/8)^{-/-} and VAMP-(2/3)^{Δ/Δ}(8)^{-/-} platelets showed significant reductions. Clustering the cargo molecules into quartiles, based on their levels, showed a notable pattern as more than 80% of cargo in NBL2^{-/-}, VAMP-(2/3)^{Δ/Δ}(8)^{-/-} and VAMP-(2/3)^{Δ/Δ}(7/8)^{-/-} platelets were less than 75% of wild-type. About 50% of cargo in VAMP-(3/7)^{-/-} and 70% of cargo in VAMP-(7/8)^{-/-} platelets were less than 75% of the WT. These patterns suggest that all VAMP isoforms contribute to platelet cargo trafficking to some extent. The data further suggest that cargo distribution is stochastic, non-thematic, and could be regulated overlapping functions of the VAMPs. This is the first report indicating the relative contributions of VAMPs in platelet trafficking on a global level.

Aaron Chacon, MS¹ • Wen Su, MD² • Tianfei Hou, PhD² • Ming Gong, MD, PhD² • Zhenheng Guo, PhD¹
Pharmacology & Nutrition Sciences University of Kentucky¹ • Physiology University of Kentucky²

Targeting the GLP-1 Receptor as New Chronotherapy Against Nondipping Blood Pressure In Diabetes

Graduate Student

Objective:

It is well established that a regular blood pressure (BP) rhythm is critical for maintaining cardiovascular health. Nondipping BP (<10% reduction during rest period) is prevalent in type 2 diabetes (T2DM). Exenatide, a short half-life GLP-1 receptor agonist used to treat hyperglycemia in T2DM, has also shown to lower BP and inhibit food intake. However, whether timing of its administration has an effect on nondipping BP in T2DM has not yet been explored.

Approach & Results:

13-week old diabetic *db/db* mice, who exhibit nondipping BP and poor food intake rhythm, were injected i.p. with exenatide at either onset of light (ZT0 Ex) or dark (ZT12) phases. BP was recorded via radiotelemetry, allowing for fully conscious, free-moving data collection. Food intake was collected via BioDAQ (Research Diet, New Brunswick, NJ) allowing for continuous food intake recording. BP dipping was achieved following daily ZT0 administration and worsened to “reversed dipping” (increase in BP over dark phase levels) from daily ZT12 administration; 10.5 and -4.5% in mean arterial pressure (MAP), respectively. MAP rhythms were evaluated by cosinor analysis revealing significant changes in robustness of +37.4% (ZT0 Ex) and -3.2% (ZT12 Ex) over basal levels. Amplitude increased significantly in ZT0 Ex but not in ZT12 Ex. Acrophase shifted 10.5 hours, peaking in the middle of the light phase for ZT12 Ex with no significant difference in ZT0 Ex. Both treatment groups saw a significant reduction in MESOR of 10.86 (ZT0 Ex) and 10.26 (ZT12 Ex) mmHg, demonstrating equivalent BP-reducing efficacy. Correlating with BP changes, light/rest phase food intake was significantly reduced by 10.5% (ZT0 Ex) and increased 20.3% (ZT12 Ex) over basal levels. 24-h food intake was not significantly affected in either treatment group.

Conclusion:

While treatment groups saw equivalent reductions in BP, their rhythms were flipped. This reveals an important, previously unexplored role of exenatide in the treatment of nondipping BP in T2DM, potentially mediated by the improvement in food intake rhythm, independent of caloric intake.

Harry Chanzu¹ • Joshua Lykins, ¹ • Smita Joshi, PhD ¹ • Martin Chow, PhD ¹ • Irina Pokrovskaya, MS ² • Brian Storrie, PhD ² • Gunnar Pejler, PhD ³ • Sidney W. Whiteheart, PhD ¹

Molecular and Cellular Biochemistry University of Kentucky ¹ • Physiology and Biophysics University of Arkansas for Medical Sciences ² • Medical Biochemistry and Microbiology Uppsala University ³

Serglycin, an Intragranular Proteoglycan with Many Effects on Platelet Function

Postdoc

Background

Upon vascular injury, platelets are activated and release molecules that affect the vascular microenvironment, promoting coagulation, wound healing, and clot architecture. Previously, we have shown that serglycin (SRGN), an intra-granular proteoglycan, plays multiple roles during platelet granule cargo packaging, retention and release, and in the extracellular environment by affecting receptor shedding.

Aims

To investigate SRGN's function in platelet cargo packaging and release and granule-plasma membrane pore dynamics upon platelet activation. Second, to define SRGN's role in platelet surface proteins shedding and downstream signaling.

Methods

Anti-SRGN nanobodies were produced in alpacas using recombinant, unglycosylated SRGN. These were used in detecting SRGN/PF4 complex and will be a crucial tool in pulldown assays to study the interaction of SRGN with platelet releasate proteins to identify interacting partners. Serial block face EM was used to study how SRGN affects granule-plasma membrane pore dynamics and release kinetics upon activation. Western blotting was used to determine how SRGN affects membrane protein shedding and downstream signaling.

Results

Platelets from SRGN^{-/-} showed reduced α -granule decondensation and swelling upon stimulation. We have generated platelets from SRGN^{-/-} and wild-type control mice to examine fusion pore expansion by 3D EM analysis. In 3D data analysis, we have observed striking details in α -granule morphology of SRGN^{-/-} platelet compared to SRGN^{+/+} platelets. Resting platelets for SRGN^{-/-} mice contain α -granule that are interconnected and elongated. Expressed recombinant SRGN protein to be used as an antigen and for screening our cDNA library. Using ELISA, we screened sera from immunized alpaca to confirm the immune response. The initial panning of the libraries shows promising clones that recognize the recombinant SRGN protein, and one tested nanobody pulls down SRGN containing complexes, as demonstrated by heparin treated SRGN/PF4 complex assay. GPVI shedding increased in SRGN^{-/-} platelets after convulxin treatment, but GP1b was unaffected compared to SRGN^{+/+} controls suggesting different roles of SRGN in receptor shedding and downstream signaling.

Conclusions

SRGN regulates α -granule decondensation and swelling after stimulation, affects granule morphology in resting platelets, affects convulxin-induced GPVI shedding in platelets, and influences cargo composition and release in both megakaryocytes and platelets. Nanobodies generated will be an invaluable reagent for studying SRGN interacting partners and determining SRGN's localization in a growing clot.

Nicholas McVay, MS¹ • Bryana Levitan, Other¹ • Andrea Sebastian² • Garrett Elmore² • Douglas Andres, PhD³ • Jonathan Satin, PhD²

Physiology University of Kentucky¹ • Physiology University of Kentucky² • Biochemistry University of Kentucky³

Hyperglycemia Modulates the L-type Calcium Channel in the Heart

Graduate Student

Background: A 2-hit hypothesis has been suggested for hyperglycemia to promote arrhythmogenesis in large mammals, whereby compromised repolarization reserve (hit 1), in addition to hyperglycemia (hit 2), leads to action potential duration (APD) prolongation. By contrast in mice, acute elevated glucose alone prolongs APD. Hyperglycemia is a pleiotropic trigger that initiates diverse effects such as PKA activation, and O-linked GlcNAcylation of proteins such as CaMKII and CaV1.2 – the pore-forming subunit of the L-type calcium channel (LTCC). We have been studying Rad-mediated PKA modulation of $I_{Ca,L}$. It is unknown whether cardiomyocyte $I_{Ca,L}$ responds similarly to elevated glucose.

Hypothesis: Hyperglycemia acutely modulates LTCC current ($I_{Ca,L}$). *Ceteris paribus*, increased late-phase $I_{Ca,L}$ will prolong the QT interval.

Methods/Approach: $I_{Ca,L}$ was measured from isolated ventricular cardiomyocytes using the whole cell configuration of the patch clamp technique. To dissect Rad-dependent versus -independent effects we used Rad-expressing (CTRL) and adult induced, cardiomyocyte-restricted Rad knockout mice (cRadKO). Surface ECG recordings, before and after a glucose tolerance test were also performed. streptozotocin-treatment modeled type 1 diabetes (T1D). Echocardiography measured *in vivo* function in non-diabetic (ND) and T1D, and CTRL and cRadKO mice. Statistical treatments consider diabetes-effect and gene-effect.

Results: Acute glucose increased $I_{Ca,L}$ in CTRL ($13 \pm 3.1\%$, $n=7$) and cRadKO ($14 \pm 2.3\%$, $n=12$). *In vivo*, acute glucose increased QT interval ($+5.0 \pm 0.8$ ms, $p=0.01$; $N=5$ mice). In T1D, evidence for CTRL cardiomyocyte remodeling is manifested as acquisition of significantly increased $I_{Ca,L}$ facilitation (5.3% to 35%, ND to T1D, respectively); however in cRadKO no further increase of facilitation was observed. In T1D acute glucose increased $I_{Ca,L}$ in CTRL ($11 \pm 3\%$, $n=3$) and in cRadKO ($8.3 \pm 3\%$, $n=5$). T1D did not significantly decrease $I_{Ca,L}$ in CTRL (ND -3.5 ± 0.5 pA/pF, T1D -2.4 ± 0.5 pA/pF) or in cRadKO (ND -5.4 ± 0.5 pA/pF, T1D -6.2 ± 0.8 pA/pF). Despite the dramatic facilitation increase caused by T1D CTRL, facilitated $I_{Ca,L}$ in T1D remained significantly elevated by cRadKO (CTRL -2.7 ± 0.3 pA/pF, cRadKO -8.3 ± 0.9 pA/pF).

Conclusions: Glucose acutely modulates $I_{Ca,L}$, and Rad is dispensable for glucose modulation; however, this does not preclude synergistic modulatory effects. In T1D glucose modulation trends towards attenuated levels. During a glucose tolerance test QT interval is also prolonged by elevated glucose. Mechanistically, persistent activated CaMKII in T1D promotes pathological remodeling. The presence of facilitated $I_{Ca,L}$ in ND, cRadKO suggests that CaMKII local to the LTCC promotes positive inotropic function without remodeling effects. Ongoing studies will evaluate the ability of cRadKO to blunt progression of diabetic cardiomyopathy.

Xian Li, PhD¹ • Xiao-Hong Song, MD² • Martha M.S. Sim, MD³ • Jeremy P. Wood, PhD⁴

Saha Cardiovascular Research Center University of Kentucky¹ • Saha Cardiovascular Research Center University of Kentucky² • Saha Cardiovascular Research Center University of Kentucky³ • Saha Cardiovascular Research Center University of Kentucky⁴

Protein S Coordinates the Synergistic Inhibition of Prothrombinase by Tfpia and Activated Protein C

Staff

Background: Protein S (PS) is a cofactor for the anticoagulants activated protein C (APC) and tissue factor pathway inhibitor alpha (TFPI α), which inhibit factors Va (FVa) and Xa (FXa), respectively. FVa and FXa form prothrombinase, which activates prothrombin. Neither the PS/APC nor PS/TFPI α system is independently effective at inhibiting thrombin generation by prothrombinase. We hypothesize that they instead function cooperatively.

Aims: To elucidate the regulation of prothrombinase by PS/APC/TFPI α .

Methods: The anticoagulant activities of PS, APC, and TFPI α were measured in purified protein and plasma-based assays, utilizing recombinant proteins to assess the individual cofactor functions of PS.

Results: FXa protected FVa from degradation by APC/PS, as described by other groups, but TFPI α dose-dependently reversed this protection. Similarly, exogenous TFPI α reduced plasma thrombin generation (ETP) 2-fold more when thrombomodulin was added to promote APC activation. Conversely, antibodies against TFPI α and APC had a synergistic effect and, when combined, promoted plasma thrombin generation and fibrin formation to the same extent as an antibody against PS alone.

We expressed a protein consisting of the APC-binding domains of PS (EGF1-2) to assess the effect of APC on PS/TFPI α function. In a purified protein assay, EGF1-2 dose-dependently blocked the APC cofactor activity of 50nM PS, but had no effect on the TFPI α activity. In the presence of EGF1-2, APC still promoted prothrombinase inhibition by PS/TFPI α (ETP decreasing 58.2% vs control).

We similarly assessed the impact of PS/APC on TFPI α , using a protein from the saliva of black flies, "black fly protease inhibitor" (BFPI), which mimics TFPI α but does not bind PS. In the absence of APC, with or without PS, BFPI had no effect on thrombin generation. However, in the presence of APC and PS, BFPI decreased the maximum rate of thrombin generation by 17.3+/-3.3%.

Conclusions: The PS/APC and PS/TFPI α systems work synergistically to downregulate prothrombinase and prevent thrombosis.

Kanakanagavalli Shravani Prakhya¹, Hemendra Vekaria, PhD¹ • Danielle Coenen, PhD² • Patrick Sullivan, PhD¹ • Sidney Whiteheart, PhD³

Department of Neuroscience University of Kentucky¹ • Department of Cellular and Molecular Biochemistry University of Kentucky² • Department of Cellular and Molecular Biology University of Kentucky³

Understanding the role of mitochondria in platelet function

Graduate Student

To mediate hemostasis, platelets use energy-dependent processes (e.g., activation, aggregation, granule secretion, clot formation, and contraction), yet it is unclear what metabolic fuels and energy-producing pathways are required for which platelet function. Platelets have metabolic flexibility, using several fuels (glucose, glycogen, etc.) and switching between glycolysis and oxidative phosphorylation (OxPhos); however, the relative roles of these ATP-generating processes are unclear. We are developing tools and models to study platelet bioenergetics and mitochondrial function in hemostasis.

To study platelet bioenergetics, we developed a continuous tracking clot contraction assay that yields multiple kinetic parameters: lag time, rate, extent, and the area under the curve (AUC). Metabolic inhibitors and a platelet-specific TFAM (Transcription Factor A Mitochondrial) deletion were used to probe the importance of platelet bioenergetics and mitochondrial function. TFAM is a transcription factor that is important for mitochondrial genome compaction (like histones). It is not only essential for maintaining the integrity of the mitochondrial genome but also for transcription of mitochondrial genes which encode for subunits of Electron Transport Chain complexes. To study platelet mitochondrial function, we created a platelet-specific KO of TFAM.

Clot contraction of TFAM^{-/-} platelets (TFAM^{flox/flox::PF4^{Cre+}}) showed defective rate, extent, and AUC at low thrombin concentration (5 mU/mL), but were normal at higher (20 mU/mL). When clot contraction was measured in the presence of a glycolysis inhibitor (2-Deoxyglucose or a glycogen phosphorylase inhibitor (CP 316819), platelets from TFAM mice showed decreased rate and extent of clot contraction. Other low energy-dependent processes such as secretion and aggregation were not affected. Using Bioflux, a microfluidic flow channel system, we have observed that TFAM^{-/-} platelets had an impaired and unstable thrombus formation showing that the formation of thrombi and its stability is energy-dependent and platelet mitochondrial bioenergetics is important for thrombus formation underflow. These experiments are supported by a preliminary *in vivo* Ferric Chloride injury model where we noted an increase in occlusion time but there was no significant change in the tail-bleeding assay.

In conclusion, we have developed a continuous tracking clot retraction assay to study platelet bioenergetics and developed a new mouse model with dysfunctional mitochondrial bioenergetics. We have seen that low energy-demanding processes like secretion and aggregation were not affected in TFAM KOs but clot contraction at low thrombin and thrombus formation under shear was impaired. We also observed no hemostatic effects but impaired thrombosis with our KOs. This model can be an important model to better understand how platelet mitochondrial bioenergetics plays a role in metabolic disorders like diabetes and aging.

Yasir Alsiraj, PhD ¹ • Heba M Ali ² • Lisa Cassis, PhD ²

Pharmacology and Nutritional Sciences University of Kentucky ¹ • Pharmacology and Nutritional Sciences University of Kentucky ²

Role of two X sex chromosomes in the development of atherosclerosis

Faculty

Background: Circulating lipids and atherosclerosis are different between women and men. Estrogens promote favorable lipids, but hormone replacement therapy in postmenopausal women increased the risk of heart disease. We recently demonstrated that sex chromosomes, namely an XX sex chromosome complement, promoted levels of circulating proatherogenic lipids and the development of atherosclerosis in mice. In this study, we hypothesized that XX female (XXF) mice will have higher levels of circulating pro-atherogenic lipids and atherosclerosis than XO females (XOF) through a gene dosage mechanism.

Methods and Results: We bred male low-density lipoprotein receptor deficient (Ldlr^{-/-}) mice with a structurally re-arranged Y chromosome to female XX Ldlr^{-/-} mice to generate female mice with one or two X chromosomes. Mice were fed a Western diet (42% kcal as fat; 0.15% cholesterol, Teklad TD88137) for 3 months. At the study endpoint, body weight was not significantly different between XXF and XOF mice (XXF: 24.5 ± 1.2; XOF: 22.6 ± 0.6 g; P>0.05). Similarly, total serum cholesterol concentrations were not significantly different between XXF and XOF mice (XXF: 1,746 ± 93; XOF: 1,702 ± 61 mg/dL; P>0.05). In contrast, the percentage of atherosclerotic lesions in the aortic arch was significantly lower in XOF than XXF mice (XXF, 20.6 ± 10.3; XOF, 8.1 ± 4.4 % lesion surface area; P<0.05). To investigate gene dosage effects from two X chromosomes, we quantified the mRNA abundance of genes known to escape X-inactivation in thoracic aortas (the site for atherosclerotic lesion formation) from XXF and XOF mice. Two genes known to escape X-inactivation (Kdm5c and Kdm6a; lysine histone demethylases) exhibited higher mRNA abundance in thoracic aortas of XXF than XOF mice (Kdm5c: XXF, 1.09 ± 0.19; XOF, 0.33 ± 0.21; P<0.05; Kdm6a: XXF, 1.05 ± 0.15; XOF, 0.43 ± 0.15; P<0.05).

Conclusion: These data indicate that two X chromosomes in female mice augment the development of atherosclerosis compared to females with one X chromosome. Higher atherosclerosis of XXF than XOF mice was not accompanied by increased levels of circulating cholesterol. Rather, genes escaping X-inactivation in thoracic aortas, such as Kdm5c and Kdm6a, may contribute to gene dosage influences from two X chromosomes.

Madison Hickey, Thomas Tribble BA, CST¹ • Sibuh Saha MD, MBA²

Gill Heart and Vascular Surgery University of Kentucky¹ • Cardiovascular and Thoracic Surgery University of Kentucky²

Interhospital ECMO transport of patients experiencing ARDs and/or Cardiogenic shock and their survival outcomes

Medical Student

Introduction:

Extracorporeal membrane oxygenation (ECMO) has grown considerably in the past decade among patients experiencing cardiogenic shock and/or acute respiratory distress syndrome (ARDS). ECMO is not yet utilized in all hospitals because of limited access to resources, staff, or technology needed to support these complex patients. The University of Kentucky (UK) is currently considered an ECMO center of excellence, meaning they partner with regional hospitals to help support and treat complex patients on ECMO. Regional hospitals often transfer these patients to UK for further management of care.

Objective: To investigate differences in survival outcomes among patients transferred to UK on Venous-arterial (VA) vs Venous-venous (VV) ECMO and those started on ECMO at UK.

Methods: With IRB approval, data was retrospectively gathered and analyzed from electronic medical records of 95 adult patients transferred to the University of Kentucky (UK) on ECMO or placed on ECMO upon arrival. The average distance traveled was 113.31 miles and the average time was 113.80 minutes. The data that was extracted included sex, BMI, age, procedure prior to ECMO cannulation, type of ECMO (Venous-arterial or Venous-venous), time of ECMO placement (before transportation to UK or at UK), and patient outcome (expired or survived to hospital discharge).

Results: Between August 2015 and December 2019, 95 patients were placed on ECMO and transported to UK for further management of care or transferred to UK to be placed on ECMO. 53 patients were placed on Venous-arterial ECMO, while 35 patients, were placed on Venous-venous ECMO, and 2 patients were placed on both throughout their care. Patients placed on VV ECMO had higher survival to discharge, 54.5%, compared to VA ECMO, 37%. VV ECMO patients were on ECMO for an average longer amount of time, 10.21 days, compared to VA ECMO, 4.35 days. VV ECMO also had shorter average travel time, 102.24 minutes, and average travel distance, 109.76 miles, compared to VA ECMO which had an average travel time of 125.28 minutes, and an average travel distance of 119.79 miles.

Conclusions: Interfacility VA or VV ECMO transport can be done safely with an experienced team. UK continues to be a leading center of excellence in regional ECMO patient care, meaning many patients are transferred here. Patients experiencing cardiogenic shock or acute respiratory distress syndrome can have improved chances of survival following transfer to UK.

Jacob DeMott¹ • Tyler W. Benson, PhD¹ • Kelsey A. Conrad, PhD¹ • J. Mark Brown, PhD² • Stanley Hazen, MD, PhD² • A. Phillip Owens III, PhD¹

Internal Medicine University of Cincinnati¹ • Cardiovascular and Metabolic Sciences Cleveland Clinic²

Inhibition of the TMAO formation pathway attenuates abdominal aortic aneurysm (AAA) incidence and survival in an angiotensin II mouse model

Staff

Introduction: Trimethylamine N-oxide (TMAO) is an inflammatory mediator derived from dietary carbon fuel sources. Our lab has demonstrated circulating TMAO is highly correlated with abdominal aortic aneurysm (AAA) diameter and growth rate in human cohorts. Moreover, mice fed a choline-enriched diet have significantly elevated plasma TMAO with augmented AAA incidence and diameter. However, a causal link has not yet been demonstrated. As such, the objective of these studies was to inhibit TMAO formation along the meta-organismal pathway to definitively determine causality in aneurysm formation.

Methods/Results: Two separate approaches were employed to inhibit the production of TMAO. First, fluoromethylcholine (FMC), an inhibitor of the CutC/D enzymatic complex, was supplemented in the drinking water of *Ldlr*^{-/-} mice for two weeks prior and throughout the study, whereas control *Ldlr*^{-/-} mice were maintained on standard water. Mice were switched to a high choline (1.2% wt/wt) and high cholesterol (0.2% cholesterol) diet 1 week prior to infusion with angiotensin II (AngII; 1,000 ng/kg/day) via osmotic mini-pump. After 28 days, all surviving mice were euthanized, plasma was collected, and the aortic diameters measured. Analysis of plasma samples revealed a significant reduction in circulating trimethylamine (TMA) and TMAO. FMC significantly reduced the incidence of AAA and rupture-induced death compared to control mice ($P < 0.001$). FMC treated significantly attenuated CD68 macrophage into the aneurysmal region of the aorta as measured by fluorescent microscopy ($P = 0.011$). To confirm these results, we utilized flavin-containing monooxygenase 3 deficient (*Fmo3*^{-/-}) mice on a *Ldlr*^{-/-} background, which were similarly placed on a high choline and high cholesterol diet and infused with AngII as described above, with littermate and age-matched *Fmo3*^{+/+} mice as controls. *Fmo3*^{-/-} mice had significantly reduce AAA incidence ($P < 0.05$) and mortality due to aortic rupture ($P < 0.005$) when compared their *Fmo3*^{+/+} littermates.

Conclusions: Our results demonstrate that inhibition of TMAO production significantly attenuates rupture-induced mortality and aneurysm incidence. As such, TMAO and associated enzymes along the metaorganismal pathway, are potential therapeutic targets for the treatment of AAA.

Sarah Kosta, PhD¹ • Kenneth Campbell, PhD¹
Physiology University of Kentucky¹

Cardiac myosin-binding protein C regulates calcium sensitivity and sarcomere force production: a computational study

Postdoc

Cardiac myosin-binding protein C (cMyBP-C) is an essential regulator of cardiac function. Mutations in cMyBP-C are one of the major causes of hypertrophic cardiomyopathy, the most common inherited form of heart disease. At the sarcomere scale, cMyBP-C is able to bind to the thick and thin filaments, and changes to its phosphorylation status affect cMyBP-C affinity for both. Despite its significance in cardiac health, surprisingly little is known about how cMyBP-C mediates its functional effects. Computational modelling tools may provide new quantitative insights into the cMyBP-C regulatory role.

FiberSim is a flexible open-source model of myofilament-level contraction. The code tracks the position and status of each contractile molecule within the half-sarcomere lattice. This allows the model to simulate some of the mechanical effects modulated by cMyBP-C and investigate its regulatory role. In this study, we tested two hypotheses about the cMyBP-C interaction with myofilaments. The first mechanism (M1) is the cMyBP-C stabilization of the super-relaxed state of myosin dimers. This myosin state is associated with a low ATPase activity and an absence of interaction with actin. The other mechanism (M2) is cMyBP-C binding to actin and modulating the thin filament activation.

We ran tension-pCa curves simulations for four situations: the absence of any cMyBP-C-mediated mechanism (CTRL), SRX-stabilization by cMyBP-C (M1), cMyBP-C binding to actin (M2), and finally both M1 and M2. The results show that M1 decreases calcium sensitivity as well as the maximal isometric force compared to the CTRL case. M2 increases calcium sensitivity and leaves the maximal isometric force unchanged. M1 + M2 increases calcium sensitivity and decreases the maximal isometric force, similar to experimental observations. This demonstrates the complex role of cMyBP-C, which acts both as a “crossbridge inhibitor” and as a “calcium-sensitizer”. Further investigations need to be carried out to determine how the cMyBP-C phosphorylation status modulates its interaction with both thin and thick filaments.

Audrey Poupeau, PhD¹ • Gertrude Arthur¹ • Kellea Nichols¹ • Frederique Yiannikouris, PhD¹
Pharmacology and Nutritional Sciences University of Kentucky¹

Circulating human sPRR increased blood pressure in female mice fed a low-fat diet

Postdoc

Elevated plasma soluble prorenin receptor (sPRR) is associated with essential hypertension and obesity-hypertension in men. Additionally, our laboratory previously found that the infusion of mouse sPRR elevates systolic blood pressure (SBP) in high-fat (HF) fed male mice through activation of the sympathetic nervous system but did not elevate SBP in HF-fed female mice. Interestingly, mouse sPRR infusion increased renal and hepatic angiotensinogen (AGT) and plasma renin concentration in female mice fed a low-fat diet. However, whether sPRR-activates the renin angiotensin system (RAS) and increases blood pressure in low-fat fed female mice remains to be investigated. Additionally, little is known concerning the influence of human sPRR on blood pressure in women. Therefore, we developed a humanized mouse model with high circulating human sPRR. Human sPRR-Myc-tag transgenic mice were bred with mice expressing Alb/Cre recombinase to induce human sPRR release in the circulation. Control and Alb-HsPRR female mice were fed a LF-diet for 8 months (n=11/groups). Body weight and body composition were examined and blood pressure assessed by radiotelemetry. Human sPRR-Myc-tag was detected in the liver of Alb-HsPRR female mice and plasma sPRR levels increased by 50-fold (CTL: 3.6±0.5 ng/ml, HsPRR:190.5±24.4 ng/ml; P<0.05), which validated the humanized mouse model. Elevated circulating human sPRR did not change body weight (CTL: 22.2±0.37, HsPRR:23.0±0.32g) or fat mass (CTL: 2.5±0.2, HsPRR:3.1±0.2g). Liver-derived human sPRR significantly elevated SBP in Alb-HsPRR compared to control female mice (Night SBP: CTL, 130.5±1.2 mmHg; Alb-HsPRR, 135.9±2 mmHg; P<0.05) and acute injection of AngII exacerbated SBP elevation. Interestingly, the decrease in blood pressure mediated by losartan was not different between Alb-HsPRR and control female mice (Night DSBP: CTL, -13.11±2.2 mmHg; Alb-HsPRR, -14.8±2.7 mmHg; P>0.05). Plasma AGT and renin activity were similar between Alb-HsPRR and control female mice. Therefore, whether the local RAS or the sympathetic nervous system are involved in human sPRR-mediated increase of SBP remains to be examined. Altogether, our results suggest an important role of circulating human sPRR in blood pressure control in women.

Dan Hao ¹ • Ling Guo ¹ • Qian Wang ¹ • Misa Ito ¹ • Chieko Mineo ² • Philip W Shaul ² • Xiang-An Li ¹

Physiology and Saha Cardiovascular Research Center University of Kentucky ¹ • Pediatrics University of Texas Southwestern Medical Center ²

Adrenal insufficiency is a risk factor in pediatric sepsis

Graduate Student

Introduction: The Sepsis Guideline recommendation for glucocorticoid (GC) treatment in pediatric sepsis changed from high recommendation (grade 1A) in 2012 to weak recommendation (grade 2C) in 2020, due to the high controversy over the beneficial of GC therapy in pediatric septic patients, suggesting an urgent need to re-evaluate the efficacy of GC therapy. Importantly, relative adrenal insufficiency (RAI), a status of insufficient inducible GC (iGC) production in stress conditions, is a poor prognosis factor in pediatric sepsis. Currently, a lack of RAI animal model presents a barrier to assess the contribution of adrenal insufficiency to sepsis and to evaluate the efficacy of GC therapy in pediatric sepsis. Here, we developed a new RAI model using adrenal specific knockout of scavenger receptor BI (SR-BI) mice and test our hypothesis that RAI is a risk factor and a precision medicine approach should be used for GC therapy in sepsis-only applying GC to young mice with RAI.

Methods: SR-BI is a well-established high density lipoprotein (HDL) receptor. It mediates cholesterol updated from HDL, which provides cholesterol for GC synthesis in the adrenal gland. SF1CreSRBIfl/fl conditional knockout mice exhibited specific depletion of SR-BI in the adrenal gland, resulting in a lack of production of iGC in response to ACTH stimulation without affecting basal GC levels—a status of RAI. Using SF1CreSRBIfl/fl mice as an RAI model, we tested our hypothesis in two sepsis models: cecal ligation and puncture (CLP) and cecal slurry induced sepsis.

Results: We found that 21-day old SF1CreSRBIfl/fl young mice are susceptible to sepsis (86.67% survival in SRBIfl/fl mice versus 12.5% in SF1CreSRBIfl/fl mice, $p=0.001$ in CLP induced sepsis; 33% survival in SRBIfl/fl mice versus 0% in SF1CreSRBIfl/fl, $p<0.05$ in cecal slurry induced sepsis). Supplementation of hydrocortisone significantly improved the survival rate in CLP-treated SF1CreSRBIfl/fl mice, but had no effect on CLP-treated SRBIfl/fl mice. Further mechanistic study reveals that iGC production is essential for effectively controlling immune responses with multiple protective effects during septic stress.

Conclusions: Using the unique RAI mice model, we demonstrated that the production of iGC is essential for controlling immune responses to septic stress with multiple protective effects and these protective effects are lost in RAI due to lack of iGC. Our finding that GC treatment benefits young mice with RAI provides a proof of concept to support the use of a precision medicine approach for GC therapy—selectively applying GC therapy for pediatric patients with RAI.

Renee Donahue, MS¹ • Hsuan Peng² • Kazuhiro Shindo, MD, PhD¹ • Erhe Gao, MD, PhD³ • Brooke Ahern⁴ • Bryana Levitan⁴ • Hlmi Tripathi, PhD¹ • David Powell, PhD⁵ • Ahmed Noor, MD⁶ • Jonathan Satin, PhD⁴ • Ashley Seifert, PhD⁷ • Ahmed Abdel-Latif, MD, PhD⁶

Cardiovascular Research Center University of Kentucky¹ • University of Kentucky² • The Center for Translational Medicine Temple University³ • Physiology University of Kentucky⁴ • MRISC University of Kentucky⁵ • Gill Heart and Vascular Institute and Division of Cardiovascular Medicine University of Kentucky⁶ • Biology University of Kentucky⁷

Adult spiny mice (*Acomys*) exhibit endogenous cardiac recovery in response to myocardial infarction.

Staff

Complex tissue regeneration is extremely rare among adult mammals with the exception of the superior tissue healing of multiple organs in spiny mice (*Acomys*). While *Acomys* species exhibit the remarkable ability to heal complex tissue with minimal scarring, their cardiac structure and response to cardiac injury are unknown. In this study, we first examined baseline *Acomys* cardiac anatomy and function in comparison with commonly used laboratory *Mus* strains (C57BL6J and outbred Swiss Webster). Our results demonstrate comparable cardiac anatomy and function between *Acomys* and *Mus*, however; *Acomys* exhibit a higher percentage of mononuclear diploid cardiomyocytes and T-type Calcium channels, rarely seen in adult mammals. In response to myocardial infarction, all strains experienced a comparable level of initial cardiac damage of the left ventricular wall and apex. However, *Acomys* demonstrated superior ischemic tolerance and cytoprotection in response to injury as evidenced by higher survival rate, cardiac functional stabilization, increased angiogenesis, and smaller scar size 50 days after injury compared to the inbred and outbred mouse strains. Overall, these findings demonstrate augmented myocardial preservation in spiny mice post-MI and establish *Acomys* as a new adult mammalian model for cardiac research.

Xufang Mu ¹ • Shu Liu, PhD ¹ • Wen Su, MD ² • Timothy McClintock, PhD ¹ • Arnold Stromberg, PhD ³ • Ming Gong, PhD ¹ • Zhenheng Guo, PhD ²

Department of Physiology University of Kentucky ¹ • Department of Pharmacology and Nutritional Sciences University of Kentucky ² • Department of Statistics University of Kentucky ³

PD-1 pathway upregulation by orchiectomy attenuates the aldosterone and high salt induced aortic aneurysms in male mice

Graduate Student

Objective - Male sex is a well-established risk factor for abdominal aortic aneurysms (AAA) but the underlying mechanisms remain to be fully understood. Using an aldosterone and high salt (Aldo/salt) induced AAA mouse model, we have demonstrated that androgen and its receptor mediate the high susceptibility to Aldo/salt induced AAA. The current study further investigates the mechanisms downstream of androgen.

Approaches and Results - To dissect the mechanisms connecting androgen and AAA, aortas were collected for RNA sequencing from 3 groups of 10-month-old wild-type mice #1 intact mice; #2 orchiectomized mice; and #3 orchiectomized mice plus DHT. All mice were given Aldo/salt for 7 days. Differentially expressed genes were analyzed using DESeq2 in R. We filtered genes that were upregulated in group #2 compared to group #1 and the up-regulation was reversed in group #3 by the DHT, or vice versa (fold change >1.5 and padj <0.05). Selected genes were run for gene ontology analysis in Enrichr (database Bioplanet 2019). Many pathways related to T cell activity were significantly enriched, particularly PD-1 signaling was one of the top pathways upregulated in orchiectomy group #2. PD-1 is known for its role as an immune checkpoint, and inflammation is a major hallmark for AAA development. Therefore to explore the role of PD-1, we first confirmed the PD-1 mRNA changes in aorta by qPCR. Secondly, IHC staining also showed PD-1 protein was significantly increased in the spleen of orchiectomized mice compared to intact controls. Finally, to investigate the potential causal role of PD-1 in the androgen-mediated aortic aneurysms formation, we injected α PD-1 antibody or control IgG antibody to orchiectomized mice 3 days before and during the 8 weeks of Aldo/salt administration. Results showed that 5 out of 12 α PD-1 mice, while none of the 8 control mice developed aortic aneurysms ($p < 0.05$).

Conclusions - PD-1 pathway is involved in the androgen associated high susceptibility of Aldo/salt induced aortic aneurysms in mice.

Sidney Johnson, MS¹ • Elizabeth Schroder, PhD¹ • Don Burgess, PhD¹ • Makoto Ono, MD, PhD¹ • Tanya Seward¹ • Claude Elayi, MD² • Karyn Esser, PhD³ • Brian Delisle, PhD¹
Physiology University of Kentucky¹ • CHI Saint Joseph Hospital² • Physiology and Functional Genomics University of Florida³

The Role of the Cardiomyocyte Circadian Clock Mechanism in Heart Rate and Ventricular Repolarization

Staff

Background: Previous studies have shown significant changes in heart rate (HR) and ventricular repolarization (VR) when eating behaviors change in mice. We hypothesize that these changes are influenced by the cardiomyocyte circadian clock mechanism.

Objective: To determine how the cardiomyocyte circadian clock mechanism in mice contributes to changes in HR and VR when food is restricted to the light cycle.

Methods: To disrupt the cardiomyocyte circadian clock mechanism, we induced deletion of *Bmal1* in cardiomyocytes in adult mice (iCSDB*Bmal1*^{-/-}). The iCSDB*Bmal1* mice were generated by crossing a floxed *Bmal1* mouse and a cardiac-specific, *Myh6-MerCreMer* recombinase mouse. The mice were either treated with a vehicle injection for control mice (iCSDB*Bmal1*^{+/+}) or a Tamoxifen injection (iCSDB*Bmal1*^{-/-}). Both groups were housed in 12-hr light and dark cycles and were subjected to ad libitum feeding (ALF) conditions and time-restricted feeding (TRF) conditions, in which feeding is restricted to the light cycle. To measure HR and VR, electrocardiography (ECG) telemetry was used. RR- and QT-intervals were analyzed, which correspond to heart rate and ventricular repolarization respectively. A nonlinear sinusoidal model was used to quantify the 24-hr rhythms associated with the RR- and QT intervals. This model calculates the period (the time between peak amplitudes), phase (the timing of the peak rhythm relative to the start of the light phase, ZT = 0), amplitude (one-half of the peak to trough levels), and the rhythm adjusted mean.

Results: The daily RR-intervals for both groups were prolonged in TRF conditions compared to ALF conditions. Analysis of light and dark cycles showed longer RR-intervals in the light cycle during ALF conditions and longer RR-intervals in the dark cycle after switching to TRF conditions. QT-interval analysis showed longer daily QT-intervals in iCSDB*Bmal1*^{-/-} mice compared to iCSDB*Bmal1*^{+/+} mice. For iCSDB*Bmal1*^{-/-} mice, the QT-intervals were more prolonged in TRF conditions than in ALF conditions. During ALF conditions, the daily QT-intervals during the light cycle were longer for both groups compared to the dark cycle. During TRF conditions, the QT-intervals in the dark cycle were longer for both groups, but the increase was larger in iCSDB*Bmal1*^{-/-} mice.

Conclusion: The data suggests that changes in HR and VR are not dependent on the cardiomyocyte circadian clock mechanism because these changes persisted in both iCSDB*Bmal1* groups. There were differences between ALF and TRF conditions, which suggests that extrinsic factors play a role. However, the data also suggests that the clock mechanism plays a role in limiting QT-interval prolongation when the heart rate slows. Abnormal QT-interval prolongation is associated with increased risk for ventricular arrhythmias and sudden cardiac death, so if conserved in humans, then disrupting the cardiomyocyte clock mechanism in people could increase their risk for sudden cardiac death.

Jennifer Torres Yee, MD ¹ • Evan R. Stearns, MD ² • Vidant Gupta, MD ³

Internal Medicine University of Kentucky ¹ • Internal Medicine University of Kentucky ² • University of Kentucky ³

Cardiovascular Implications in Refractory TTP: A Single Case with Review of Literature

Postdoc

The TTP mortality rate has increased over time despite reports of significant improvement in survival associated with clinical use of plasma infusion and plasma exchange. Cardiac events in suspected TTP patients are the most common presentation of a rare occurrence with an incidence of less than 0.0004% in the United States. The most frequently associated cardiac events are acute MI followed by decompensated heart failure, syncope, pump-failure shock, and lastly SCD. Patients with refractory TTP have a poorer prognosis given lack of effective therapies which are limited by cost availability in hospital across the country. Recent outcome predictors associated with in-hospital mortality have not shown improved clinical outcomes in patients. to date, early and prompt initiation of early extracorporeal therapy as initial treatment has shown association with positive clinical outcomes and reduced morbidity during same hospitalization. We present a special case of refractory recurrent TTP presenting as an outside hospital transfer who received initial non-invasive medical management with emergent plasma exchange shortly after her arrival to our facility with course complicated by extensive micro-clot formation and anterior wall STEMI in the setting of previous MI from prior TTP flare. She received subsequent second line treatment with humanized anti-von Willebrand factor, Caplacizumab in addition to anti-platelet therapy with low dose aspirin daily for secondary prevention. Patient was discharge clinically stable to L-TACH facility 3 weeks later with new cerebral infarcts complicated by new-focal deficits.

Matako Ono 1 • Don Burgess, PhD 1 • Tanya Seward 2 • Sidney Johnson, MS 1 • Ezekiel Rozmus, MS 2 • Elizabeth Schroder, PhD 1 • Brian Delisle, PhD 1

Physiology University of Kentucky 1 • Physiology University of Kentucky 2

Time-restricted Feeding to the Light Cycle Exacerbates QT Interval Prolongation At All Heart Rates In 24-hour Rhythm In Mice of Long QT Syndrome Type3

Postdoc

Background: Long QT syndrome type 3 (LQT3) is caused by mutations in the SCN5A-encoded Nav1.5 channel. LQT3 patients exhibit time of day-associated abnormal increases in their QT intervals and risk for life-threatening episodes. Heart rate and QT interval each have a circadian rhythm over 24-hours. The light/dark cycle entrains the circadian clock in the suprachiasmatic nucleus and the timing of feeding entrains circadian clocks in the peripheral organs.

Objective: We determined how time restricted feeding (TRF) to the light (inactive) cycle affects to heart rate and QT interval in wild-type (WT) and LQT3 mice.

Methods: We measured the RR and QT intervals in male mice (WT and LQT3, n=6 respectively) housed in 12-hour light and 12-hour dark conditions where food was made available at all times of day (ad libitum or ALF) or only during the middle 8 hours of the light phase (time restricted feeding or TRF). After the initial adjustment, mice consumed equivalent calories. 24-hour rhythms in RR and QT intervals were calculated by fitting data to a cosine function in ALF, 24 hours or 2-weeks after switching to TRF.

Results: During ALF, both WT and LQT3 mice showed aligned 24-hour rhythms in the RR- and QT-intervals that peaked at the beginning of the light cycle (WT; peak RR interval= 128.4 ± 1.0 ms and peak QT interval= 50.5 ± 1.6 ms, LQT3; 132.4 ± 2.4 ms and 56.7 ± 0.7 ms). Switching to TRF for 24 hours caused a sudden and large phase shift in the peaks of 24-hour rhythms to the dark cycle (WT; peak RR interval= 175.3 ± 3.0 ms and peak QT interval= 61.9 ± 1.4 ms, LQT3; 187.1 ± 3.7 ms and 69.4 ± 1.3 ms, $p < 0.001$ compared to ALF). After 2 weeks of TRF, the RR- and QT-intervals still peaked at dark cycle (WT; peak RR interval= 167.2 ± 3.8 ms and peak QT interval= 58.1 ± 1.1 ms, LQT3; 183.5 ± 2.2 ms and 67.3 ± 1.0 ms, $p < 0.001$ compared to ALF). There was a significant difference in peak RR- and QT-intervals after TRF between WT and LQT3 mice (RR-interval; $p < 0.01$, QT-interval; $p < 0.001$).

TRF also increased nadir RR interval in LQT3 mice (105.7 ± 1.4 ms in ALF, 114.6 ± 1.4 ms in TRF 2weeks, $p < 0.05$) and nadir QT interval in both WT (45.2 ± 1.3 ms in ALF, 48.2 ± 1.4 ms in TRF 2weeks, $p < 0.01$) and LQT3 mice (49.9 ± 1.1 ms in ALF, 55.8 ± 1.5 ms in TRF 2weeks, $p < 0.01$). There was a significant difference in nadir QT interval after TRF between WT and LQT3 mice ($p < 0.05$).

Conclusion: The timing of food intake significantly shifts and amplifies the 24-hour rhythms in heart rate and QT interval of WT and LQT3 mice. At all heart rates, QT interval prolongation was observed in both mice and there was a significant difference in QT prolongation at fastest HR between WT and LQT3 mice. If conserved in humans, the timing of food intake could represent a previously underappreciated modifiable risk factor for arrhythmic triggers.

Gertrude Arthur ¹ • Audrey Poupeau ¹ • Kellea Nichols ¹ • Jacqueline Leachman ¹ • Analia Loria ¹ • Jeffrey Osborn ² • Frederique Yiannikouris ¹

Department of Pharmacology and Nutritional Sciences University of Kentucky ¹ • Department of Biology University of Kentucky ²

Collecting duct cells-derived human sPRR impairs the antihypertensive effects of losartan and upregulates ERK1/2 and AQP2 expression

Graduate Student

Recent studies showed that soluble prorenin receptor (sPRR) plays an important role in blood pressure regulation and in water balance. In rodent models, sPRR contributes to AngII production by increasing renin activity, systolic blood pressure (SBP) and aquaporin2 (AQP2)-dependent antidiuretic action. However, there is a gap of knowledge concerning the functional role of locally produced sPRR from the kidney. Therefore, we evaluated the kidney-derived human sPRR role in SBP control and fluid homeostasis.

Human sPRR-Myc-tag transgenic mice were bred with mice expressing Hoxb7/Cre to selectively express human sPRR in the collecting duct (RHsPRR). RHsPRR and control (CTL) male mice were fed a standard diet for 10 months (n=8-11/group). Body weight and urine volume were examined and SBP measured by radiotelemetry. Western blot analysis depicted the presence of human sPRR-Myc-tag (28 KDa) in the cortex and medulla of RHsPRR male mice validating the humanized mouse model. Body weight did not change and 24hr-SBP was similar between CTL and RHsPRR mice (128±2 and 122±5 mmHg, respectively). However, the chronic response to losartan treatment was reduced in RHsPRR compared to CTL (Δ SBP: CTL: -9±3; RHsPRR: -5±1 mmHg, P<0.05). Kidney-derived human sPRR did not change GFR (838±75 vs 1088±163 μ l/min/100g BW) and urinary vasopressin (0.62±0.21; 0.72±0.20 ng/mg creatinine), while modestly decreasing urine excretion rate by ~40% (CTL: 1.04±0.20; RHsPRR: 0.57±0.25 ml/day). Furthermore, RHsPRR mice had higher AQP2 protein expression in renal cortex (CTL: 0.24±0.07; RHsPRR: 4.11±0.70 AU, P<0.05) and medulla (CTL: 0.11±0.04; RHsPRR: 4.03±1.74 AU, P<0.05) than CTL mice. Kidney-derived human sPRR significantly increased phosphorylation of ERK 1/2 in the cortex compared to CTL (CTL: 5.4±1.0; RHsPRR: 9.2±1.4 AU, P<0.05), an MAPK involved in the regulation of water balance.

In addition, RHsPRR mice showed increased plasma osmolality compared to CTL mice (CTL: 349±2; RHsPRR: 357±2 mOsm/kg, P<0.05). Overall, our data suggest that renal human sPRR could contribute to the increase in plasma tonicity by promoting the activation of ERK1/2-AQP2 pathway. Whether this signaling is associated with impaired antihypertensive effects of AT1R blockage remains under investigation

Joshua Lykins ¹, Sidney W. Whiteheart, PhD ¹

Dept. of Molecular and Cellular Biochemistry University of Kentucky ¹

Megakaryocyte secretion of cytokines is influenced by α -granule retention proteins

Graduate Student

Background/Objectives: Platelets are produced by megakaryocytes (MK) in the bone marrow. Disorders affecting the development of platelet granules are well documented. These storage pool disorders (SPDs) lead to disrupted trafficking of granule cargo. The trafficking of cargo to these granules is integrated with the development of MK, and the α -granule stores several growth factors that affect the HSC niche and the bone marrow microenvironment, such as PF4 and TGF- β respectively. Many SPDs also exhibit myelofibrosis in the bone marrow, indicating that the aberrant trafficking of α -granule cargo is affecting the surrounding milieu of the bone marrow and the HSC niche. The purpose of this study was to assess the release of PF4 from MKs *in vivo* and *in vitro* in knockout mice that lack two key α -granule packaging proteins: Serglycin and NBEAL2, and how alterations in extramedullary PF4 affect MK development.

Methods: To investigate this relationship, we have utilized primary MKs from Serglycin^{-/-} and NBEAL2^{-/-} mice. Whole bone marrow was isolated from euthanized mice, mature cells were removed by magnetic separation with lineage depletion kit (Miltenyi Biotec), and immature cells were then cultured in 50 ng/ml TPO. Samples for western blot and ELISA were taken daily. PF4 levels were then assessed by western blot and ELISA (R&D systems). Daily samples were taken for FACS analysis to assess DNA content. To address *in vivo* levels of PF4 we isolated bone marrow plasma by centrifugation.

Results and Conclusions: The results of these experiments showed that PF4 is secreted by MKs normally during their development as shown in WT mice. However, the deletion of Serglycin led to increased secretion of PF4 during earlier stages of MK development, and near-complete depletion of internal PF4 by day 5. Comparison to NBEAL2^{-/-} MKs showed a lack of internal PF4 and very low levels of secreted PF4. These results are supported by the *in vivo* measurements of PF4 in bone marrow plasma, which showed much higher levels of extramedullary PF4 in Serglycin^{-/-} compared to WT, and almost no detectable PF4 in NBEAL2^{-/-} bone marrow plasma. Analysis of DNA content revealed that over the course of culture there was an increase in cells in the 4n, 8n, and 16n populations as expected. These populations decreased in both Serglycin^{-/-} and NBEAL2^{-/-} cultures. Consistently, examination of sternal marrow from Serglycin^{-/-} and NBEAL2^{-/-} mice showed decreased MK size. These results taken together indicate that: Serglycin and NBEAL2 are necessary for proper PF4 storage and secretion in MKs; that Serglycin is needed to retain PF4 inside the MK, and that without Serglycin, PF4 secretes or “leaks” from α -granules and MKs into the extracellular space; MKs derived from Serglycin^{-/-} and NBEAL2^{-/-} mice do not mature to the same extent as those from WT mice, possibly due to alterations in the levels of PF4 and potentially other cytokines in the media.

Hisashi Sawada, MD, PhD², Chen Zhang, MD, PhD¹ • Yanming Li, PhD¹ • Yuriko Katsumata, PhD² • Ying Shen, MD, PhD¹ • Scott LeMaire, MD³ • Hong Lu, MD, PhD⁴ • Alan Daugherty, PhD, D.Sc⁴
Department of Surgery Baylor College of Medicine¹ • Department of Bioinformatics University of Kentucky² • Department of Surgery University of Kentucky³ • Department of Physiology University of Kentucky⁴

Transcriptomic modulation of second heart field-derived smooth muscle cells in angiotensin II-infused mice promotes aortopathy

Faculty

Objective: Smooth muscle cells (SMCs) in the ascending aorta are derived from both the cardiac neural crest and second heart field (SHF). The importance of cardiac neural crest-derived SMCs on development of thoracic aortic aneurysms has been reported, while functional roles of SHF-derived SMCs are controversial. The aim of this study was to profile the transcriptome of SHF-derived SMCs in ascending aortas of angiotensin II (AngII)-infused mice by single cell RNA sequencing.

Methods and Results: Female ROSA26 mT/mG mice were bred to male mice expressing Cre under the control of the Mef2c promoter (Mef2c Cre). Angiotensin II (AngII, 1,000 ng/kg/day) was infused subcutaneously into Mef2c Cre +/- mice and ascending aortas were harvested at day 3 of AngII infusion (n=5). Ascending aortas without AngII infusion were harvested as control (n=4). SHF-derived cells were sorted based on mGFP signal by FACS and single cell sequencing was performed using SHF-derived cells. Single cell RNA sequencing detected mRNA in multiple cell types, and AngII altered mRNA abundance of 3,658 genes in the SMC cluster. Several SMC contractile-related genes, such as *Acta2*, *Tagln* and *Cnn1*, were increased by AngII compared to control SHF-derived SMCs. Conversely, *Klf4*, a proliferative gene, was decreased in SHF-derived SMCs of AngII-infused mice. In addition, AngII increased multiple extracellular matrix component genes, including fibrillin1 and elastin. AngII also upregulated *Serpine1* and *Fn1* that are important for extracellular matrix organization. Thus, AngII led to transcriptomic modulations in SHF-derived SMCs. Of note, AngII infusion decreased mRNA abundance of *Tgfrb2* and *Lrp1*, key regulators of extracellular matrix maturation, in SHF-derived SMCs. To further investigate the importance of SHF-derived SMCs, we deleted either *Tgfrb2* or *Lrp1* in SHF-derived cells. SHF-specific *Tgfrb2* deletion was embryonic lethal with peritoneal hemorrhage and outflow tract dilatation. SHF-specific *Lrp1* deletion augmented AngII-induced thoracic aortic rupture and dilatations.

Conclusion: SHF-derived SMCs play an important role in maintaining aortic integrity, and exhibit transcriptomic modulations by AngII infusion that may contribute to aortopathies.

Martha Sim, MS¹ • Hammodah Alfar¹ • Melissa Hollifield, MS² • Dominic Chung, PhD³ • Xiaoyun Fu, PhD³ • Meenakshi Banerjee, PhD¹ • Xian Li, PhD¹ • Alice Thornton, MD⁴ • James Porterfield, MD, PhD⁴ • Jamie Sturgill, PhD⁵ • Gail Sievert, PhD⁶ • Marietta Baxton-Baxter, PhD⁶ • Kenneth Campbell, PhD⁶ • Jerold Woodward, PhD² • Jose Lopez, PhD³ • Sidney Whiteheart, PhD¹ • Beth Garvy, PhD² • Jeremy Wood, PhD⁷

Molecular and Cellular Biochemistry University of Kentucky¹ • Microbiology, Immunology and Molecular Genetics University of Kentucky² • Bloodworks Northwest³ • Infectious Disease University of Kentucky⁴ • Internal Medicine University of Kentucky⁵ • Center for Clinical and Translational Science University of Kentucky⁶ • Saha Cardiovascular Research Center University of Kentucky⁷

HIV-1 and SARS-CoV-2 Both Cause Protein S Deficiency, but through Different Mechanisms

Graduate Student

Background: The critical plasma anticoagulant protein S (PS) circulates in two pools in plasma: free PS, and PS bound to complement factor 4-binding protein (c4bp), which blocks its anticoagulant function. PS deficiency commonly occurs in Human Immunodeficiency Virus-1 (HIV-1)+ patients and is associated with higher thrombotic risk. We hypothesized a similar process contributes to thrombosis in COVID-19 patients.

Aims: To assess the regulation of PS in viral coagulopathies.

Methods: This study was approved by the Institutional Review Board. Citrated plasma was collected from consenting HIV-1+ (19 on first diagnosis/ naïve, 11 on antiretroviral therapy/ ART) or SARS-CoV-2+ (28 inpatients, 49 outpatients) and healthy controls for both populations (10, 31, respectively). Plasma thrombin generations were measured using calibrated automated thrombography method, plasma proteins concentrations were measured with ELISAs, plasma Tissue Factor activity was measured with a centrifugation method and factor Xa generation assays, and enzyme activity assays were performed with spectroscopic methods.

Results: HIV-1+ patients had lower total PS than controls (94.12±8.71% vs 133.77±10.45%, p=0.008), in both naive (42%) and ART-treated (27%) patients. Total PS negatively correlated with endogenous thrombin potential (p=0.01), suggesting PS deficiency contributes to increased thrombin generation in these patients.

Total PS was not reduced in SARS-CoV-2+ patients, but free PS was (103.7±51.7% vs 142±50.4%, p=0.01). To determine the cause of free PS deficiency, we measured known PS-binding proteins C4BP, protein C (PC), and Mer, and found no differences between patients and controls. By native gel, we identified PS bound to C4BP, Mer, PC, tissue factor pathway inhibitor (TFPI), and von Willebrand Factor (VWF). VWF was markedly elevated in inpatients (378.1±176.7% compared to controls, p=0.0001). Purified VWF dose-dependently decreased free, but not total, PS when added to control plasma, and blocked the TFPI cofactor activity of PS. PS was also identified as a plasma binding partner of VWF by mass spectrometry, and this interaction increased 10-million-fold with shearing. Finally, despite anticoagulation, plasma thrombin generation in inpatient samples was comparable to controls, suggesting a profound hypercoagulability, possibly exacerbated by PS deficiency.

Conclusions: In HIV-1, PS consumption leads to total PS deficiency. In SARS-CoV-2, VWF increases and binds PS, reducing the free anticoagulant pool. Thus, viruses can cause PS deficiency through multiple mechanisms, promoting thrombosis by shifting the procoagulant-anticoagulant balance.

David Alexander¹, Lauren Bell¹, Xiang-An Li Ph.D.² and Guigen Zhang Ph.D.¹

¹F. Joseph Halcomb III, M.D. Department of Biomedical Engineering, University of Kentucky

²HDL Receptor Laboratory, Saha Cardiovascular Research Center, University of Kentucky College of Medicine, University of Kentucky

A Chip-Based Biosensor for Detecting Cortisol Levels

Undergraduate

The goal of this research is to conduct a feasibility study for developing a biosensor to detect cortisol levels using the electrochemical cyclic voltammetry method. Several biosensors are developed through functionalization of electrode formed on a chip in a three-electrode design. To functionalize the working electrode on the chip, a self-assembled monolayer (SAM) is first formed at its surface which is followed by binding of anti-cortisol antibody (C-M_{ab}) through its amine group to the succinimidyl group of the SAM layer. For detection, a biosensor is first exposed to cortisol in solution to allow proper antibody-cortisol binding and the binding characteristic is assessed by running electrochemical cyclic voltammetry in a solution filled with redox species of ferro/ferricyanide. The results we obtained demonstrate a success in establishing the feasibility of detecting trace amounts of cortisol in solution. The peak currents obtained reflect the underlying kinetic as well as transport mechanisms. Our next step is to further develop the sensor and calibrate it for possible use in a clinical setting. Our long-term goal is to provide a rapid in-vitro means to detect physiological cortisol levels accurately.

M. BATES, C. HADDIX, E.S. POWELL, L. SAWAKI, S. SUNDERAM;
University of Kentucky, Lexington, KY

Discrimination of different levels of finger extension from the EEG in hemiparetic stroke

Graduate Student

Assistive technologies such as brain-computer interfaces (BCIs) offer individuals with neural injury the means to interact with external devices by monitoring and interpreting their mental commands using electroencephalography (EEG). However, the ability to extract EEG features associated with fine motor control is limited, especially in stroke victims who may have large cortical lesions. Here we test the feasibility of predicting graded motor effort associated with finger extension from the EEG.

We conducted an IRB-approved study on three stroke patients with left hand paresis and three age-matched controls. Subjects were prompted by a visual display to extend their fingers outward from rest every few seconds to one of four levels—Low, Medium, High, or “No-Go”—and then return to rest. This task was performed for six runs of 16 cues each, switching hands after every run. Hand movement and muscle activity (extensor digitorum communis) were monitored using a motion capture glove and bipolar EMG, respectively. The glove recorded each phalange’s position in Cartesian space, to track extension of each digit relative to the wrist. The angle of extension in response to each cue was thus measured and averaged over index, middle, and ring fingers. EEG was simultaneously recorded over 32 locations and the mean-squared power in a moving window estimated in the 8–30 Hz band during each cue relative to a reference period preceding the cue. A quadratic classifier was trained on samples of this feature vector and the accuracy of prediction of test samples assessed using four-fold cross-validation.

For controls, the mean accuracy of the EEG classifier was 55-60% on each hand over the four levels of finger extension, much greater than the chance level of 25%; confusion between low and medium extension was the major source of error. Accuracy was strikingly similar—about 60%—on either hand for the stroke subjects, despite there being no measurable extension with the motion capture glove on the impaired hand. An EMG classifier predicted graded finger extension with only 40% accuracy on the stroke-impaired hand but 80% in the unimpaired hand and in controls.

Our findings show that the EEG can predict gradations in finger extension related to both actual and intended movement in individuals with hemiparetic stroke. This offers BCIs a measure of fine control for interactive rehabilitation protocols. Future work will focus on closing the loop using these distinguishable signals to provide real-time feedback, which can be incorporated into existing regimens to promote functional recovery.

Support: National Science Foundation Grant 1849213.

Disclaimer: This work was performed while Lumy Sawaki was employed at University of Kentucky. The opinions expressed in this article are the author’s own and do not reflect the view of the National Institutes of Health, the Department of Health and Human Services, or the United States government.

Chase Haddix¹ • Elizabeth Powell, MS² • Lumy Sawaki-Adams, MD, PhD² • Sridhar Sunderam, PhD¹
Biomedical Engineering University of Kentucky¹ • Departments of Physical Medicine and Rehabilitation University of Kentucky²

Discrimination of different levels of finger extension from the EEG in hemiparetic stroke

Graduate Student

Assistive technologies such as brain-computer interfaces (BCIs) offer individuals with neural injury the means to interact with external devices by monitoring and interpreting their mental commands using electroencephalography (EEG). However, the ability to extract EEG features associated with fine motor control is limited, especially in stroke victims who may have large cortical lesions. Here we test the feasibility of predicting graded motor effort associated with finger extension from the EEG.

We conducted an IRB-approved study on three stroke patients with left hand paresis and three age-matched controls. Subjects were prompted by a visual display to extend their fingers outward from rest every few seconds to one of four levels—Low, Medium, High, or “No-Go”—and then return to rest. This task was performed for six runs of 16 cues each, switching hands after every run. Hand movement and muscle activity (extensor digitorum communis) were monitored using a motion capture glove and bipolar EMG, respectively. The glove recorded each phalange’s position in Cartesian space, to track extension of each digit relative to the wrist. The angle of extension in response to each cue was thus measured and averaged over index, middle, and ring fingers. EEG was simultaneously recorded over 32 locations and the mean-squared power in a moving window estimated in the 8–30 Hz band during each cue relative to a reference period preceding the cue. A quadratic classifier was trained on samples of this feature vector and the accuracy of prediction of test samples assessed using four-fold cross-validation.

For controls, the mean accuracy of the EEG classifier was 55-60% on each hand over the four levels of finger extension, much greater than the chance level of 25%; confusion between low and medium extension was the major source of error. Accuracy was strikingly similar—about 60%—on either hand for the stroke subjects, despite there being no measurable extension with the motion capture glove on the impaired hand. An EMG classifier predicted graded finger extension with only 40% accuracy on the stroke-impaired hand but 80% in the unimpaired hand and in controls.

Our findings show that the EEG can predict gradations in finger extension related to both actual and intended movement in individuals with hemiparetic stroke. This offers BCIs a measure of fine control for interactive rehabilitation protocols. Future work will focus on closing the loop using these distinguishable signals to provide real-time feedback, which can be incorporated into existing regimens to promote functional recovery.

Support: National Science Foundation Grant 1849213.

Disclaimer: This work was performed while Lumy Sawaki was employed at University of Kentucky. The opinions expressed in this article are the author’s own and do not reflect the view of the National Institutes of Health, the Department of Health and Human Services, or the United States government.

Danny Orabi^{1,2,6,8} • Anthony D. Gromosky¹ • Stephanie Marshall¹ • Daniel Ferguson¹ • Kevin Fung¹ • William Massey^{1,2} • Rakhee Banerjee^{1,2} • Venkateshwari Varadharajan^{1,2} • Iyappan Ramachandiran^{1,2} • Daniel J. Silver^{1,2} • Lucas Osborn^{1,2} • Chase K. A. Neumann¹ • Rebecca Schugar¹ • Chelsea Finney¹ • Amanda Brown^{1,2} • Anthony Horak^{1,2} • Shijie Cao¹ • Preeti Pathak¹ • Dominik Bulfon³ • Yat Hei Leung⁴ • Olga Sergeeva⁵ • Robert Zimmerman³ • Marc Prentki⁴ • Zhenghong Lee⁵ • Frederico Aucejo⁶ • Daniella Allende⁷ • Justin D. Lathia^{1,8} • J. Mark Brown^{1,2,8}

Department of Cardiovascular and Metabolic Sciences, Lerner Research Institute, Cleveland Clinic¹

Center for Microbiome and Human Health, Cleveland Clinic Foundation²

Institute of Molecular Biosciences, University of Graz³

The Serine Hydrolase ABHD6 is a Therapeutic Target in Obesity-Associated Hepatocellular Carcinoma

Postdoc

Primary liver cancer ranks third in world-wide cancer-related mortality, with hepatocellular carcinoma (HCC) accounting for the great majority of these tumors. Recently there has been an emphasis on metabolic syndrome and non-alcoholic fatty liver disease (NAFLD) in the development of cirrhosis and HCC, as their attributable disease burden continues to sharply rise. We previously identified the lipid hydrolase alpha-beta hydrolase domain 6 (ABHD6) as a critical signaling node and molecular driver of metabolic syndrome, making it a prime target for investigation in NAFLD-related HCC. ABHD6 displays higher expression within HCC tumor cores when compared to adjacent non-tumor tissue in human subjects. Using an *in vivo* antisense oligonucleotide (ASO)-driven knockdown approach, we have shown that inhibition of ABHD6 prevents the development and progression of HCC in an obesity/NAFLD-driven mouse model. Additionally, a xenograft mouse model using the human Huh7 cell line displayed reduced tumor engraftment and growth with ABHD6 genetic deletion and small molecule inhibition. HCC cells genetically lacking ABHD6 demonstrated increased levels of bis(monoacylglycerol)phosphates (BMPs), lipids localized to the late endosome/lysosome. Challenged by an *in vitro* model of palmitic acid-mediated lipotoxicity, ABHD6 knockout cells demonstrated alterations in lysosomal function and autophagic flux, both of which are strongly associated with metabolic syndrome as well as HCC. These studies reveal novel lipid signaling mechanisms by which NAFLD progresses towards HCC and provide support for ABHD6 as a potential therapeutic target in HCC.

****Larry Rudel Award Lecture****

Rupinder Kaur ¹ • Garrett Anspach ² • Gregory Graf, PhD ²
Pharmaceutical Science University of Kentucky College of Pharmacy

Trans-Intestinal Cholesterol Excretion Is Dependent On The Luminal Cholesterol Content

Graduate Student

Biliary cholesterol excretion is a major route for the elimination of excess cholesterol. The ABCG5/ABCG8 transporter heterodimer (G5/G8) accounts for >70% of biliary cholesterol elimination. However, whole body sterol balance is maintained under a variety of conditions in which biliary cholesterol secretion is disrupted. This indicates the presence of an adaptive, non-biliary route of cholesterol elimination in the gastrointestinal tract termed trans-intestinal cholesterol excretion (TICE). The present study investigates the time course, degree, and location of these adaptive changes in cholesterol efflux when G5/G8 is inactivated in the liver of adult mice. *Abcg5/8^{fllox}* (control), *Abcg5/8^{fllox}* administered AAV_TBG-Cre at 8 weeks of age (acute-LKO), and *Abcg5/8^{fllox/Alb-cre}* (chronic-LKO) were maintained on standard rodent chow and feces were collected two days prior and up to 28 days after AAV administration. Despite significant reductions in biliary cholesterol secretion (54% in acute-LKO and 66% in chronic-LKO mice), no differences were detected in fecal neutral or acidic sterols at any point following AAV administration, indicating that adaptive changes to maintain sterol balance happen rapidly. In a separate cohort of control and chronic-LKO mice stomach, 5 segments of small intestine, cecum and colon were collected, and tissue sterols were extracted and analyzed via GC/MS. Cholesterol content of the first segment of chronic-LKO mice was 15% lower than that of control mice, showing 60% of the cholesterol deficit exiting the bile duct is closed within the first segment of the small intestine. In another cohort of control and chronic-LKO mice, the proximal small intestine was perfused with cholesterol poor or rich bile acid micelles and biliary and intestinal cholesterol secretion rates were determined. Despite significant reductions in biliary cholesterol secretion in chronic-LKO mice, no differences were detected in intestinal cholesterol secretion rates. Perfusion of cholesterol poor model bile resulted in net secretion of cholesterol in both groups of mice, while cholesterol rich model bile showed net absorption. We conclude that TICE, and the adaptation to disruptions in biliary cholesterol secretion, are dependent on the cholesterol concentration of the luminal content rather than a physiological adaptive process that accelerates TICE to maintain sterol balance.

****Selected Abstracts Presentation****

Jamie Morris ¹ • Hannah Sexmith ² • Scott Street ¹ • John T. Melchior, PhD ¹ • Amy S. Shah, MD ³ • W. Sean Davidson, PhD ¹
Pathology and Laboratory Medicine University of Cincinnati ¹ • Endocrinology Cincinnati Children's Hospital Medical
Center ² • Endocrinology Cincinnati Children's Hospital Medical Center ³

Apolipoprotein A-II Increases Cholesterol Efflux Capacity of Human Plasma High-density Lipoproteins

Staff

The ability of high-density lipoprotein (HDL) to promote cellular cholesterol efflux (CEC) is a more robust predictor of cardiovascular disease protection than its plasma quantity. Previously, we found that fully lipidated HDL containing apolipoprotein A-II (APOA2) promotes cholesterol efflux via the ATP binding cassette transporter (ABCA1). This was surprising given that ABCA1 is thought to primarily interact with lipid-poor apolipoproteins. Having previously focused on isolated lipoproteins, we moved into human plasma with the hypothesis APOA2 can enhance ABCA1-mediated CEC in this more complex environment. Human plasma was incubated with increasing amounts of lipid-free APOA2. The samples were assayed for CEC from macrophages +/- cAMP for ABCA1 stimulation. APOA2 dose dependently increased whole plasma CEC - due mostly to HDL as the effect persisted in apoB-depleted plasma. Next, plasma was incubated with lipid-free APOA1 or APOA2, immediately fractionated by size exclusion chromatography and each fraction assayed for CEC. In unmodified plasma, cholesterol effluxed to peaks corresponding to LDL, HDL and lipid-free apolipoproteins with the latter exclusively increased by ABCA1 expression, as expected. When lipid-free APOA1 was added, efflux to LDL and HDL remained largely unchanged. However, there was a dramatic increase in ABCA1-mediated CEC to the lipid-poor apolipoprotein fractions, likely due to the added APOA1. When APOA2 was added, we noted a similar increase of ABCA1-mediated CEC in the lipid-poor apolipoprotein fractions as the APOA1 sample, likely due to displacement of lipid-poor APOA1 by APOA2 from HDL. Strikingly, APOA2 doubled ABCA1-mediated cholesterol efflux to the fully lipidated HDL fractions. Proteomic analyses indicated that APOA2 increased in HDL though some APOA1 was retained. To explore the mechanism, we reconstituted HDL particles with APOA1 that either contained or lacked its C-terminal lipid binding helix. APOA2 lost the ability to stimulate ABCA1 efflux to HDL when the C-terminal domain of APOA1 was deleted. Our current hypothesis states that APOA2 displaces the C-terminal helix of APOA1 from the HDL surface which can then interact with ABCA1 - much like it does in lipid-poor APOA1. Reconstituted forms of APOA1 are under development as a therapy to rapidly clear cholesterol from coronary arteries in patients with acute coronary syndrome. Our work suggests APOA2 may be a novel target given its dual benefits for cholesterol efflux.

****Selected Abstracts Presentation****

Alexis Smith ¹ • Smita Joshi, PhD ¹ • Sidney Whiteheart, PhD ¹
Molecular and Cellular Biochemistry University of Kentucky ¹

α -Synuclein: a VAMP Chaperone in the Platelet Release Reaction

Graduate Student

Background: Platelets use SNARE-mediated exocytosis to maintain hemostasis and thrombosis. These processes are maintained by the exocytosis of platelet releasate from the three types of granules in platelets: dense, alpha, and lysosomal. Understanding how the process of exocytosis is regulated in secretion, we look for potential SNARE regulators and found the protein α -synuclein. α -Synuclein appears to be the only member of the synuclein family present in platelets and is very abundant.

Aims: To address the role of α -synuclein in platelet exocytosis.

Methods: We examined the phenotype of platelets from α -synuclein^{-/-} mice. Secretion from each granule population was measured and hemostasis was evaluated using a tail-bleeding time assay. Western blotting was used to assess the levels of the platelet secretory machinery.

Results: Secretion kinetic and dose-response assays showed that platelets from α -synuclein^{-/-} mice have defective release from the dense granules and less so from lysosomal granules. Tail bleeding times for α -synuclein^{-/-} mice were increase compared to the wild-type mice. To understand the mechanism of this defect, we asked whether α -synuclein is acting as a VAMP-chaperone in platelets and thus modulates secretion by controlling V-SNARE levels. The two dominant T-SNARES SNAP-23 and Syntaxin-11 were not altered in α -synuclein^{-/-} mice. However, the dominant V-SNARE VAMP-8 was reduced. Other V-SNARES VAMP-2, VAMP-3, and VAMP-7 were normal. Additional western blotting experiments demonstrated the presence of the α -synuclein-interactor Cysteine String Protein, added a new element to the known platelet secretory machinery.

Conclusion: These experiments demonstrate a role for α -synuclein in platelet exocytosis and hemostasis and will further fill a gap in our knowledge on α -synuclein's physiological function and understanding how the process of platelet exocytosis is regulated. This work is supported by grants from the NIH and NHLBI (HL56652, HL138179, and HL150818), and a VA Merit Award to S.W.W. This work is also supported by an NSF KY-WV LSAMP BD Fellowship (NSF HRD 2004710) awarded to A.N.S.

****Selected Abstracts Presentation****

Woosuk Steve Hur, PhD¹ • Y-Van Nguyen¹ • Matthew Flick, PhD¹

Pathology and Laboratory Medicine University of North Carolina at Chapel Hill¹

Protective Role of Plasminogen Deficiency in Non-Alcoholic Fatty Liver Disease and Glucose Dysmetabolism

Postdoc

Obesity is a major public health problem of global significance with ~40% of the world population being classified as overweight (BMI > 25) and 13% as obese (BMI > 30). Obesity drives chronic metabolic inflammation leading to metabolic syndrome that precipitates cardiovascular disease, fatty liver disease, Type II diabetes, and certain cancers. The obese phenotype is characterized by a markedly perturbed blood system characterized by exacerbated procoagulant activity, suppressed fibrinolytic function and the accumulation of extravascular fibrin deposits within white adipose tissue and liver. Recently, we showed that high fat diet (HFD)-challenged mice expressing a fibrinogen variant that does not engage macrophages through the integrin receptor α_{MB2} had reduced weight gain and associated pathologies (*e.g.*, fatty liver disease, insulin resistance) secondary to reduced macrophage-mediated metabolic inflammation. Here, we analyzed the impact of elimination of the fibrinolytic protease plasminogen on HFD-driven weight gain, metabolic inflammation, and obesity-associated pathologies. Over the course of 20 weeks, plasminogen-deficient (Plg-) mice gained as much weight as the control mice (Plg+) on HFD, although the epididymal white adipose tissue of HFD-fed Plg- mice had a greater mass than that of HFD-fed Plg+ mice. In contrast, the liver mass of HFD-challenged Plg+ mice were significantly higher than that of HFD-fed Plg- mice and were comparable to low fat diet (LFD)-fed mice. HFD-fed Plg+ animals displayed a fatty liver disease phenotype characterized by histological evidence of steatosis, elevated triglyceride content, and hepatocellular injury (*i.e.*, elevated plasma ALT). HFD-fed Plg- mice were protected from developing each of these pathologies. HFD-fed Plg+ mice had significantly elevated circulating cholesterol levels at 20 weeks, whereas levels in Plg- mice were comparable to LFD-fed mice. Intriguingly, while the brown adipose tissue mass was comparable between diet and genotype, there was an upregulation of uncoupling protein-1 (*Ucp1*) expression in BAT of HFD-fed Plg- mice. Notably, whereas HFD-fed Plg+ mice showed evidence of diabetes compromised glucose clearance, HFD-fed Plg- mice were partially protected from these pathologies. Collectively, our data suggest that plasmin(ogen) contributes to HFD-induced fatty liver disease and glucose dysmetabolism.

****Selected Abstracts Presentation****

WE VALUE YOUR FEEDBACK!

Thank you for attending this year's event
Please take a few moments to comment on your experience.

[Click here to be directed to the survey](#)

Will be available Friday, September 10

SEE YOU IN 2022

- NOVEMBER 4, 2022 -

